

University of Windsor

Scholarship at UWindor

Electronic Theses and Dissertations

Theses, Dissertations, and Major Papers

1-1-1972

Hydrofluoric acid production studies: An investigation into the kinetics of reaction between fluorspar and sulfuric acid.

Danilo Candido
University of Windsor

Follow this and additional works at: <https://scholar.uwindsor.ca/etd>

Recommended Citation

Candido, Danilo, "Hydrofluoric acid production studies: An investigation into the kinetics of reaction between fluorspar and sulfuric acid." (1972). *Electronic Theses and Dissertations*. 6111.
<https://scholar.uwindsor.ca/etd/6111>

This online database contains the full-text of PhD dissertations and Masters' theses of University of Windsor students from 1954 forward. These documents are made available for personal study and research purposes only, in accordance with the Canadian Copyright Act and the Creative Commons license—CC BY-NC-ND (Attribution, Non-Commercial, No Derivative Works). Under this license, works must always be attributed to the copyright holder (original author), cannot be used for any commercial purposes, and may not be altered. Any other use would require the permission of the copyright holder. Students may inquire about withdrawing their dissertation and/or thesis from this database. For additional inquiries, please contact the repository administrator via email (scholarship@uwindsor.ca) or by telephone at 519-253-3000ext. 3208.

INFORMATION TO USERS

This manuscript has been reproduced from the microfilm master. UMI films the text directly from the original or copy submitted. Thus, some thesis and dissertation copies are in typewriter face, while others may be from any type of computer printer.

The quality of this reproduction is dependent upon the quality of the copy submitted. Broken or indistinct print, colored or poor quality illustrations and photographs, print bleedthrough, substandard margins, and improper alignment can adversely affect reproduction.

In the unlikely event that the author did not send UMI a complete manuscript and there are missing pages, these will be noted. Also, if unauthorized copyright material had to be removed, a note will indicate the deletion.

Oversize materials (e.g., maps, drawings, charts) are reproduced by sectioning the original, beginning at the upper left-hand corner and continuing from left to right in equal sections with small overlaps.

ProQuest Information and Learning
300 North Zeeb Road, Ann Arbor, MI 48106-1346 USA
800-521-0600

UMI[®]

HYDROFLUORIC ACID PRODUCTION STUDIES:
AN INVESTIGATION INTO THE KINETICS OF REACTION
BETWEEN FLUORSPAR AND SULFURIC ACID

A Dissertation
Submitted to the Faculty of Graduate Studies through the
Department of Chemical Engineering in Partial Fulfilment
of the Requirements for the Degree of
Doctor of Philosophy at the
University of Windsor

by

Danilo Candido

Windsor, Ontario

1972

UMI Number: DC52691

INFORMATION TO USERS

The quality of this reproduction is dependent upon the quality of the copy submitted. Broken or indistinct print, colored or poor quality illustrations and photographs, print bleed-through, substandard margins, and improper alignment can adversely affect reproduction.

In the unlikely event that the author did not send a complete manuscript and there are missing pages, these will be noted. Also, if unauthorized copyright material had to be removed, a note will indicate the deletion.

UMI[®]

UMI Microform DC52691
Copyright 2008 by ProQuest LLC
All rights reserved. This microform edition is protected against
unauthorized copying under Title 17, United States Code.

ProQuest LLC
789 East Eisenhower Parkway
P.O. Box 1346
Ann Arbor, MI 48106-1346

ABX 7529

APPROVED BY:

[Signature]

E. Demelle

[Signature]

J. P. Mathew

H.S. Muralidharan

A. Raouf

698773

Dedicated to

Sally, Paul and Cathy.

ABSTRACT

The reaction between flotated fluorspar and concentrated sulfuric acid was investigated in a batch and a continuous reactor system.

Conversion-time data were obtained with the batch reactor in the range of 250 - 350°F.

Two series of runs were conducted in the continuous reactor. The first, varying temperature (300 - 450°F) and the acid:spar ratio (0.95 - 1.05) and the second, a 2^{4-1} fractional factorial design of experiments, varying temperature (370 and 450°F), mixing speed (15.8 and 25 r.p.m.), calcium carbonate content of the fluorspar (3.5 and 7.14 % by wt.) and the fineness of the fluorspar (2 levels).

By means of statistical analysis of the data, it was shown that three rate models provide a satisfactory fit.

The results indicated that the reaction is diffusion controlled (activation energy 16,000 Btu/lb.mole), and that the reactivity of the spar is appreciably enhanced by an increase in the calcium carbonate content. No appreciable change in the reactivity was detected with a change in the fluorspar fineness. The mixing speed seems to enhance the reaction at 25 r.p.m. levels only when the calcium carbonate of the fluorspar is 3.5 % by wt.

ACKNOWLEDGEMENTS

The author primarily wishes to express his gratitude to Dr. G. P. Mathur for his able guidance and encouragement. His sense of perspective was of great help during the course of this work.

My thanks also go to Dr. M. Adelman whose knowledge of chemical analysis techniques was of great help.

The co-operation of the many people at Alcan is also acknowledged; Mr. Gerard Auger of the Alcan Works Laboratory, who was responsible for the chemical analysis of the many samples, and Messrs. Edgar Dervedde and Steve Monahan who were most helpful with their suggestions.

I also wish to take this opportunity to thank Mr. Otto Brudy, Superintendent of the Central Research Shop who helped me in the construction of the equipment. Thanks are due also to Mr. George Ryan, the Chemical Engineering Technician, for his capable help.

The financial support of the Aluminum Company of Canada (ALCAN) who funded the project is gratefully acknowledged. Also, the aid of the National Research Council of Canada by way of Graduate Fellowships is truly appreciated.

TABLE OF CONTENTS

	Page
ABSTRACT	ii
ACKNOWLEDGEMENTS	iii
TABLE OF CONTENTS	iv
LIST OF FIGURES	ix
LIST OF TABLES	xi
I. INTRODUCTION	1
II. LITERATURE SURVEY	5
III. THEORY	10
A. General	10
B. Classification of Solid Fluid Reactions	11
1. Classification Based on the Phases in Which Various Species Appear.	11
2. Classification According to the Manner by which the Reaction Progresses.	12
a. Heterogeneous reactions.	12
b. Homogeneous reactions.	13
c. Reactions accompanying phase changes of solid components or evolution of volatiles.	13
3. Order of Solid-Fluid Reactions.	13
C. Unreacted-Core Shrinking Model.	16
D. Temperature Effects.	23
E. The Abyss.	25

	Page
IV. APPARATUS AND EXPERIMENTAL PROCEDURE	27
A. The Continuous Reactor.	28
1. The Reactor.	28
2. Solids Feeding.	31
3. Acid Feeding.	32
4. Solids Removal.	33
5. The Scrubber.	33
B. Experimental Procedure for the Continuous Reactor Runs.	34
C. The Batch Reactor.	36
D. Experimental Procedure for the Batch Reactor.	37
E. Operational and Equipment Difficulties.	37
1. The Reactor.	38
2. The Solids Feed System.	38
3. Acid Feed System.	40
4. Solids Removal System.	42
5. The Scrubber.	42
V. REACTOR AND KINETIC MODELS	52
A. The Continuous Reactor.	52
B. The Rate Equation.	54
VI. EXPERIMENTAL RESULTS AND ANALYSIS	61
A. Experimental Results.	61

	Page
1. Qualitative Observations.	61
a. Batch reactor.	61
b. The continuous reactor.	62
2. Continuous Reactor Data.	63
3. Batch Reactor Data.	64
B. Analysis of Batch Data.	65
C. Analysis of Continuous Reactor A-Runs.	73
D. Fitting the Arrhenius Equation to the Batch and Continuous Reactor Data Simultaneously.	77
E. Predicted Conversion Errors.	79
F. The Factorial Experimental Design.	84
1. Planning the Design.	85
2. Analysis of Factorial Runs Data.	89
VII. DISCUSSION OF RESULTS	151
A. The Results.	151
1. The Batch Reactor.	151
2. The Continuous Reactor.	152
B. Interpretation of Results.	155
1. Mixing in the Continuous Reactor.	155
a. The effect of calcium carbonate content.	155
b. The effect of mixing rate.	158

	Page
2. Effect of Fluorspar Size Reduction.	159
C. Interpretation of Rate Equations.	161
D. Comparison of Results to Previous Works.	167
1. The Work of Ostrovskii and Amirova.	167
2. The Works of Gnyra and Menard and Whicher.	168
E. Thermal Effects.	169
F. The Silica Reaction.	170
VIII. CONCLUSIONS	172
BIBLIOGRAPHY	175
NOMENCLATURE	179
APPENDICES	185
I. MODEL DISCRIMINATION AND DETERMINATION OF RATE CONSTANTS	185
A. Using Batch Data.	185
B. The Continuous Reactor Data.	187
1. Initialization.	190
2. Linear Approximation and Steepest Descent.	192
II. THERMODYNAMIC CONSIDERATIONS.	204
III. ANALYSIS OF THE DATA OF PUXLEY AND WOODS..	208
IV. SAMPLE TREATMENT AND MASS BALANCES	210
A. Sample Treatment.	212
B. Mass Balances .	222

C. Discussion.	228.
D. Nomenclature for Mass Balance Program.	231
VITA AUCTORIS	281

LIST OF FIGURES

		Page
III.1	Schematic Diagram of Concentration Profile for the Unreacted-Core Shrinking Model	17
IV.1	Schematic of Reactor Assembly	45
IV.2	Reactor Details	46
IV.3	Reactor Mixers	47
IV.4	Reactor Interior Showing Position of Central and Rear Flange Thermocouples	48
IV.5	Solids Metering Hopper Assembly	49
IV.6	Metering Auger	50
IV.7	Solids Out Auger and Solids Out Port	51
V.1	A Typical Tracer Response	58
VI.1	Batch Reactor Conversion-Time Data and Conversion Curves Predicted by the Least Squares Fit of Model 6	97
VI.2	Batch Reactor Conversion-Time Data and Conversion Curves Predicted by the Least Squares Fit of Model 7	98
VI.3	Batch Reactor Conversion-Time Data and Predicted Conversion Curves from the Least Squares Fit of Model 9	99
VI.4	Batch Reactor Conversion-Time Data and Conversion Curves Predicted by the Least Squares fit of Model 10	100
VI.5	Batch Reactor Conversion-Time Data and Conversion Curves Predicted by the Least Squares Fit of Model 11	101
VI.6	Arrhenius Plot of Apparent Rate Constants of Model 9 with Non-Linear Equation Lines of Best Fit	102

		Page
VI.7	Arrhenius Plot of Apparent Rate Constants of Model 9 with Linearized Equation Lines of Best Fit	103
VI.8	Arrhenius Plot of Apparent Rate Constants of Model 10 with Non-Linear Equation Lines of Best Fit	104
VI.9	Arrhenius Plot of Apparent Rate Constants of Model 10 with Linearized Equation Lines of Best Fit	105
VI.10	Arrhenius Plot of Apparent Rate Constants of Model 11 with Non-Linear Equation Lines of Best Fit	106
VI.11	Arrhenius Plot of Apparent Rate Constants of Model 11 with Linearized Equation Lines of Best Fit	107
VII.1	Reacting Scheme of Lumps	160
AIV.1	Initial Solids Out Samples Handling Scheme	245
AIV.2	Modified Solids Out Samples Scheme	246

LIST OF TABLES

Page

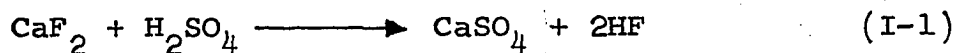
V.1	List of Reaction Models	59
VI.1	Fluorspar Compositions	108
VI.2	Run Parameters for the Continuous Reactor Runs with Mixers at 10 r.p.m., Using Fluorspar Newfluor-A	109
VI.3	Run Parameters for the Continuous Reactor Factorial Runs	110
VI.4	Fractional Age Distribution of Solids Leaving Reactor $(E(t)\Delta t)_i$	112
VI.5	Batch Conversion-Time Data	116
VI.6	Least Squares Analysis of Models Using Batch Data	117
VI.7A	Least Squares Fit of the Batch Data Apparent Rate Constants to the Non-Linear Arrhenius Equation	118
VI.7B	Least Squares Fit of the Batch Data Apparent Rate Constants to the Linearized Arrhenius Equation	119
VI.8	Average Conversion of Spar and Apparent Rate Constants for A-Runs	120
VI.9	Least Squares Fit of the Continuous Reactor Data Apparent Rate Constants to the Linearized Arrhenius Equation	121
VI.10	Least Squares Fit of the Continuous Reactor Data Apparent Rate Constants to the Linearized Arrhenius Equation	122
VI.11	Least Squares Fit of the Continuous Reactor and Batch Reactor Data Apparent Rate Constants to the Non-Linear Arrhenius Equation	123

VI.12	Least Squares Fit of the Continuous Reactor and Batch Reactor Apparent Rate Constants to the Linearized Arrhenius Equation	124
VI.13	Table of Residuals for the Least Squares Fit of the Apparent Rate Constants of the A-Runs of the Continuous Reactor to the Non-Linear Arrhenius Equation	125
VI.14	Table of Residuals for the Least Squares Fit of the Apparent Rate Constants of the A-Runs of the Continuous Reactor to the Linearized Arrhenius Equation	128
VI.15	Table of Residuals for the Least Squares Fit of the Apparent Rate Constants of the A-Runs of the Continuous Reactor and the Batch Reactor to the Non-Linear Arrhenius Equation	131
VI.16	Table of Residuals for the Least Squares Fit of the Apparent Rate Constants of the A-Runs of the Continuous Reactor and the Batch Reactor to the linearized Arrhenius Equation	134
VI.17	Predicted Conversions	137
VI.18	Observed Conversion of CaF_2 and Apparent Rate Constants of Runs 1F to 10 F	140
VI.19	Natural Logarithm of the Apparent Rate Constants with the Coded Factors	141
VI.20	Mean Differences of $\ln k$	142
VI.21	Analysis of Variance	143
VI.22	Regrouping the F-Runs	144
VI.23	Least Squares Estimate of the Parameters of Equation (VI-42) from the Factorial Experiments Apparent Rate Constants	145

	Page	
VI.24	Least Squares Estimate of the Parameters of Equation (VI.42) Using the Apparent Rate Constants of the A and F runs as well as the Batch Reactor	146
VI.25	Analysis of Residuals for Least Squares Fit of Equation (VI-42) to all the Apparent Rate Constants	147
VI.26	Predicted Conversions	150
AII.1	Thermodynamic Data of Reactants and Products	206
AII.2	Thermodynamic Quantities for the Principle Reactions Occuring in the Reactor	207
AIII.1	Reaction Constants for Puxley's Data Assuming Zero Order Kinetics	209
AIV.1	Utility of Sample Analysis	247
AIV.2	Analysis of Synthetic Samples	249
AIV.3	Results of Solids Out Sample Analysis	250
AIV.4	Scrubber Liquor Samples Analysis	252
AIV.5	Gas Transfer Line Sludge	256
AIV.6	SiO ₂ Content of Solids, of Solids out Sample Where Only The Scrubber Effluent Analysis was Done	257
AIV.7	Mass Balances and Conversions Using the Reported Solids Out Analysis Assuming CaCO ₂ Formation During Filtration; No Solids Out Flow Correction	259
AIV.8	Mass Balances and Conversions Using Reported Solids Out Analysis Assuming CaCO ₃ Formation During Filtration; Solids Out Flow Corrected to Force a Sulfate Balance	262

I INTRODUCTION

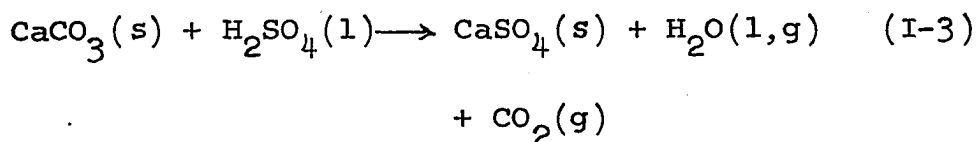
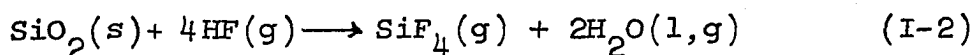
Hydrofluoric acid was produced for the first time about 200 years ago by the treatment of fluorspar (calcium fluoride) with concentrated sulfuric acid according to the endothermic reaction



Industrial manufacture of HF began in 1931 and HF has since become an important chemical product. Some of its uses are in the manufacture of fluorinated hydrocarbons (freons), in the manufacture of fluorocarbons and their polymers (Teflon or Kel-F), as a catalyst and reaction medium for the alkylation of olefins, etc. However, the main use for HF is in the manufacture of cryolite (Na_3AlF_6), which is used as electrolyte in the manufacture of aluminum.

Hydrofluoric acid is largely produced by contacting fluorspar with concentrated sulfuric acid (93-98% by weight) in heated, stationary or rotary, steel reactors 50-60 feet long in which the HF and CaSO_4 are produced and removed continuously. In stationary reactors mixing is accomplished with internal paddles.

Crude fluorspar varies in its calcium fluoride content from 50 to 90%, and after grinding to the desired fineness, must be passed through a flotation process to remove undesirable impurities. The chief impurities remaining in the flotated spar are silica (SiO_2) and calcite (CaCO_3) in concentrations of 1 - 3 % and 1 - 5% respectively and lead to the side reactions.



The two reactions, of course, reduce the yield of HF as well as cause contamination of the gaseous stream.

The chief difficulties with this method of HF manufacture are:

- (1) poor mixing of the reactants upon initial contact
- (2) high corrosion of the reactor walls and mixing paddles
- (3) inefficient heat transfer through the reactor walls due to deposition of scale.

Many attempts have been made to enhance the mixing and heat transfer and to reduce the corrosion of the reactor. While they are not discussed here one may refer

to the patents in the Bibliography for details.

The present state of the art of hydrogen fluoride production from fluorspar and sulfuric acid is largely based upon qualitative and often conflicting evidence. No data are available on the effects of temperature, mixing rate, and fluorspar impurities on the reaction.

Lump formation within the reactor has been observed to affect the HF production to a significant degree (refer to patents in Bibliography). Studies of the reaction under batch conditions undertaken thus far (24,26) do not account for this lump formation due to the small quantities of reactants used in those studies.

The scope of this study was to estimate the effect of

- (a) temperature
- (b) mixing speed
- (c) moles of acid per mole of CaF_2 added
- (d) fineness of the fluorspar
- (e) CaCO_3 content of the spar

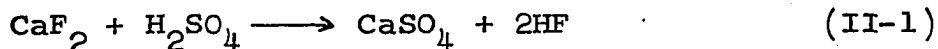
on the reaction, by carrying out experimentation using a stirred, continuously fed reactor, under isothermal conditions. The data of the continuous reactor were augmented by carrying out additional experimentation in

a batch reactor also maintained at isothermal conditions. Sufficient quantities of reactants were added to the batch reactor so as to make lump formation possible.

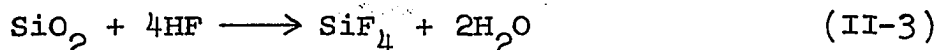
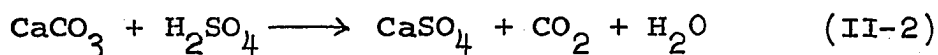
The approach was to obtain batch conversion-time data and analyse this data with the aim of obtaining a suitable rate model. The rate model found to suitably correlate the batch data was then to be used to analyse the continuous reactor data in order to determine the apparent rate constants for each run, to determine the effects of temperature, mixing rate, spar fineness and the CaCO_3 content of the fluorspar.

II. LITERATURE SURVEY

As indicated in the previous chapter, the major reaction that occurs upon contacting fluorspar with sulfuric acid is

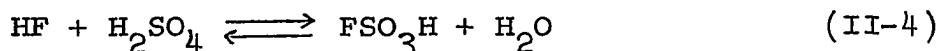


Several side reactions that occur simultaneously are



These reactions are due to impurities present in the flotated fluorspar.

Traube and Reubke (32) found that an additional reaction can occur in the mix according to the equation



Data on the reaction kinetics of reaction (II-1), (II-2) and (II-3) are scarce.

Puxley and Woods (26) obtained batch data in the temperature range 125-250°C, using a platinum crucible while stirring the mix with a platinum bar. However, their data suffer because of a lack of temperature control. They also encountered difficulties in mixing

the reaction mass.

Rowe (27) in 1955, analysed the data of Puxley and Woods and hypothesized a possible kinetic model of the form

$$R_A = 1 - \frac{2}{\sqrt{2\pi}} \int_0^s \exp \left[-\frac{1}{2} s^2 \right] ds$$

(II-5)

$$s = \frac{1}{\sqrt{t} (a + bt^n)}$$

where R_A represents the rate of disappearance of the acid or spar on a molar basis, and a , b and n are parameters. Rowe was inclined to believe that the diffusion of H_2SO_4 to the reacting interface controls the reaction rate. However, he stressed that the equation was identical for the case where diffusion of HF away from the reacting interface is the controlling step.

More recently Ostrovskii and Amirova (24) conducted batch experiments on the fluorspar-sulfuric acid reaction by suspending a platinum dish in a steel tube furnace. The furnace temperature was maintained at $\pm 2^\circ C$ of the desired temperature. Dry air was passed through the tube at a rate of 5 litres per hour. The extent of reaction was determined by following weight loss with

time. They used 99.2% sulfuric acid and fluorspar of 98% purity. The temperature range in their investigation was 85 - 145°C. Ostrovskii and Amirova concluded that in this temperature range, the rate of disappearance of CaF_2 is controlled by the chemical reaction at the unreacted core surface. They fitted their data to the model

$$(1 - x_B)^{-2/3} - 1 = \frac{kt}{R_p} \quad (\text{II-7})$$

Where x_B is the fractional degree of conversion; t is the reaction time (min.); k is the rate constant (cm/min.); R_p is the original diameter of the reacting particle (cm). If the particle size of the fluorspar is maintained constant equation (II-7) reduces to the form

$$(1 - x_B)^{-2/3} - 1 = k^1 t \quad (\text{II-8})$$

where k^1 is the apparent rate constant (min.^{-1}).

Equation (II-7) was derived from the pseudo steady-state unreacted shrinking core model to be discussed in

Chapter II. Ostrovskii and Amirova found that $k^1 = 7.75 \times 10^{10} \exp \left[-\frac{20800}{RT} \right]$ (min.^{-1}) in the range

of 85 - 105°C and $k^1 = 1.38 \times 10^4 \exp - \frac{9200}{RT}$ (min.⁻¹) in the range of 105-145°C. Differences in the values of the activation energy were attributed to the lack of formation of FSO₃H above 100°C

Blumberg (4) and Blumberg and Starvinou (5) as well as Palmer, (25) in carrying out various experimental studies of the reaction of silica particles with aqueous solutions of hydrofluoric acid, concluded that the reaction may be restricted by any diffusion process and can be described by the rate model

$$R_A = k_o \exp \left[-\frac{\Delta E}{RT} \right] S[HF] . \quad (\text{II-9})$$

where S is the exposed area of the solids, k_o the frequency factor and [HF] the concentration of HF in the reacting solution.

Unfortunately, information on the silica reaction for the fluorspar-acid system is limited to qualitative speculation. Gnyra and Whicher (16) in a qualitative experimental study observed that the state of primary mix was an important criterion for the silica reaction. The longer the initial mix remains wet the greater was the extent of conversion of the silica.

Gnyra (15) carried out a qualitative study on the effects of the CaCO_3 content in the fluorspar. He observed an enhancement of acid penetration into the spar with increased CaCO_3 content. Menard and Whicher (21) in a semiquantitative study found that CaCO_3 enhances the setting rate of the reaction mass thus impedes further mixing of the reactants.

Traube and Lange (31) report a study on the effects of temperature on the evolution of hydrogen fluoride from the equimolar mixtures of 98% H_2SO_4 and 99.7% fluorspar. They found that after one hour of contact time at 60°C approximately 12% of the HF generated reacted with H_2SO_4 to produce FSO_3H . For identical contact times the amount of FSO_3H formation decreased to 7% at 80°C and to nil at 100°C .

Traube and Lange further point out that FSO_3H formation is detrimental to the reaction of the spar with the acid since the monobasic fluosulfonic acid takes the place of the dibasic more reactive sulfuric acid, thus retards the progress of the reaction.

III. THEORY

A. General

In spite of the unquestionable importance of solid-fluid reactions relatively few studies have been made on the chemical kinetics and transfer rates of mass and energy in heterogeneous non-catalytic systems. This is partially due to the intricate relationships among the rates of chemical reaction and the rates of mass and energy transfer. Even in an isothermal reaction system the overall reaction rates are influenced not only by the rate of chemical reaction occurring in or at the surface of the solid, by the mass transfer rates of fluids through the solid and across the fluid-film surrounding the solid, but also by factors such as solid reactivity, crystallite orientation, crystallite size, surface characteristics, impurities, etc.

A typical solid-fluid reaction may be considered to occur through the following steps: (1) diffusion of the fluid reactants across the fluid film surrounding the solid, (2) diffusion of the fluid reactants through a porous layer, (3) adsorption of the fluid reactants at the solid reactant surface, (4) chemical reaction with the solid surface, (5) desorption of the fluid products from the

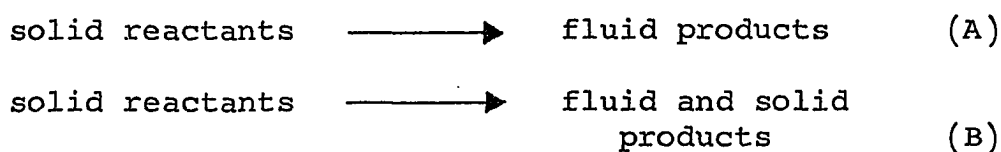
solid reaction surface, and (6) diffusion of the product away from the reaction surface through the solid porous media and through the fluid film surrounding the solid. In some particular systems the steps may be somewhat altered. Since these steps occur consecutively, if any one of them is much slower than the others that step becomes the controlling or rate-determining step. However, the majority of solid-fluid reactions are apparently influenced simultaneously by more than one step.

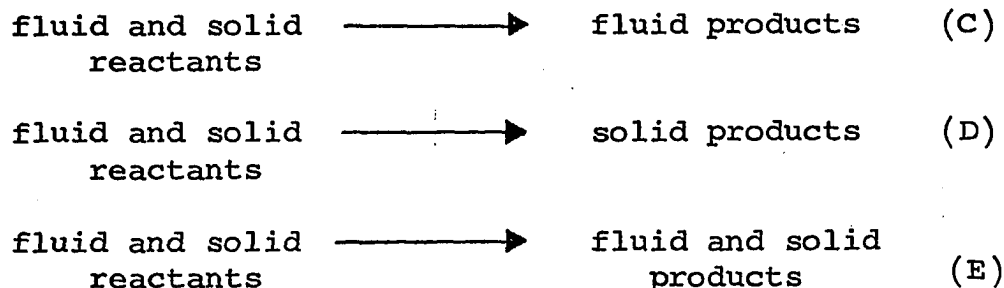
A rigorous treatment of the phenomenon seems unattainable even for the solid of simplest geometry. Besides, a great number of difficulties exist in practical systems, such as the changing size and shape of the solids during the reaction and formation of product around the solid reactant which may crack or ablate.

B Classification of Solid-Fluid Reactions

1. Classification Based on the Phases in Which Various Species Appear

Noncatalytic fluid-solid reactions may be characterized by one of the following schemes:





Examples of each type of reaction may readily be found in industry.⁽³⁴⁾ The reaction of sulfuric acid with fluorspar is of type E.

2. Classification According to the Manner by Which the Reaction Progresses.

Heterogeneous noncatalytic fluid solid reactions may also be classified by the manner by which the chemical reaction occurs, the internal structure of the solid, the geometry, and the relative velocities of chemical reactions and diffusion of the reactants and products are four of the many possible parameters that may be considered in following the manner of occurrence.

a. Heterogeneous reactions. When the porosity of the unreacted solid is so small as to make it impervious to the fluid reactants, the reaction will occur at the surface of the solid or at the interface between the unreacted solid and the porous product layer. Also, when the chemical reaction is very rapid and the diffusion

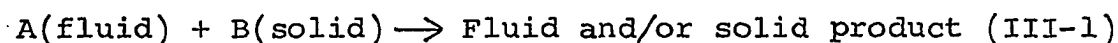
sufficiently slow, the zone of reaction is narrowly confined to the interface between the unreacted solid reactant and the product.

b. Homogeneous reactions. In many cases the solid contains enough voidage to allow free passage of the fluid reactants and products, and the solid reactants are distributed homogeneously throughout the solid phase. In this case one can reasonably consider that the reaction between fluid and solid phases occurs homogeneously throughout the solid phase. This case has been treated thoroughly by Wen (34).

c. Reactions accompanying phase changes of solid components or evolution of volatiles. In some cases, prior to the chemical reaction the solid changes phase because of poor heat conduction in an exothermic reaction. The solid may melt or sublime prior to or during contact with the fluid. In such cases a homogeneous vapor phase reaction takes place either on the outside of the solid or in the solid product layer formed around the unreacted solid.

3. Order of Solid-Fluid Reactions

Consider the following isothermal equimolar non-catalytic reaction:



If diffusion rates through the fluid-film and porous solid layer are very fast the overall rate of solid-fluid reaction is solely determined by the inherent chemical reactivity of the solid and fluid reactants. In the case of a gaseous fluid one can also quantitatively describe the mechanism on the basis of the Langmuir adsorption isotherm (31). However the resulting equations involve more than two arbitrary constants and often as many as seven (34). The resulting equations, although desirable from a theoretical viewpoint, are in practice difficult to handle.

Provided no extrapolation beyond the range investigated is allowed, and the surface phenomenon controls the rate of the solid-fluid reaction one may often use an n^{th} order rate model to fit the data. Based on adsorption isotherms the order may vary from zero to two depending on whether the gas reactant is strongly or weakly adsorbed (34). Experimental studies indicate many gas solid reactions to have this range of order of reactions, depending on conditions such as reactant activity, pressure, temperature activity, etc. (34)

Thus the rate of reaction of fluid component A, r_A and for solid reactant S, r_S can be represented as

$$r_A = ar_S = - ak_S C_S^m C_A^n = - ak_v C_S^m C_A^n \quad (\text{III-2})$$

where a is the stoichiometric coefficient (the number of moles of fluid component A that will react with 1 mole of solid reactant S, and m and n are the order of reaction with respect to solid reactant S and fluid reactant A respectively. Depending upon particular conditions the rate may be expressed in terms of surface area or volume. The units of r_A or r_S depend on the rate expression, namely, if k_S is used the rate is in moles per unit area per unit time, whereas if k_V is used the rate is in moles per unit volume per unit time.

In many instances the concentration of solid reactant may be considered constant so that the reaction rate expression reduces to

$$r_S = k'_S C_A^n \quad (\text{III-3})$$

where $k'_S = k_S C_S^m$

C. Unreacted-Core Shrinking Model

Consider the case where a fluid reacts with the solid producing a fluid and a porous solid product or an ash layer according to equation (III-1). The porous product shall hitherto be referred to as the ash layer. The unreacted solid is impervious to fluid A because it is densely packed but the porous product allows fluid A to diffuse in, and the fluid product to diffuse out.

Consider a spherical particle having an initial radius R_p being reacted by A. Initially the reaction occurs on the outside surface of the particle but as the reaction proceeds the reaction surface will withdraw into the interior of the solid phase. The external radius is considered to remain the same. This assumes that no deformation of the ash layer occurs and that the bulk density of the ash is the same as that of the solid reactant. The fluid reactant A must first move through various layers of resistance prior to reaching the unreacted core. Figure III.1 illustrates the resistances as well as the concentration profile within the particle. Referring to Figure III.1 C_{Ao} , C_{As} , and C_{Ac} are designated as the fluid reactant concentrations in

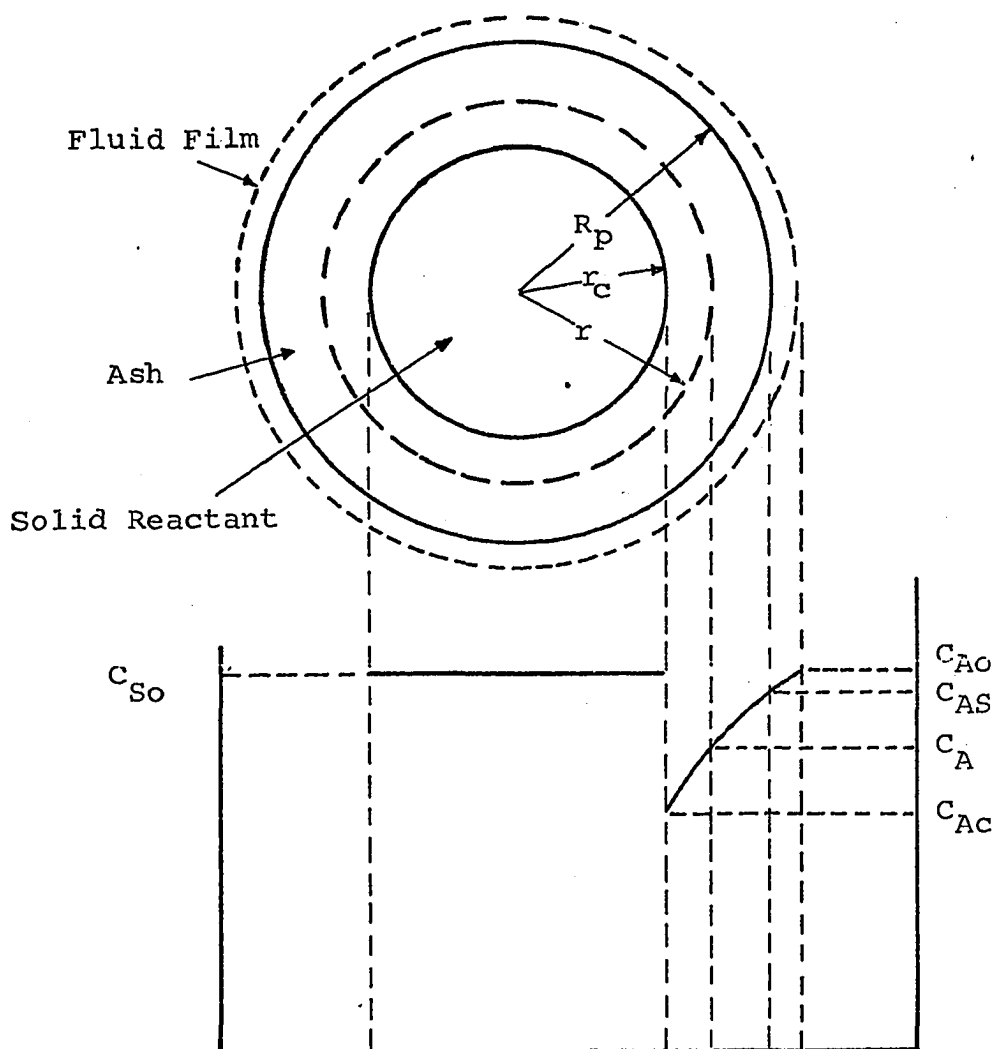


Figure III.1, Schematic Diagram of Concentration Profile for the Unreacted-Core Shrinking Model.

the bulk stream, at the particle surface, and at the surface of the core, respectively R_p , r_c and r are radii of the particle, of the unreacted core and at any point in the ash layer respectively.

A fundamental equation relating the material balance of component A may be written as

$$\epsilon \frac{\partial C_A}{\partial t} = D_{eA} \left(\frac{\partial^2 C_A}{\partial r^2} + \frac{2}{r} \frac{\partial C_A}{\partial r} \right) \quad (\text{III-4})$$

$$R_p > r > r_c$$

The boundary conditions for the spherical particles are:

at the solid particle surface R_p

$$D_{eA} \left(\frac{\partial C_A}{\partial r} \right)_{R_p} = k_{mA} (C_{Ao} - C_{As})$$

at the moving interface, r_c

$$D_{eA} \left(\frac{\partial C_A}{\partial r} \right)_{r_c} = a k_s C_{Ac} \quad (\text{III-5})$$

and $- D_{eA} \left(\frac{\partial C_A}{\partial r} \right)_{r_c} = a C_{So} \left(\frac{\partial r_c}{\partial t} \right)$

where k_{mA} is the mass transfer coefficient of component A

from the bulk of the fluid phase to the solid surface across the film, and C_{S_0} is the solid reactant concentration in the unreacted core which is assumed constant, ϵ is the voidage of the porous layer of the particle and D_{eA} is the effective diffusivity coefficient of the fluid reactant in the ash layer at $t = 0$, $r_c = R_p$

The reaction at the solid surface is assumed to be first order with respect to the fluid reactant A and zero order with respect to the solid reactant.

Analytical solutions to equation (III-4) using the boundary conditions of equation (III-5) are difficult except in a few special cases (34). It is customary to let $\epsilon(\partial C_A / \partial t) = 0$ and obtain an approximate solution. This technique is known as the pseudo steady state solution and is reasonably accurate in most solid-gas reaction systems except for systems at extremely high pressures and very low solid reactant concentrations. However, for solid-liquid systems the error involved becomes excessive unless the liquid reactant concentration is very low (3,34).

If we let $\partial C_A / \partial t = 0$ in equation (III-4) it becomes

$$0 = D_{eA} \left(\frac{\partial^2 C_A}{\partial r^2} + \frac{2}{r} \frac{\partial C_A}{\partial r} \right) \quad R > r > r_c \quad (\text{III-6})$$

and using the boundary conditions the solution is readily

obtained to yield a concentration profile:

$$\frac{C_A}{C_{Ao}} = \frac{\left(1 + \frac{D_{eA}}{a k_s r_c}\right) \frac{1}{r_c} - \frac{1}{r}}{\left(1 + \frac{D_{eA}}{a k_s r_c}\right) \frac{1}{r_c} - \left(1 - \frac{D_{eA}}{k_{mA} R_p}\right) \frac{1}{R_p}} \quad (\text{III-7})$$

The time required for the particle to reduce the unreacted core from R_p to r_c is given by

$$t = \frac{a R_p C_{So}}{C_{Ao}} \left\{ \frac{1}{3} \left(\frac{1}{k_{mA}} - \frac{1}{D_{eA}} \right) \left(1 - \frac{r_c^3}{R_p^3} \right) + \frac{1}{a k_s} \left(1 - \frac{r_c}{R_p} \right) + \frac{R_p}{2 D_{eA}} \left(1 - \frac{r_c^2}{R_p^2} \right) \right\} \quad (\text{III-8})$$

If one wishes to reduce these equations to the usual reaction rate form, one considers the number of moles of A disappearing per unit time, M_A , which can be expressed as

$$M_A = 4\pi R_p^2 N_{As} = 4\pi r_c^2 N_{A,ash} = 4\pi r_c^2 N_{Ac}$$

and

$$M_A = 4\pi C_{Ao} \left/ \left\{ \frac{1}{R_p^2 k_{mA}} + \frac{1}{r_c^2 a k_s} + \frac{1}{D_{eA}} \left[\frac{1}{r_c} - \frac{1}{R_p} \right] \right\} \right. \quad (\text{III-9})$$

In order for the fluid to react at the surface of the

core it must diffuse through the film and ash layer to the reacting surface. The three terms in the denominator of equation (III - 9) represent the three resistances in series for the reaction considered.

If the fluid-film resistance is much greater than that of the ash diffusion and surface reaction it is said to be a film resistance controlled phenomenon and equation (III - 9) reduces to

$$-\frac{dr_c}{dt} = \frac{a k_{mA} C_{Ao}}{C_{So}} \left(\frac{R_p}{r_c} \right)^2 \quad (\text{III - 10})$$

When ash diffusion controls then

$$-\frac{dr_c}{dt} = \left(\frac{a D_{eA} C_{Ao}}{C_{So} r_c} \right) \left(\frac{1}{1 - \frac{r_c}{R_p}} \right) \quad (\text{III-11})$$

When chemical reaction controls

$$-\frac{dr_c}{dt} = \frac{a k_s C_{Ao}}{C_{So}} \quad (\text{III-12})$$

In terms of the fractional conversion of B.

$$x_B = 1 - \frac{\left[\frac{4}{3} - \pi \frac{r_c^3}{R_p^3} \right]}{\left[\frac{4}{3} - \pi \frac{R_p^3}{P} \right]} = 1 - \left(\frac{r_c}{R_p} \right)^3 \quad (\text{III-13})$$

equations (III-10)(III-11) and (III-12) may be expressed as follows:

$$\frac{dx_B}{dt} = \frac{3a k_m C_{Ao}}{C_{So} R_p} \quad (\text{III-14})$$

for film diffusion controlling

$$\frac{dx_B}{dt} = \frac{3a D_{eA} C_{Ao}}{C_{So} R_p} \frac{(1 - x_B)^{1/3}}{1 - (1 - x_B)^{1/3}} \quad (\text{III-15})$$

for ash diffusion controlling, and

$$\frac{dx_B}{dt} = \frac{3a k_s C_{Ao}}{C_{So} R_p} (1 - x_B)^{2/3} \quad (\text{III-16})$$

when chemical reaction controls.

The above derivations are based on a system where the concentration of the fluid reactant is constant. In some instances this reactant concentration decreases in proportion to the degree of conversion of the solid reactant. Or

$$C_A = C'_{So} (A - ax_B) \quad (\text{III-17})$$

$$\text{and } A = C'_{Ao} / C'_{So} \quad (\text{III-18})$$

where C'_{So} is now the initial solid concentration on a fluid concentration basis (moles of solid reactant initially present per volume of fluid), and C'_{Ao} is the initial fluid

reactant concentration.

Applying equation (III-17) to equations (III-14), (III-15) and (III-16) one obtains

$$\frac{dx_B}{dt} = \frac{3a k_{ma} C'_{So}}{C_{So} R_p} (A - ax_B) \quad (\text{III-19})$$

when film diffusion is controlling,

$$\frac{dx_B}{dt} = \frac{3aD_{eA} C'_{So}}{C_{So} R_p^2} \frac{(A - ax_B) (1 - x_B)^{1/3}}{1 - (1 - x_B)^{1/3}} \quad (\text{III-20})$$

for the case where ash diffusion is controlling, and

$$\frac{dx_B}{dt} = \frac{3a k_s C'_{So}}{C_{So} R_p^2} (A - ax_B) (1 - x_B)^{1/3} \quad (\text{III-21})$$

for a chemical reaction controlled reaction.

D. Temperature Effects

The Boltzmann law describing the energy distribution of molecules in a substance establishes the character of the relationship between the rate of a physical or a chemical process and temperature.

$$N_i = \frac{N}{Z} e^{-E_i/kT} \quad (\text{III-22})$$

where N is the total number of molecules, N_i is the number of molecules with energy E_i , k is the Boltzmann constant and

Z is the distribution function.

The form of the equation for the distribution of the molecules in terms of energy will depend on the form of the problem, but the distribution will always take the form containing the Boltzmann factor $e^{-Q/RT}$ (9). Accordingly, the constant for the reaction rate involving solids is expressed by

$$K = Ae^{-Q/RT} \quad (\text{III-23})$$

in which the value of A and Q will depend on the limiting process of the reaction.

If the process is limited by the chemical reaction itself, the pre-exponential multiplier A is equal to pZ_0 , p being the probability or steric factor and Z_0 the number of binary encounters between reacting particles; Q is the energy of activation of the chemical action and it depends on the bond forces between the particles of each of the original species and the repulsive forces between the approaching particles (for heterogeneous processes which include reactions in the crystalline mixtures Q is the apparent energy of activation).

In a process limited by the diffusion of a species, the velocity of reaction is determined by the value of the diffusion coefficient which may often be expressed in the form

$$D_{eA} = Ae^{-Q/RT}$$

(III-24)

where A now depends on the frequency of oscillations of the diffusing species and Q is the energy of motion of the diffusing species.

In any case, the greater the value of Q, the activation energy, the greater the change in the process rate with changes in temperature. In diffusion controlled processes, the activation energy will be relatively low yielding velocity changes of 10-40% with temperature changes of 10°C. When the process is limited by the chemical step the activation energies will be relatively high and a 10°C rise in temperature will increase the velocity by 2-4 times or more⁽⁹⁾.

E. The Abyss

To reiterate, the shrinking core model is a reasonable description of the phenomenon when a fluid reactant reacts with an impervious spherical solid producing a fluid reactant and a solid ash. The particle radius remains constant and does not deform during the reaction. In order for the pseudo steady state equations to remain valid, the fluid reactant should be in relatively low concentrations.^(3,34)

As is true of many fairy tales, the real situation is far from the ideal that one would wish it to be.

No attempts have been made here to account for heat transfer effects. For a highly exothermic reaction the interior of the particle would increase in temperature while for an endothermic reaction cooling would occur. This problem has been treated elsewhere^(9,28) but the resulting equations are much too bulky to consider here.

Another problem which has received little or no attention is the treatment of non-spherical particles. As well, very little treatment has been accorded to changes in the surface area of the unreacted core as pointed out by Cannon and Denbigh⁽¹⁰⁾. In the latter phenomenon, if the reaction rate per unit area of core decreases with greater conversion, the surface non-uniformity will tend to be smoothed out, because the rate of reaction will be less at a point of deeper penetration. If the rate of reaction per unit area remains constant, the non-uniformity will be constant or increase.

IV APPARATUS AND EXPERIMENTAL PROCEDURE

Because the reaction of fluorspar with sulfuric acid may be strongly affected by imposed dynamic forces, it was necessary that the reaction be studied under dynamic conditions similar to those imposed by the industrial process. More specifically, mixing cannot be properly accounted for in a batch reacting system, because of the nature of the reacting material.

Furthermore, because the reaction is highly endothermic, the temperature of the reacting mass is difficult to control in a batch process unless very small quantities are used. But with very small quantities of reactants, one cannot but help avoiding the lump formation which may play a significant role in the reaction.

At the same time, the usefulness of the continuous reactor data have limitations if they are not isothermal and the feed rates are not constant.

In the construction of the continuous reactor assembly attention was focussed towards achieving the following:

- (a) Temperature was to be maintained constant at all reactor points.
- (b) The acid and feed rates had to be accurate.

- (c) Solids entrainment in the product gases was to be kept to a minimum.
- (d) An accurate measure of the amount of hydrogen fluoride produced had to be obtained.
- (e) The mixing rate was to be constant during any run.

Figure IV.1 is a schematic diagram of the continuous reactor assembly.

As discussed in section VI the data of the continuous reactor are limited in their usefulness for testing kinetic models. To supplement the continuous reactor data it was necessary to carry out batch experiments.

In the construction of the batch reactor, all the attention was focussed towards temperature control.

A. The Continuous Reactor

1. The Reactor

The reactor was a 5 inch diameter, flanged, cold rolled steel pipe 14 inches long. A semicylindrical heater along the reactor bottom was used to heat the main reactor body. Flange heaters, on the flange perimeters, were used to eliminate axial temperature variations. Figure IV.2 shows the details of the reactor.

The semicylindrical heater was $5 \frac{3}{4}$ inch I.D. and was 12 inches long, fitting snugly between the reactor flanges.

It was rated at 2300 watts at 230 volts.

The flange heaters were of 9 inch I.D. and 1 1/2 inches wide. Both heaters were rated at 1225 watts at 115 volts.

A proportional controller using the central thermocouple as sensor served to control the semicylindrical heater. The flange heaters were manually controlled by way of variable transformers.

The reactor contents were mixed by 1/8 inch thick, 1 inch wide, paddles constructed from old lawnmower blades. A photograph of the mixers is provided in Figure IV.3. Some space between the two sets of paddles was necessary to provide clearance for the central thermocouple.

The forward paddles were coated with a hard stellite alloy to prevent excessive corrosion by the environment.

To prevent undue fouling of the reactor walls, which would hinder heat transfer, the clearance between the paddle edges and the reactor wall was kept to as low a value as possible.

A 1/4 h.p. electronically controlled D.C. motor provided the drive for the mixers. The range of mixing could be varied from 1 to 44 r.p.m. with an accuracy of roughly 2%. To achieve the low r.p.m. values a 60 to 1 gear reducer was necessary. The high reduction provided for a very powerful mixing.

Three chromel-alumel thermocouples were used to measure temperatures at various points in the reactor. These were ceramic insulated thermocouples protected by a stainless steel sheath of $1/8$ inch diameter. To prevent error in temperature measurement due to stray currents or stray magnetic fluxes, the thermocouple junctions were ungrounded. One eighth inch NPT adjustable compression fittings were used to fasten the thermocouples to the reactor walls.

The first thermocouple was inserted through the forward flange $1\ 3/4$ inches above the reactor bottom. It extended approximately $3/4$ inches into the reactor. It was installed so as not to interfere with the stirrers.

The second thermocouple was inserted through the top of the reactor and extended to about $1/8$ in above the reactor bottom. This thermocouple was held in place by a $3/8$ inch diameter slotted stainless steel rod. This rod does not interfere with the thermocouple reading as illustrated in the photograph in Figure IV.4. The restraining rod prevented the thermocouple from becoming fouled in the mixer paddles.

The third thermocouple was inserted through the rear flange and its position is also illustrated in Figure IV.4.

A Honeywell multipoint strip chart recorder measured and recorded the temperatures.

All the thermocouples used were checked for accuracy by immersion into boiling distilled water and noting the temperature response.

2. Solids Feeding

Fluorspar was fed to the reactor through a double hopper arrangement. The first hopper, as illustrated in Figure IV.5, was equipped with a $3/8$ inch diameter helical auger. The auger was driven by an electronically controlled variable speed, $1/6$ h.p. D.C. motor. The auger rotation rate determined the rate of spar flow.

As shown in Figure IV.6, a 5 inch long mixing auger pushed the solids toward the feeding tube where it was carried off by the smaller auger. However, unless further mechanical aid was provided, tunneling occurred, producing erratic or no flow. To overcome this, two 3 inch diameter variable speed stirrers were installed in the hopper to maintain the powder in a semifluid state.

The powder out of the metering auger fell into a second hopper equipped with a constant speed $5/8$ inch diameter constant speed auger. This auger, similar to the solids out auger shown in Figure IV.7, had a substantially higher capacity than the metering auger, and easily pushed all of the powder falling into this second hopper into the reactor.

The accuracy of the spar feeding system was usually better than 1%.

3. Acid Feeding

Sulfuric acid was pumped by means of an electronically controlled variable speed Masterflex[®] tubing pump. The pump tubing was of Viton but the rest of the line was 1/4 inch teflon tubing. A rotameter was used to measure the flow which was controlled by the r.p.m. of the pump.

The viscosity of concentrated sulfuric acid is highly dependent on temperature. This meant that day to day temperature variations caused deviation of the rotameter calibration, which is highly dependent on the fluid viscosity. To overcome this problem, it was necessary to insure that the temperature of the acid as it entered the rotameter be constant.

To achieve constant temperature, the acid was passed through a glass coil immersed in a constant temperature bath. The bath temperature was controlled so as to maintain the desired temperature (about 39°C) at the rotameter entrance. A thermometer with 0.1°C graduations was installed at the rotameter entrance to indicate the acid temperature.

The teflon tubing between the rotameter and the reactor

was wrapped with heating tape to heat the acid to approximately 200°F prior to its entry into the reactor.

The accuracy of the acid feeding was better than 1 per cent.

4. Solids Removal

The solid products from the reaction were removed by means of a 1 inch diameter wood auger bit. This auger, as shown in Figure IV.7, extended 1 inch into the reactor and was encased in a teflon sheath. To facilitate flow, a solids out port, also shown in Figure IV.2, was installed inside the reactor wall.

The auger was driven at speeds of 1-60 r.p.m. by an electronically controlled variable speed 1/6 h.p. D.C. motor.

5. The Scrubber

The fumes produced in the reactor were drawn out of the reactor through a 1 inch teflon tube. This line was wrapped with heating tape to prevent undue condensation of the vapours.

The schematic of Figure IV.1 gives an adequate view of the scrubber assembly.

The vent scrubber provided the vacuum necessary to withdraw the reactor fumes. This vacuum was controlled by adjusting the exhaust valve.

The caustic makeup (Na_2CO_3 solution) was filtered to prevent fouling of the control valve.

The circulating pump provided outlet pressures of about 40 p.s.i. to create more than an adequate vacuum.

The efficiency of the vent scrubber was 100 % as substantiated by analysis of the exhaust by means of a Drager gas detector. The analysis indicated that no hydrogen fluoride was present in the exhaust.

B. Experimental Procedure for Continuous Reactor Runs

Prior to reactor startup, the solids and acid feeding systems were both calibrated at the desired levels. Recalibration of the solids feeder was necessary because temperature and humidity conditions altered the calibration from day to day. The recalibration of the acid rotameter was necessary because of slight variations in the concentration of the acid used.

The reactor was then heated to the desired temperature level and feeding of spar and acid was begun. The reactor was operated for about four hours to allow steady-state conditions to be achieved. At about that time, 5 grams of nickel sulfate were added to the reactor by way of the second hopper. The nickel sulfate served as a tracer for the determination of the residence time distribution.

Samples of the solids out for tracer analysis were taken in the following intervals of time, 0-3, 3-6, 6-9, 9-12, 12-15, 15-20, 20-25, 25-30, 30-40, 40-50, 50-60, 60-70, 70-80, 80-100, 100-120, 120-140, 140-160, 160-180, 180-200, 200-220, and 220-240 minutes. Sufficient time was allowed to insure that all the tracer had left the reactor. These samples also served for the determination of the solids out flow rate.

Solids out samples for chemical analysis, were taken in the time intervals of 120-140, 140-160, 160-180, 180-200, 200-220 and 220-240 minutes. These samples were taken simultaneously with the tracer samples, and were collected with a spoon and immediately quenched in 500 ml of 1 N NaOH solution. Scrubber liquor effluent samples were taken in the same time intervals.

While the reactor was running, the variable transformers for the flange heaters needed adjusting to maintain temperatures constant.

Periodic checking of the solids feeder accuracy was also done during each reactor run. This was easily accomplished by collecting the solids from the metering auger for a 1 minute interval. If a slight deviation of flow was noted, the r.p.m. of the drive motor was adjusted to compensate. This constant checking of feed rate was mandatory

because variation in flow could occur during a run due to ambient temperature and humidity variations. In this way slight deviations could properly be remedied before they became serious.

The spar sample collected from the metering auger, was not discarded, but slowly added to the reactor when the next sample to check the feed rate was being taken.

After shutdown, the reactor was completely disassembled and washed, then reassembled for the next run.

The treatment of the samples is discussed in Appendix IV.

C. The Batch Reactor

To supplement the data of the continuous reactor, the batch reactor was constructed and operated.

It is a fairly simple piece of equipment consisting of a 3" diameter steel pipe with a blind flange. The pipe walls were machined down to 1/8 inch thickness to facilitate good heat transfer. The flange was also 1/8 inch thick to facilitate good heat transfer. Heaters were used on the bottom plate and on the wall. A thermocouple was centrally located on the flange. The temperature was recorded on a strip chart recorder and controlled by an on-off temperature controller which regulated the bottom heater.

D. Experimental Procedure for the Batch Reactor

The reactor, with a pre weighed amount of fluorspar was preheated to the desired temperature level. A preweighed amount of acid was simultaneously heated to about 10°C higher than the desired running temperature.

The acid was then added to the preheated fluorspar while manually stirring with a stainless steel spatula. Stirring was continued until the mixture hardened and the spatula was employed to break up the larger granules.

In each of these runs roughly 40 grams of spar and 48 grams of acid were used. Great care was taken to ensure that equimolar quantities of reactants were used.

Four samples were taken at predetermined times for each of the runs and quickly quenched in 100 mls of 1N NaOH solution.

Although the temperature dropped about 20°F upon initial contact of the reactants the period of this drop was only about 45 seconds to one minute, after which the temperature was maintained to $\pm 8^{\circ}\text{F}$.

E. Operational and Equipment Problems

Some of the difficulties which were encountered, and could recur, with the equipment have already been briefly dealt with in the previous discussion. Here an attempt

is made to make the reader aware of other problems which had to be overcome. The chief of these problems was the solids feed system.

1. The Reactor

In a move to save costs, a variable transformer rather than a temperature controller was employed to control the heating of the semicylindrical heater. Although this manual control was satisfactory below 350°F it proved to be rather poor at the higher temperatures.

2. The Solids Feed System

The original solids feed system consisted of a hopper with a machined screw for feeding and stirrers to maintain the spar in a fluid state. The stirrers were necessary to prevent ratholing (a stable arch forming). Moreover the spar tended to adhere to the screw, often causing all flow to cease. At best, the spar flow rate was erratic and dependent more on the position of the hopper stirrers than on the screw rotation rate.

The same hopper was equipped with a different screw (a wood bit auger) which provided better stability of the spar flow rate so long as the position of the hopper stirrers was not disturbed. However, when the calcium balance

problems, as discussed elsewhere arose, it was suspected that during the actual running of the reactor the outlet port of the feeder was clogging. Since no adequate method of measuring the spar feed rate during reactor operation was available no adjustment to the screw r.p.m. could be made to compensate for the fouling action.

At that time, the solids feed port was on the forward reactor flange rather than in the portal above the reactor as shown in Figure IV.2. The putty-like reactor contents could easily have been the cause of the fouling. In addition, the corrosive action of the reactor fumes caused substantial corrosion of the screw feeder and enhanced the adherence of the spar to the screw.

In desperation a solids feeder was rented from the Vibra Screw Corporation. This feeder was found to be unsatisfactory due to its inconsistent performance. Furthermore, it was bulky and extremely noisy.

However, the design of their auger was considered to be satisfactory and a new feeder was designed employing this auger. The new feeder was described previously and it proved to be quite satisfactory.

Initially, it was thought advisable to vibrate the hopper by use of pneumatic vibrators. However, vibration

was found to be unnecessary so long as the hopper stirrers were powerful enough to rotate at a constant r.p.m..

To eliminate blockage of the solids feed a solids feed port was constructed atop the reactor. However this did not prevent corrosion of the feeding auger by the fumes.

To allow for periodic checking of the solids flow rate, a second hopper was employed to transfer the solids into the reactor. This last change was very important on two counts. Firstly, it eliminated all interference of the solids metering by the fumes and solids in the reactor. Secondly, the solids flow rate could be monitored continuously even during reactor operation allowing one to compensate for minor deviations in flow rates.

3. Acid Feed System

Originally the sulfuric acid was gravity fed through insulated 1/4 inch sch. 40 mild steel pipe from a heated 5 litre glass tank. Due to the extremely low flow rates required (7 - 15cc/min), it was necessary to use needle valves to regulate flow. A rotameter was used for metering purposes. Corrosion of steel pipe is reportedly low enough to make its use practical for this purpose. However, sufficient corrosion occurred to cause fouling of the needle valves. The steel pipe was subsequently replaced with teflon

tubing. The performance of this line was satisfactory until such time when commercial grade acid was fed to the system in place of the analytical grade used for testing. Severe fouling with the commercial grade acid led to the belief that a metering pump would need to be used to improve flow control.

A metering pump was subsequently purchased and proved satisfactory for a while. After a period of time, the pump check valves began to foul badly resulting in undesirable flow rate inaccuracies.

The final solution proved to be the use of a variable speed tubing pump to control the flow rate, and the rotameter for metering. Although this arrangement gave steady acid flows, the rotameter calibration still fluctuated from day to day. This fluctuation was eventually attributed to day to day room temperature fluctuations. To overcome this inaccuracy the use of the temperature bath was initiated.

Simultaneously, because of the extremely low flow rates involved, it was found that heating the acid in the reservoir was undesirable because by the time it entered the reactor it would be cooled down considerably. Wrapping the teflon tubing with heating tape to heat the acid prior to its entry into the reactor proved to be a practical solution.

It must be pointed out that these changes were not necessarily made in chronological order.

4. Solids Removal System

Initially this system used a 3/4 inch diameter machined screw to remove the solids. This screw proved unsatisfactory even when the solids out port was added. When a 3/4 inch diameter wood bit auger replaced that screw, satisfactory results were obtained.

The size of the auger was later changed to 1 inch diameter to facilitate a more efficient solids removal. Although this large auger will handle partially wet solids it will not work if the solids are too wet.

5. The Scrubber

The first scrubber consisted of a flanged 36 inch long 5 inch diameter steel pipe. The pipe was packed with P.V.C. rings. A vacuum was applied to the scrubber by means of two laboratory size jet ejectors. The fumes were drawn out of the reactor through a 3/4 inch aluminum and steel pipe. Steel pipe was used to construct a U-tube trap to catch any liquid that might flow from the scrubber into the transfer line. Other parts of the transfer line were of aluminum.

The major problem encountered with this equipment was the rapid corrosion of the transfer line pipe and the fouling of both the transfer line and the scrubber with solids entrained in the gases.

Fouling of the transfer line caused vacuum build up in the scrubber followed by flooding of the scrubber because the vacuum prevented the liquid from flowing out.

All this, of course, led to a very unstable operation and sometimes led to the profuse spewing of dangerous fumes into the immediate area.

By fortunate circumstance, the author was made aware of a new piece of equipment available that could eliminate these problems. A pilot plant size jet scrubber that would serve to scrub the gases, as well as provide the necessary vacuum for withdrawing the fumes out of the reactor, was being marketed.

Deployment of this jet scrubber proved very satisfactory. Although some fouling of the teflon transfer line did occur when the equipment was initially put into operation, adequate adjustment of the exhaust valve prevented undue solids carryover. The use of heating tapes on the transfer line also helped to maintain it fairly dry and eliminated fouling.

Another problem which also needed to be dealt with was the fouling of the caustic makeup needle valve. Solids precipitated out by caustic addition to tap water were the direct cause of this problem. The addition of a filter to the feed line was a simple solution to the problem.

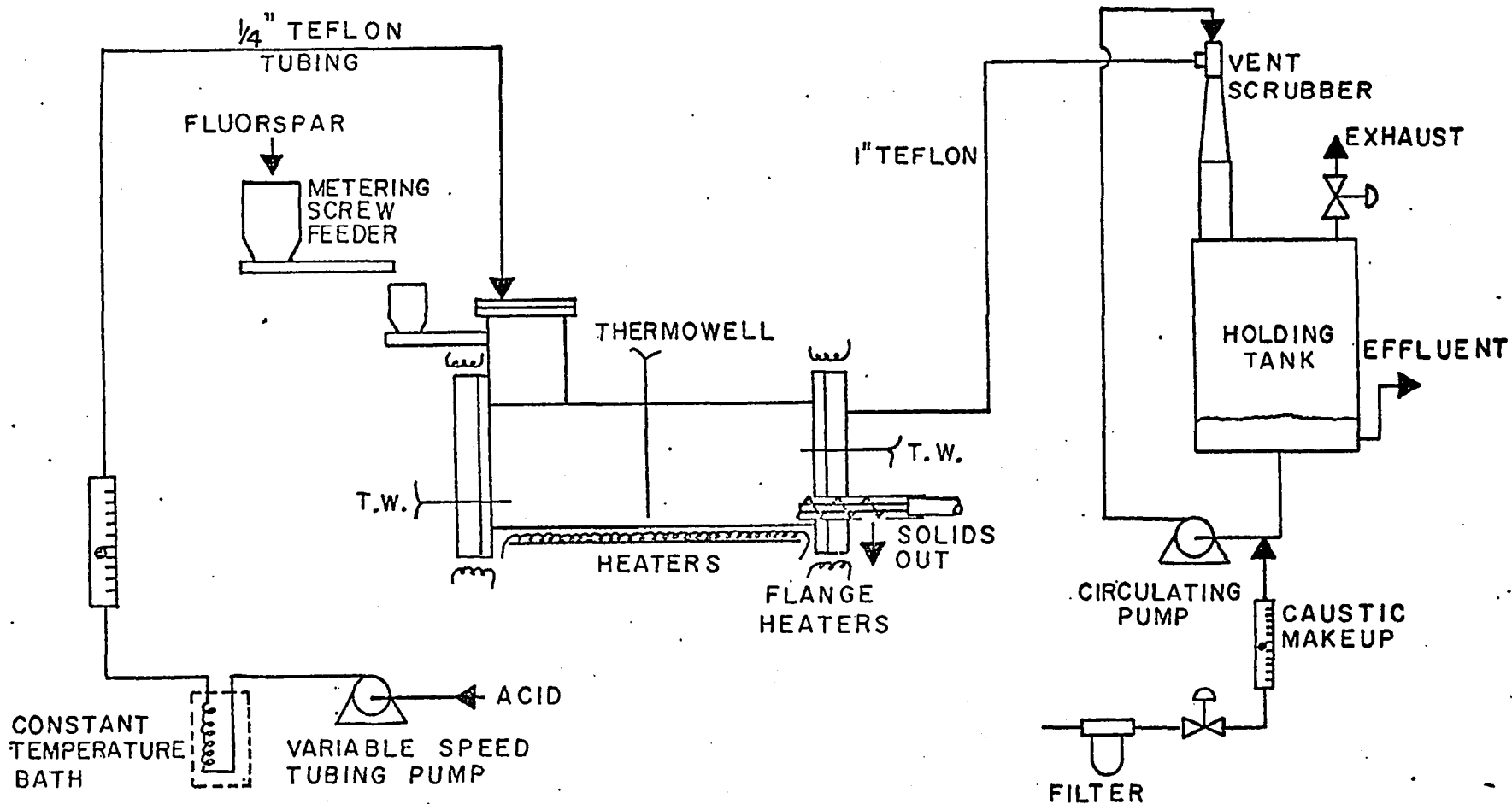
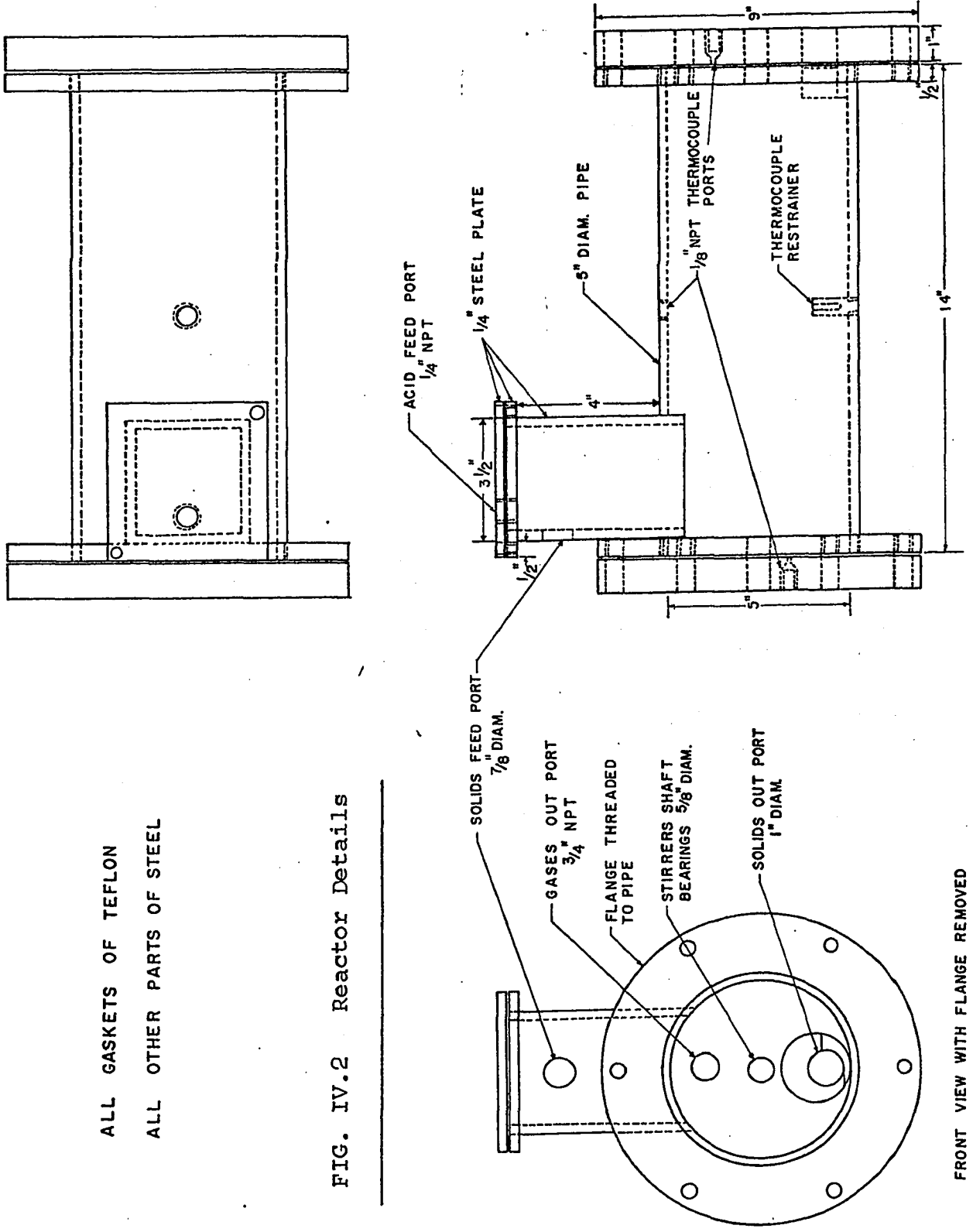
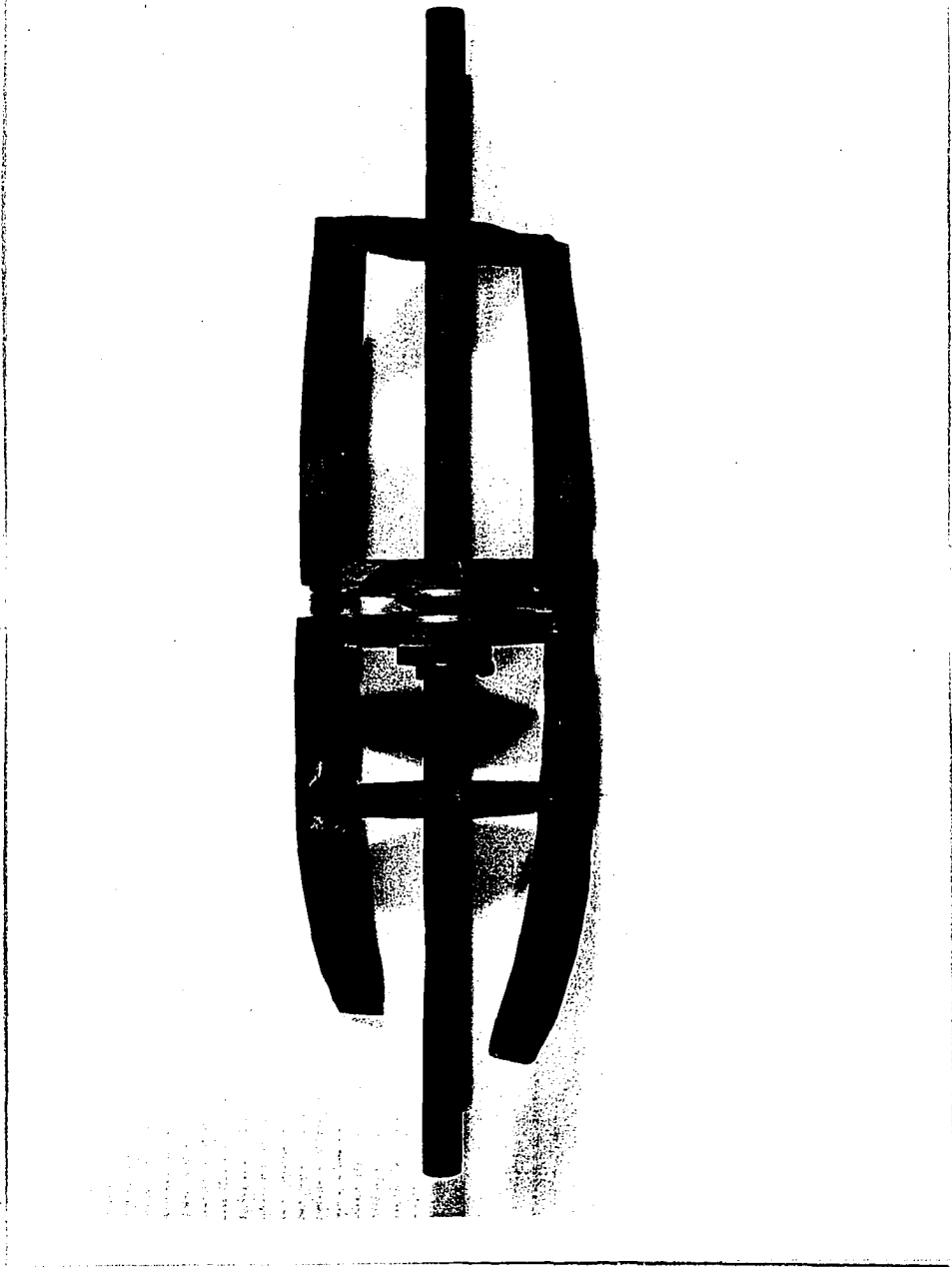


FIG. IV.1, Schematic of Reactor Assembly

ALL GASKETS OF TEFLON
ALL OTHER PARTS OF STEEL

FIG. IV.2 Reactor Details



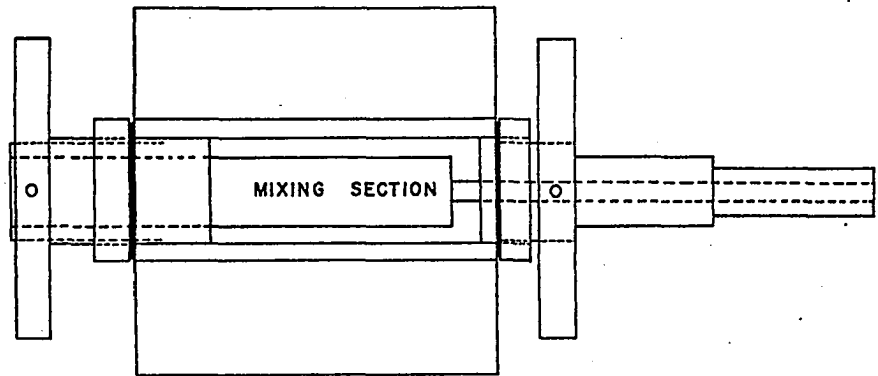


Reactor Mixers

FIG. VI.3



FIG. IV.4 Reactor Interior Showing Positions of Central and Rear Flange Thermocouples.



MATERIALS OF CONSTRUCTION
 HOPPER; STAINLESS SHEET
 HOPPER FLANGES AND
 PILLOW BLOCKS; ALUMINUM

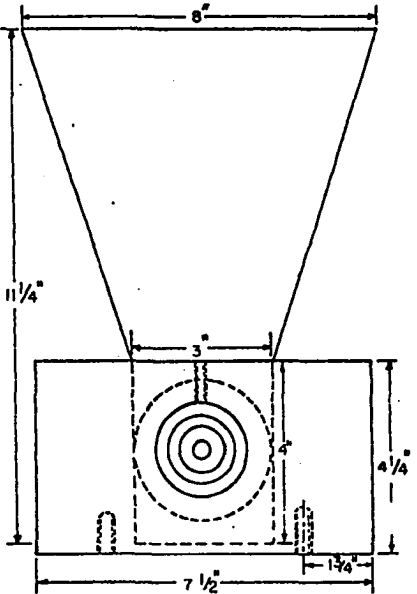
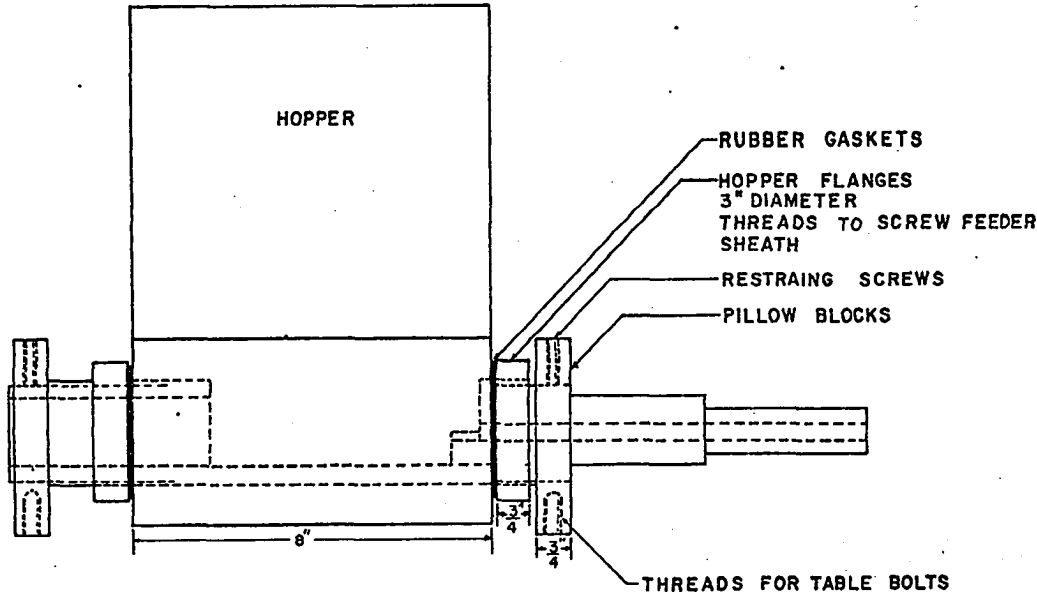


FIG. IV.5 Solids Metering Hopper Assembly

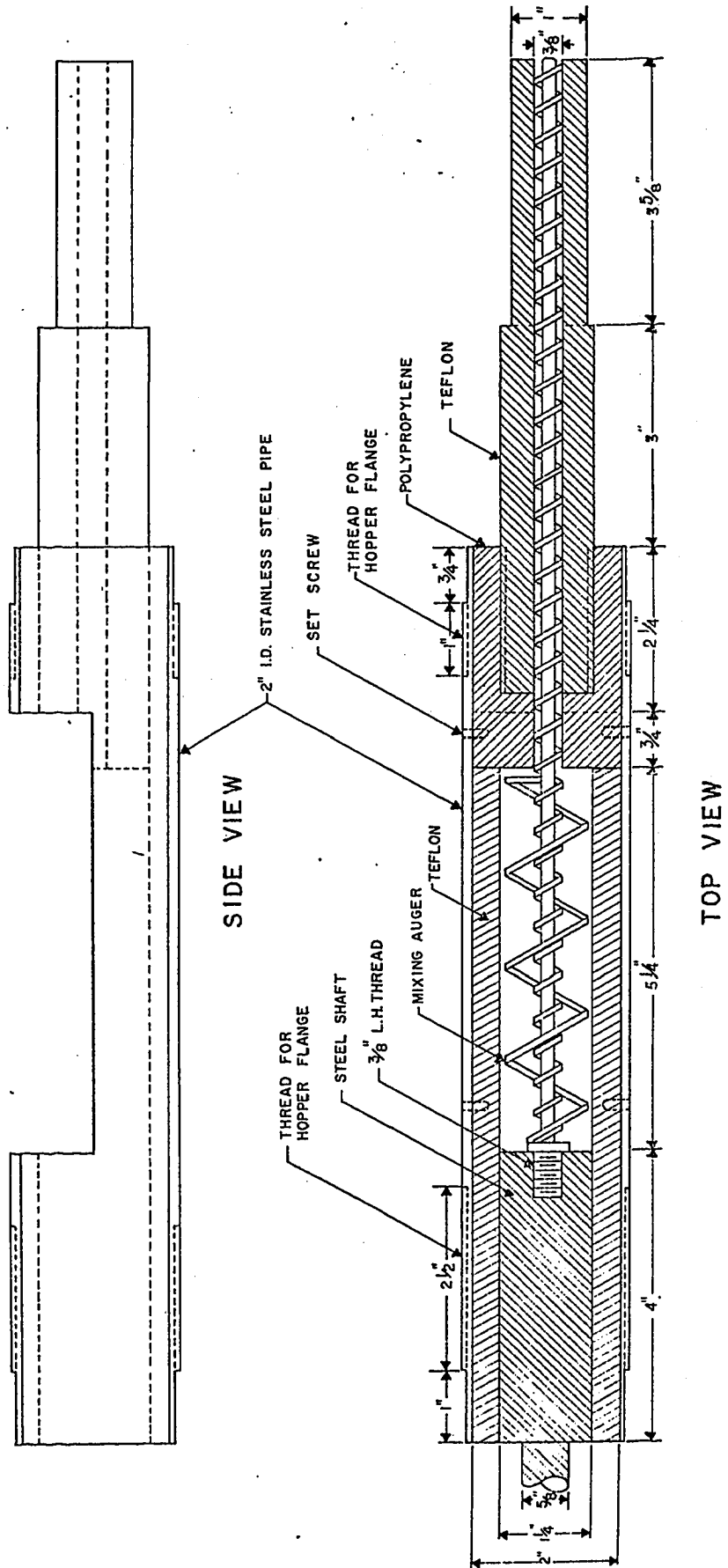


FIG. IV.6 Metering Auger

SIDE VIEW

TOP VIEW

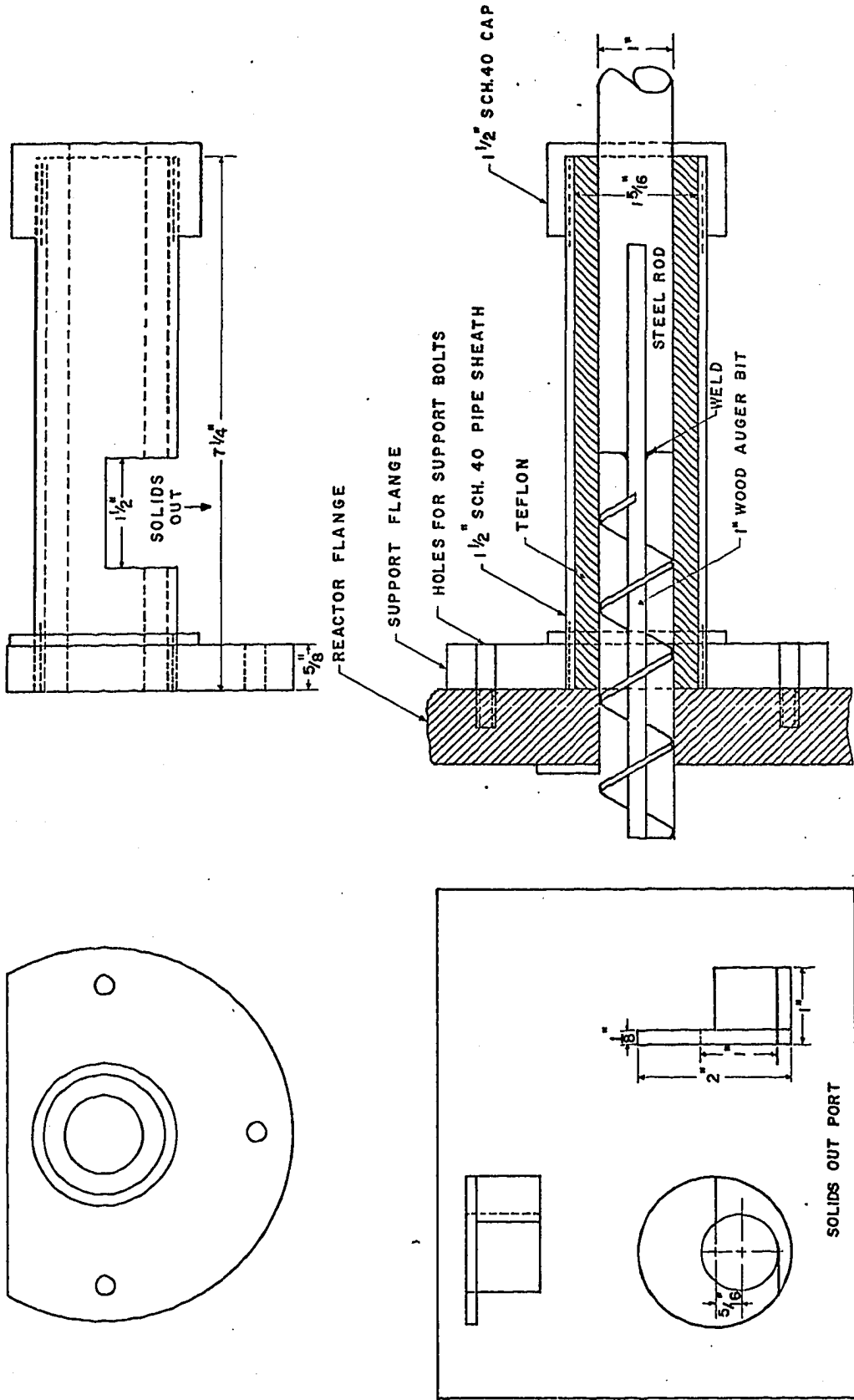


FIG. IV.7 Solids Out Auger and Solids Out Port

V. REACTOR AND KINETIC MODELS

A. The Continuous Reactor

Tracer data (a typical output curve is shown in Figure V.I), indicated that the reactor was not an ideal plug flow reactor, nor was it an ideal continuous stirred tank reactor.

The initial approach was to consider mass and energy balances of both the macroscopic flow and of the microscopic reacting particles. This approach was taken by Sood,⁽²⁷⁾ but led to an impractical set of equations solvable, if at all, by use of advanced numerical techniques. The second approach was to eliminate energy balances, and treat the reactor as a tanks in series model (18,19,20). The third approach was dramatically different, and was based on the premise that mixing in the reactor does not occur in the manner assumed by the first two approaches. The approach outlined below, attempts to account realistically for the observed phenomena occurring in the reactor.

At the entrance, the reactor is partially filled with a pasty mixture of reactants and products. The rest of the reactor is partially filled with hard, grey, substantially dry granules. This is not a step change, but the transformation from a wet to a dry mixture occurs in the early

sections of the reactor. In any case, once the granules have formed interaction among them is negligible. This results in many non-interacting batch reactors which remain in the reactor for varying lengths of time due to non-ideal flow.

From the tracer data, one can obtain $E(t)$, the residence time distribution of the particles leaving the reactor. These data, combined with the average conversion of the output stream may be used to obtain a rate constant for an assumed kinetic model.

The starting point for this analysis is the expression

$$\left\{ \begin{array}{l} \text{Mean value of} \\ \text{the fraction of CaF}_2 \\ \text{unconverted} \end{array} \right\} = \sum_{\text{all elements}} \left\{ \begin{array}{l} \text{fraction of} \\ \text{exiting} \\ \text{granules that} \\ \text{remained in} \\ \text{the reactor} \\ \text{for time } t_i \text{ to} \\ t_i + \Delta t_i \end{array} \right\} \left\{ \begin{array}{l} \text{fraction of} \\ \text{CaF}_2 \text{ unconverted} \\ \text{for granules} \\ \text{remaining in the} \\ \text{reactor for a} \\ \text{time } t_i \text{ to} \\ t_i + \Delta t_i \end{array} \right\} \quad (V-1)$$

$$\text{or } (1 - \bar{x}_B) = \sum_{i=1}^n (E(t)(\Delta t))_i \cdot (1 - x_B(\bar{t}_i)) \quad (V-2)$$

$x_B(\bar{t}_i)$ = average conversion of B obtained for a stream of age between t_i and $t_i + \Delta t_i$

$$\bar{t}_i = \frac{(t_i) + (t_i + \Delta t_i)}{2}$$

$[E(t)(\Delta t)]_i$ = fraction of stream with ages between t_i and $t_i + \Delta t_i$

In most instances, $E(t)$ is not easily expressed in an analytic form. Also, unless the kinetic rate expression is of a simple form, $x_B(\bar{t}_i)$ is not easily expressed in analytic form. Therefore, although it is possible to express equation (V-1) in the integral form

$$\bar{x}_B = \int_0^{\infty} x_B(t) E(t) dt \quad (V-3)$$

it is impractical to work with it.

B. The Rate Equation

We begin by adopting the moles of calcium as a basis for expressing concentration. Thus X_A = gm. moles of A per gram mole of calcium present in the reacting mass. If, for example, the feed were pure CaF_2 the initial concentration of CaF_2 , X_{B0} , is unity since there is one gram mole of CaF_2 per mole of calcium in the reacting mass. This basis of concentration is chosen because the total number of moles of calcium does not change as the reaction proceeds.

Using this basis, one can write the reaction rate term as

$$-r_B = -\frac{1}{N_{\text{Ca}}} \frac{dN_B}{dt} = f(k, X_A, X_B) \quad (V-4)$$

$$\text{or } \frac{dx_B}{dt} = f(k, X_A, X_B) \quad (\text{v-5})$$

where k is an arbitrary rate constant.

The function, $f(k, X_A, X_B)$, may take many forms, one of which is

$$f(k, X_A) = k X_A \quad (\text{v-6})$$

In terms of fractional conversion one can let

$$X_B = X_{B0} (1 - x_B)$$

$$\text{and } X_A = X_{A0} - x_B X_{B0} = X_{B0} (A - x)$$

since one mole of A reacts with one mole of B. And, A is the molar ratio of acid to spar expressed as gm. moles of acid per gram mole of spar in the initial reacting mixture.

Equation (v-6) then became

$$\frac{dx_B}{dt} = k (A - x_B) \quad (\text{v-7})$$

and k has dimensions of 1/time.

The above model is one of many considered for correlating the rate of evolution of hydrogen fluoride.

Prior to discussing these equations one should list the peculiar phenomenological aspects of the reaction of sulfuric acid with fluorspar.

- (1) CaF_2 crystals are not porous and fairly pure.
- (2) The reaction yields a solid and a fluid product.
- (3) The solid product is quite porous and adheres to the unreacted material.
- (4) The liquid reactant decreases in amount in proportion to the degree of conversion.
- (5) The initial solid particles are not spherical and surface irregularities tend to be smoothed out as the reaction proceeds.
- (6) The solid particles are not of a uniform size, but are quite fine. (mean particle diameter of 20 to 30 μ)

Items (1) through (4) would seem to point to the validity of using the shrinking core model. At the same time, because the acid was of high concentration, the validity of the pseudo steady state assumption was in question. However, as discussed in Appendix I, treatment of the reacting system must be kept as simple as possible because only one rate constant value may be determined from the data on the continuous reactor. In reality, equation (III-9), which is a relatively simple equation, cannot be used because three rate constants would need to be determined.

With the restriction of having only one rate constant in

a model, one is limited in the amount of sophistication possible.

One can begin by simply attempting to fit the data to an empirical equation of the form

$$f(k, X_A, X_B) = kX_A^m X_B^n$$

For simplicity m and n were chosen to be integer values or zero. Models 1, 2, 3, 4, and 5 are of this type.

Recalling that in the reaction the surface concentration of the solid may be considered constant while the concentration of the fluid reactant is decreasing in proportion to the amount of conversion one can use equations (III-19), (III-20), and (III-21) referred to in the THEORY (section III). These equations are included in Table V.1 as Models 1, 7 and 6 respectively. Model 6 is valid for the case where one assumes a first order reaction with respect to A on the surface. If a second order reaction with respect to A is assumed the equation of Model 15 is obtained.

Models 9, 10, 11, 12, and 13 are empirical variations of the diffusion controlling equation of Model 7.

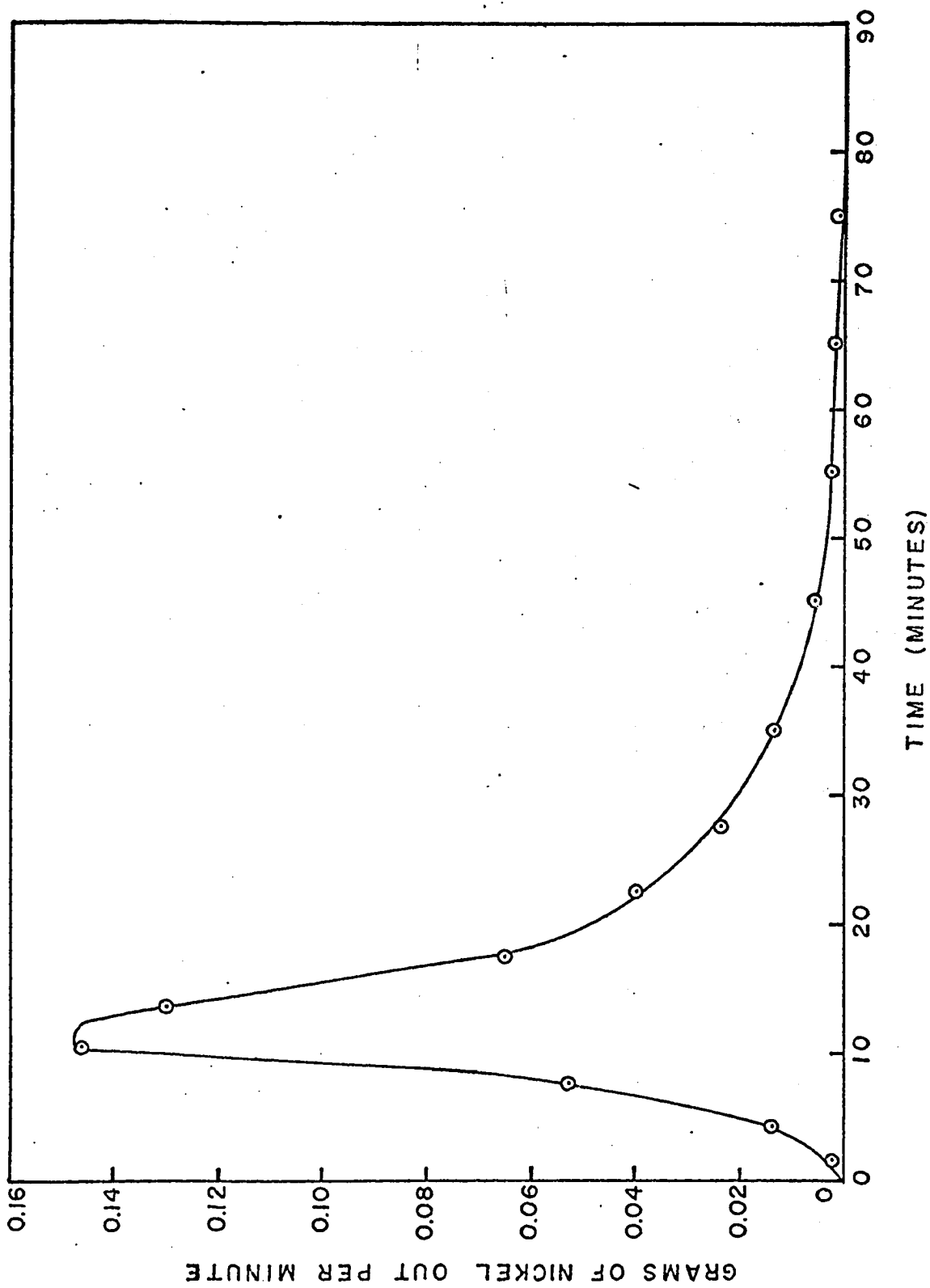


FIG. V.1 A Typical Tracer Response.

TABLE V.1 List of Reaction Models

Model No.	Units of Rate Constant (a)	Model
1	$\text{min.}^{-1} X^{-1}$	$\frac{dx_B}{dt} = k_1 X_{B0} (A-x_B)$
2	$\text{min.}^{-1} X^{-1}$	$\frac{dx_B}{dt} = k_2 X_{B0} (A-x_B)(1-x_B)$
3	$\text{min.}^{-1} X^{-2}$	$\frac{dx_B}{dt} = k_3 X_{B0}^2 (A-x_B)$
4	min.^{-1}	$\frac{dx_B}{dt} = k_4 (1-x_B)^2$
5	min.^{-1}	$\frac{dx_B}{dt} = k_5 (1-x_B)$
6	$\text{min.}^{-1} X^{-1}$	$\frac{dx_B}{dt} = k_6 X_{B0} (A-x_B)(1-x_B)^{2/3}$
7	$\text{min.}^{-1} X^{-1}$	$\frac{dx_B}{dt} = k_7 \frac{X_{B0} (A-x_B)(1-x_B)^{1/3}}{1-(1-x_B)^{1/3}}$
8	$\text{min.}^{-1} X^{-1}$	$\frac{dx_B}{dt} = k_8 \frac{X_{B0} (A-x_B)(1-x_B)^{2/3}}{1-(1-x_B)^{1/3}}$
9	$\text{min.}^{-1} X^{-2}$	$\frac{dx_B}{dt} = k_9 \frac{X_{B0}^2 (A-x_B)^2 (1-x_B)^{2/3}}{1-(1-x_B)^{1/3}}$

(a) X = concentration in moles per mole of calcium

TABLE V.1 Contd.

Model No.	Units of Rate Constants	Model
10	$\text{min.}^{-1} x^{-2}$	$\frac{dx_B}{dt} = k_{10} \frac{x_{B0}^2 (A-x_B)^2 (1-x_B)^{1/3}}{1-(1-x_B)^{1/3}}$
11	$\text{min.}^{-1} x^{-2}$	$\frac{dx_B}{dt} = k_{11} \frac{x_{B0}^2 (A-x_B)^2 (1-x_B)^{2/3}}{1-(1-x_B)^{2/3}}$
12	$\text{min.}^{-1} x^{-2}$	$\frac{dx_B}{dt} = k_{12} \frac{x_{B0}^2 (A-x_B)^2 (1-x_B)}{1-(1-x_B)}$
13	$\text{min.}^{-1} x^{-1}$	$\frac{dx_B}{dt} = k_{13} \frac{x_{B0} (A-x_B) (1-x_B)}{x_B}$
14	$\text{min.}^{-1} x^{-1}$	$\frac{dx_B}{dt} = k_{14} \frac{x_{B0} (A-x_B) (1-x_B)^{2/3}}{1-(1-x_B)^{2/3}}$
15	$\text{min.}^{-1} x^{-2}$	$\frac{dx_B}{dt} = k_{15} x_{B0}^2 (A-x_B)^2 (1-x_B)^{2/3}$
16	$\text{min.}^{-1} x^{-1}$	$\frac{dx_B}{dt} = k_{16} \frac{x_{B0} (A-x_B) (1-x_B)^{1/3} x_B}{1-x_B - (1-x_B)^{1/3}}$

VI EXPERIMENTAL RESULTS AND ANALYSIS

A Experimental Results

1. Qualitative Observations

Several points need to be documented on the basis of visual observations made during the operation of the batch and continuous reactor.

a. Batch reactor

When the hot acid was added to the preheated fluorspar a rapid frothing ensued, the intensity of which increased with increasing temperature. In the runs at 350°F the acid had to be added less rapidly to prevent boilover of the contents. Runs at temperatures above 350°F were impossible in the batch reactor because addition of the acid would necessarily have been so slow so as to affect the results.

After the frothing stage, the reactants took on a putty-like appearance, which, if left unmixed, would have set as one mass. However, with mixing by use of a spatula the setting action produced granules of various sizes (5/8 inch to 1/8 inch diameter with some powder). The larger granules seemed to be wetter than the others i.e. they contained a greater proportion of acid.

The putty-like stage lasted about 5 minutes in the 250°F runs but only about 2 minutes in the 350°F runs.

In one experiment, 1/8 inch diameter crystals of relatively pure CaF_2 were immersed in a beaker containing sulfuric acid at about 250°F . Small bubbles of gas were evolved which dissolved in the acid (HF is soluble in H_2SO_4 at 250°F to 1.8% by weight HF content). The solids product layer did not appear until the crystals had reacted for some time. This product layer formed initially on the crevices of the crystals but soon covered the entire unreacted surface and adhered very firmly to it. Examination under a microscope revealed that the product layer was not sponge-like but rather more like Plaster of Paris. The microscopic examination also revealed that the surface irregularities had been somewhat smoothed out.

b. The continuous reactor.

Some of the points mentioned here have already been covered in the other sections of this thesis. They are reconsidered here only by way of a summary.

In the feed end of the reactor, the reacting mass, which only partially filled the reactor, consisted of a putty-like material. The entire forward reactor interior was thickly coated by this putty. About 6 inches beyond the reactor entrance the paddles were only slightly coated and the reactor contents consisted of slightly wet granules which became

fairly dry as they travelled to the reactor exit. While some of the exiting granules were of 1/4 inch to 3/16 inch diameter, they were in the main about 1/16 of an inch or less in diameter.

In a run which is not documented in this thesis, pure synthetic CaF_2 was fed into the reactor. Operation of the reactor using this spar was impossible because fairly large lumps formed which could not be handled by the solids out auger. The lumps were also fairly wet indicating low conversions. With the same reactor conditions, but using the synthetic spar to which a 5% by weight CaCO_3 content had been added, the large lumps did not form nor were the solids out as wet as in the above run.

Even after 8 hours of operation the solids out flow rate pulsated to a large extent. When large pulsations occurred, the temperatures were also observed to fluctuate slightly. Runs in which high flow fluctuations occurred were normally discarded because the tracer response for these runs could not be relied upon as being representative. Only two runs were discarded for this reason.

2. Continuous Reactor Data

Table VI.1 contains the compositions, and the mean particle diameters, of the spars used in runs 10A to 19A and

1F to 10F of the continuous reactor. Sulfuric acid of 98.8% by weight purity was used in all these runs. Table VI.2 shows the experimental parameters of the A runs carried out. Table VI.3 contains the run parameters of the factorial runs 1F to 10F.

The results of the mass balances as well as the conversions obtained for all the samples taken are included in APPENDIX IV.

Table VI.4 shows the fractional age distribution of the solids leaving the reactor calculated from the percent nickel out data and the solids out flow rates using the equation

$$\left\{ \begin{array}{l} \text{Fraction of solids out} \\ \text{stream which consists} \\ \text{of elements of age} \\ \text{between } t_i \text{ and } t_i + \Delta t_i \end{array} \right\} = (E(t) \cdot \Delta t)_i = \frac{W_i C_i}{\sum_{j=1}^n W_j C_j} \quad (\text{VI-1})$$

where W_i = weight of solids out during the interval i

C_i = average % Ni content of solids out during the interval

and n = total number of intervals

3. Batch Reactor Data

The conversions-time data of the batch reactor runs using fluorspar Newfluor-A is contained in Table VI.5. The conversion values were calculated from the % CaF_2 in the filtered solids samples reported by the lab.

B. Analysis of Batch Data.

The conversion-time data of Table VI.5 were subjected to the analysis outlined in APPENDIX I. Only three models were seen to yield a fairly linear plot of integral (I) versus time (t). These models were: model 9, 10, and 11 of Table V.1.

$$\text{Model 9} \quad \frac{dx_B}{dt} = \frac{k_9 X_{Bo}^2 (A-x_B)^2 (1-x_B)^{2/3}}{1 - (1-x_B)^{1/3}}$$

$$\text{Model 10} \quad \frac{dx_B}{dt} = \frac{k_{10} X_{Bo}^2 (A-x_B)^2 (1-x_B)^{1/3}}{1 - (1-x_B)^{1/3}}$$

$$\text{Model 11} \quad \frac{dx_B}{dt} = \frac{k_{11} X_{Bo}^2 (A-x_B)^2 (1-x_B)^{2/3}}{1 - (1-x_B)^{2/3}}$$

All other models contained in Table V.1 yielded non-linear integral versus time plots.

The apparent rate constants of the three models were estimated by least squares regression as discussed in Appendix I and are shown in Table VI.6. For comparison purposes this analysis was also done for models 6 and 7.

$$\text{Model 6} \quad \frac{dx_B}{dt} = k_6 X_{Bo} (A-x_B)(1-x_B)^{2/3}$$

$$\text{Model 7} \quad \frac{dx_B}{dt} = \frac{k_7 X_{Bo} (A-x_B)(1-s_B)^{1/3}}{1 - (1-x_B)^{1/3}}$$

The correlation coefficients for I vs. t for all models are included in Table VI.6 and indicate a high association between I and t. However the correlation coefficient is only a measure of association and in no way should be interpreted as the final criterion of the goodness of fit of these models.

A more accurate measure of the goodness of fit of a model is the ratio MS_{AR}/S_E^2 where MS_{AR} is the mean square of the residuals about the regression. i.e.

$$MS_{AR} = \frac{\sum_i (x_{Bi} - \hat{x}_{Bi})^2}{(n - 1)} \quad (VI-2)$$

\hat{x}_{Bi} = the conversion predicted by the rate model at a time t_i using the determined k value.

x_{Bi} = the conversion obtained by experiment.

n = number of data points.

S_E^2 is the mean square due to pure error and was evaluated from the replicate values of x_B at a time t_i using the following equation

$$S_E^2 = \frac{\sum_{j=1}^m \sum_{i=1}^{n_j} (x_{Bij} - \bar{x}_{Bi})^2}{\sum_{j=1}^m (n_j - k)} \quad (VI-3)$$

n_j = no. of replicates available at a time t_i

\bar{x}_{Bi} = mean value of replicates at a time t_i

m = total no. of time levels at which replicates were available

The S_E^2 value calculated is 8.97×10^{-4} with 23 degrees of freedom and is a measure of the experimental error.

If a model is to fit the data and MS_{AR} value for the regression should not be significantly greater than the experimental error. If it is significant it indicates that there is a bias in the model (i.e. the residuals are unduly high).

The MS_{AR} values were calculated after having obtained the least squares estimates of the apparent rate constants. The F ratio (MS_{AR}/S_E^2) along with the 95% confidence interval of the apparent rate constants were included in Table VI.6.

The F ratios are significant at the 5% or lower level of significance for all three temperature levels for model 6, and for the 300 and 350°F temperature levels for model 7. None of the F ratios are significant for models 9, 10 and 11 indicating that these three models fit the data. As well, the MS_{AR} values in Table 6 are of equal size, indicating that none of the models may be considered a better fit.

It must be stressed that the above analysis does not prove that the three models are the correct models, but proves only that the null hypothesis that these models fit the data cannot be rejected.

Figures VI.1, VI.2, VI.3, VI.4 and VI.5, show the experimental data and the conversion curves predicted by models 6, 7, 9, 10 and 11 using the least squares estimates of the apparent rate constants. Figure VI.1 and VI.2 illustrate the lack of fit of models 6 and 7 to the data.

Having obtained the apparent rate constants for each of the models at three temperature levels, the next task was to fit these constants to the Arrhenius equation of the form

$$k = k_T \exp \left\{ \frac{-E}{R} \left(\frac{1}{T} - \frac{1}{\bar{T}} \right) \right\} \quad (\text{VI-4})$$

where E is the apparent activation energy (Btu/lb.mole), T is the temperature ($^{\circ}\text{R}$), $(1/\bar{T})$ is the mean $(1/T)$ value, and R is the gas constant (Btu/lb.mole $^{\circ}\text{R}$). The aim was to obtain the best estimate of the two parameters k_T and E.

There were two approaches used for the least squares estimate of the parameters. The first approach was to estimate the parameters of the non-linear equation (VI-4) while the other was to linearize it by taking the natural logarithm of both sides of the equation for easier approximation of the parameters. However, linearization simply for easier approximation of the parameters is an invalid procedure unless the true regression model itself is intrinsically linear (13), (17).

If the model is intrinsically non-linear, the regression

equation is

$$k_i = k_T \exp \left\{ \frac{-E}{R} \left[\frac{1}{T_i} - \left(\frac{1}{\bar{T}} \right) \right] \right\} + \epsilon_{1i} \quad (\text{VI-5})$$

$$i = 1, 2 \dots n$$

where ϵ_{1i} is the random error with the expected value of 0 and normally distributed about 0 with a variance σ_k^2 , where σ_k^2 is the variance of the apparent rate constants. Put more simply ϵ_{1i} is the increment by which an individual k_i may fall off the regression curve, the expected value of which is zero and whose variance is expected to equal the variance of k at all levels of k . If the variance of k is independent of the level of the temperature, the variance of ϵ_{1i} must also be assumed to be constant.

Using the program GAUSHAUS ⁽²¹⁾ the least squares estimates of the non-linear parameters k_T and E were obtained. The values of the parameters obtained are shown in Table VI-7A along with the variance of residuals $S_{R,k}^2$

$$S_{R,k}^2 = \frac{\sum_i (k_i - \hat{k}_i)^2}{n - p} \quad (\text{VI-6})$$

p = no. of parameters in the regression equation = 2;

n = no. of data points. Because there were only 3 temperature points $n - p = 1$ (i.e. the variance about regression had only

one degree of freedom) the resulting estimates of the standard error of E and k_T (by linear approximation) also had only one degree of freedom and the 95% confidence intervals of E and k_T were very large and ignored. The $(1/T)$ value for all three models was $1.3196 \times 10^{-3} \text{ } ^\circ\text{R}^{-1}$ so that the equation were

$$\hat{k}_9 = 0.102 \exp \left\{ \frac{-22190}{R} \left[\frac{1}{T} - \frac{1}{757.8} \right] \right\} \quad (\text{VI-7})$$

for model 9

$$\hat{k}_{10} = 0.0775 \exp \left\{ \frac{-20520}{R} \left[\frac{1}{T} - \frac{1}{757.8} \right] \right\} \quad (\text{VI-8})$$

for model 10

$$\text{and } \hat{k}_{11} = 0.176 \exp \left\{ \frac{-21480}{R} \left[\frac{1}{T} - \frac{1}{757.8} \right] \right\} \quad (\text{VI-9})$$

for model 11. The k values had units of $(\text{min.}^{-1} \times \text{ } ^\circ\text{R}^{-2})$ where X represents concentration in terms of moles per mole of calcium. The superscript $\hat{}$ denotes predicted value.

Suppose now one assumes that the regression equation is intrinsically linear, of the form.

$$k_i = k_T \exp \left\{ \frac{-E}{R} \cdot \left[\frac{1}{T_i} - \left(\frac{\bar{1}}{\bar{T}} \right) \right] \right\} \cdot \phi_i \quad (\text{VI-10})$$

$$i = 1, 2 \quad \quad n$$

which can be linearized to the form

$$(\ln k)_i = \ln k_T - \frac{E}{R} \left\{ \frac{1}{T_i} - \frac{\bar{1}}{\bar{T}} \right\} + \epsilon_{2i} \quad (\text{VI-11})$$

$$i = 1, 2 \dots n$$

so that $\phi_i = \ln^{-1}(\epsilon_{2i})$.

Rewriting equation (VI-10) in the form

$$k_i = \hat{k}_i \phi_i \quad (\text{VI-12})$$

where

$$\hat{k}_i = k_T \exp \left[\frac{-E}{R} \left[\frac{1}{T_i} - \left(\frac{\bar{1}}{\bar{T}} \right) \right] \right] \quad (\text{VI-13})$$

$$i = 1, 2 \dots n$$

\hat{k}_i is the estimate of k_i from the regression equation using the best estimates of k_T and E . However, in equation (VI-10), ϕ_i is a random factor by which the rate constant k_i differs from the regression equation and is valid only if the error $(k_i - \hat{k}_i)$ is proportional to the size of k_i .

For equation (VI - 11), ϵ_{2i} is assumed to be normally distributed about the mean zero with a constant variance

$$\sigma_{\ln(k)}^2$$

The best estimates of the linear parameters k_T and E of equation (VI-11) were determined by least

squares (13) and are reported in Table VI.7B along with the variance of residuals

$$s_{R, \ln k}^2 = \frac{\sum_i \left((\ln k)_i - \widehat{(\ln k)}_i \right)^2}{n - p} \quad (\text{VI-14})$$

Again it is fruitless to consider confidence intervals because there is only one degree of freedom for the variance of residuals. The $(\overline{1/T})$ value for the models was $1.3196 \times 10^{-30} R^{-1}$ so that the Arrhenius equations estimated were

$$\widehat{k}_9 = 0.104 \exp \left\{ \frac{-19530}{R} \left[\frac{1}{T} - \frac{1}{757.8} \right] \right\} \quad (\text{VI-15})$$

for model 9

$$\widehat{k}_{10} = 0.0812 \exp \left\{ \frac{-18150}{R} \left[\frac{1}{T} - \frac{1}{757.8} \right] \right\} \quad (\text{VI-16})$$

for model 10, and

$$\widehat{k}_{11} = 0.185 \exp \left\{ \frac{-18940}{R} \left[\frac{1}{T} - \frac{1}{757.8} \right] \right\} \quad (\text{VI-17})$$

for model 11.

Because there were only three data points it is impossible to determine which of the regression equations (intrinsically linear or intrinsically non-linear) fits best. However by either approach the activation energy was in the

order of 20,000 Btu/lb. mole.

C. Analysis of Continuous Reactor A-Runs.

Using the method outlined in APPENDIX I the apparent rate constants were determined for runs 11A to 19A. The apparent rate constant values are shown in Table VI.8. The apparent rate constants from the batch data were included in this table by way of a summary.

The acid:spar ratio (A) used in the calculation of the apparent rate constants of the continuous reactor runs were those labelled "corrected acid:spar ratio". This corrected acid:spar ratio accounted for acid boiloff and reaction with CaCO_3 .

As will be discussed in section VII of this thesis, once the reaction between spar and acid has proceeded to some degree the acid in the reaction mass is in the form of $\text{CaSO}_4 \cdot \text{H}_2\text{SO}_4$ crystals⁽²⁴⁾ or liquid H_2SO_4 in the capillaries of the ash layer. In either case the vapour pressure of H_2SO_4 would be reduced and boiloff inhibited. The boiloff, therefore, was more likely to occur in the early stages of the reaction when the mix was still wet.

When the mix is still wet and conversion was low, the term $(A-x_B)^2$ in the rate equations was not so sensitive to

the value of A. The acid boiloff was thusly best considered as an acid bypass.

Furthermore, because CaCO_3 would immediately react on contact with sulfuric acid, the acid so consumed was considered as unavailable for reaction with calcium fluoride.

Corrected acid:spar
ratio

$$= \frac{\left[\text{moles of H}_2\text{SO}_4 \text{ in} \right] - \left[\text{moles of H}_2\text{SO}_4 \text{ required for reaction with CaCO}_3 \right] - \left[\text{moles of H}_2\text{SO}_4 \text{ boiled off} \right]}{\left[\text{moles of CaF}_2 \text{ into reactor} \right]}$$

The continuous reactor data were subsequently fitted to the non-linear and linearized Arrhenius equation

Because now there were 9 data points an approximation of the 95% confidence interval was more meaningful

The least squares analysis of the data is contained in Tables VI.9 and VI.10.

The estimates of the variance of k due to pure error, $S_{E,k}^2$ values of Table VI.9 were calculated using the values of the rate constants obtained at each temperature level (i.e. at each temperature three runs were carried out varying only the acid:spar ratio).

$$s_{E,k}^2 = \frac{\sum_{j=1}^m \sum_{i=1}^{n_j} (k_{ij} - \bar{k}_j)^2}{\sum_{j=1}^m (n_j - 1)} \quad (\text{VI-18})$$

Where m = number of temperature levels at which replication was done = 3, and n_j = number of replicates at any one temperature = 3.

The use of $s_{E,k}^2$, or $s_{E,\ln(k)}^2$ (for the intrinsically linear model) as measures of variance due to pure error presupposes that the acid:spar ratio was properly accounted for by the rate equation. If the rate equation had not properly accounted for the acid:spar ratio, the errors about regression would not be randomly distributed but correlated to the level of the corrected acid:spar ratio. A plot of the errors in Tables VI.13 and VI.14 vs. the acid:spar ratio, as well as tests to ascertain the randomness of the errors, revealed that the errors were indeed randomly distributed and not correlated to the corrected acid:spar ratio. Nor was there any apparent correlation detected between the level of the rate constant (or $\ln k$) and the errors about regression.

The above statements hold for both the residuals of the non-linear and linearized Arrhenius equations. The data, therefore, do not reveal whether it is more appropriate to use the non-linear or linear models. Both approaches satisfy the data rather well.

The following equation was used to calculate the estimate of the variance due to pure error of $\ln k$, $S_{E, \ln(k)}^2$,

$$S_{E, \ln(k)}^2 = \frac{\sum_{j=1}^m \sum_{i=1}^{n_j} \left((\ln k)_{ij} - (\overline{\ln k})_j \right)^2}{\sum_{j=1}^m (n_j - 1)} \quad (\text{VI-19})$$

Because the $S_{E,k}^2$ or $S_{E, \ln(k)}^2$ values in Tables VI.9 and VI.10 were larger than the S_R^2 values in all cases there was no reason to assume that the regression equations did not adequately fit the data.

By least squares fit of the non-linear Arrhenius equation to the continuous reactor data the following equations were obtained;

$$\hat{k}_9 = 0.317 \exp \left\{ - \frac{16200}{R} \left[\frac{1}{T} - \frac{1}{828.8} \right] \right\} \quad (\text{VI-20})$$

for model 9

$$\hat{k}_{10} = 0.206 \exp \left\{ - \frac{15270}{R} \left[\frac{1}{T} - \frac{1}{828.8} \right] \right\} \quad (\text{VI.21})$$

for model 10, and

$$\hat{k}_{11} = 0.524 \exp \left\{ - \frac{15800}{R} \left[\frac{1}{T} - \frac{1}{828.8} \right] \right\} \quad (\text{VI-22})$$

for model 11, where $T = {}^\circ R$.

By least squares fit of the linearized Arrhenius equation to the continuous reactor data, the following equations were obtained;

$$\hat{k}_9 = 0.307 \exp \left\{ -\frac{17000}{R} \left[\frac{1}{T} - \frac{1}{828.8} \right] \right\} \quad (\text{VI-23})$$

for model 9

$$\hat{k}_{10} = 0.202 \exp \left\{ -\frac{15700}{R} \left[\frac{1}{T} - \frac{1}{828.8} \right] \right\} \quad (\text{VI-24})$$

for model 10

$$\hat{k}_{11} = 0.510 \exp \left\{ -\frac{16500}{R} \left[\frac{1}{T} - \frac{1}{828.8} \right] \right\} \quad (\text{VI-25})$$

for model 11.

The parameters estimated by either non-linear or linear least squares revealed that for the continuous reactor data the activation energy was in the order of 16,000 Btu/lb. mole and did not vary significantly from model to model. Furthermore, on the basis of the 95% confidence intervals, the hypothesis that the activation energy values for the non-linear models are not significantly different from the linear models, could not be rejected.

D. Fitting the Arrhenius Equation to the Batch and Continuous Reactor Data Simultaneously

In the above analysis, the batch reactor apparent rate constants and the continuous reactor apparent rate constants

were regressed to the Arrhenius equation separately. It was of interest to see if the A runs and batch data could be fitted to an overall Arrhenius equation.

The least squares estimates of E and k_T obtained for the non-linear and linearized Arrhenius equation contained in Tables VI.11, and VI.12 respectively were obtained. As in the previous analysis the S_R^2 and $S_{E, \ln(k)}^2$ (or $S_{E,k}^2$) values were compared and, as in previous results, because the $S_{E, \ln(k)}^2$ or $S_{E,k}^2$ values were larger than the S_R^2 values there was no lack of fit of either the non-linear or linear model nor was one model discernably superior to the other.

Examination of the residuals in Tables VI.15 and VI.16 did not indicate any correlation between the residuals and the size of k_i or $\ln k_i$ or between the residuals and the corrected acid:spar ratio.

More significantly, examination of the residuals of the batch reactor data points indicates that the overall Arrhenius equation does adequately fit these points.

By least squares fit of the non-linear Arrhenius equation to the batch reactor and continuous reactor data simultaneously, the following equations were obtained:

$$\hat{k}_9 = 0.247 \exp \left\{ - \frac{16400}{R} \left(\frac{1}{T} - \frac{1}{809.9} \right) \right\} \quad (\text{VI.26})$$

for model 9.

$$\hat{k}_{10} = 0.166 \exp \left\{ - \frac{15200}{R} \left(\frac{1}{T} - \frac{1}{809.9} \right) \right\} \quad (\text{VI-27})$$

for model 10, and

$$\hat{k}_{11} = 0.414 \exp \left\{ - \frac{15900}{R} \left(\frac{1}{T} - \frac{1}{809.9} \right) \right\} \quad (\text{VI-28})$$

for model 11. Using least squares for the linearized Arrhenius equation the equations were

$$\hat{k}_9 = 0.234 \exp \left\{ - \frac{17900}{R} \left(\frac{1}{T} - \frac{1}{809.9} \right) \right\} \quad (\text{VI-29})$$

for model 9,

$$\hat{k}_{10} = 0.161 \exp \left\{ - \frac{16100}{R} \left(\frac{1}{T} - \frac{1}{809.9} \right) \right\} \quad (\text{VI-30})$$

for model 10, and

$$\hat{k}_{11} = 0.396 \exp \left\{ - \frac{17200}{R} \left(\frac{1}{T} - \frac{1}{809.9} \right) \right\} \quad (\text{VI-31})$$

for model 11.

The log of the apparent rate constants vs. $1/T$ plots, with the various regression equations obtained by the least squares fit of the linear and non-linear models are shown in Figures VI.6, VI.7, VI.8, VI.9, VI.10 and VI.11.

E. Predicted Conversion Errors.

Having estimated the parameters for the non-linear and linearized Arrhenius equation by least squares, it was

appropriate to determine how well the rate equations, using the rate constants calculated from the Arrhenius equation (with the appropriate estimated parameters), predicted the conversion of spar in the continuous reactor runs 11A-19A. Again it was necessary to use the exit age distribution. Calculation of the conversions was accomplished as outlined in Appendix I.

The conversions obtained using models 9, 10 and 11 are shown in Table VI.17. For this table the conversions under columns 1, 2, 3 and 4 were obtained using the rate constants from the Arrhenius equation whose parameters were estimated as follows

- Column (1) least squares fit of the non-linear Arrhenius equation to the continuous reactor data.
- (2) least squares fit of the linearized Arrhenius equation to the continuous reactor data least squares fit of the non-linear
- (3) least squares fit of the non-linear Arrhenius equation to the continuous reactor and batch reactor data
- (4) least squares fit of the linearized Arrhenius equation to the continuous reactor and batch reactor data.

The variance of errors in Table VI.17 was obtained from the following equation

$$\text{Variance} = \sum_i \frac{(x_{Bi} - \hat{x}_{Bi})^2}{\gamma} \quad (\text{VI-32})$$

ν = degrees of freedom = 7

x_{Bi} = observed conversions

\hat{x}_{Bi} = predicted conversions

The standard deviation of the errors was the square root of the variance. The largest standard deviation obtained was 0.0124 (fractional conversion).

In order to determine if the variance calculated as above was larger than expected, it was necessary to determine the inherent errors due to sampling, analysis of the samples, and deviation of the flow rates.

Calculation of the extent of conversion of fluorspar was based on the determination of the fluorine content of the scrubber liquor samples.

% CaF_2 conversion

$$= \left\{ \begin{array}{l} \text{(g/l. of fluorine in scrubber liquor)} \\ \text{X (caustic liquor flow rate) X } \frac{\text{MW}_{\text{CaF}_2}}{2 \text{ MW}_F} \end{array} \right\}$$

CaF_2 into reactor

(VI-33)

From replication of analysis of samples it was possible to calculate the variance due to analysis as

$$s_A^2 = 0.00620 \text{ (g./l. of fluorine)}^2$$

with 176 degrees of freedom.

In addition to the analysis error there was a sampling error due to the inherent fluctuations of the reactor.

Because six samples were taken for each of the runs, the variance due to sampling, S_s^2 , could be estimated. Its value was determined to be

$$S_s^2 = 0.01068 \quad (\text{g./l. of fluorine})^2$$

with 94 degrees of freedom.

For each sample at least 2 replicate analysis were done so that the variance due to analysis and sampling for each sample, S_F^2 , was (35)

$$S_F^2 = S_s^2 + S_A^2/n \quad (\text{VI-34})$$

where n = no. of replicate analyses = 2

$$S_F^2 = 0.0137 \quad (\text{g./l. of fluorine})^2$$

The standard deviations of the spar and the scrubber liquor feed rates were both estimated at 1%.

The fluorspar feed rate for most of the runs was about 500 g/hr. and the caustic liquor feed rate was usually 70.5 litres per hour.

For a variable, y , which is calculated from a function of $x_1, x_2, x_3 \dots$ the variance of y may be estimated as

follows (33)

$$s_Y^2 = \left(\frac{\partial y}{\partial x_1} \right)^2 s_{x_1}^2 + \left(\frac{\partial y}{\partial x_2} \right)^2 s_{x_2}^2 + \left(\frac{\partial y}{\partial x_3} \right)^2 s_{x_3}^2 + \dots \quad (\text{VI-35})$$

so that for equation (VI-33) the relationship was

$$s_{x_B}^2 = s_F^2 \left\{ \frac{70.5 \times 78/38}{500} \right\}^2 + s_{SL}^2 \left\{ \frac{2.57 \times 78/38}{500} \right\}^2 + s_{SF}^2 \left\{ \frac{2.57 \times 70.5 \times 78/38}{(500)^2} \right\}^2$$

where $s_{SL}^2 = (70.5 \times 0.01)^2$ was the variance of the scrubber liquor feed rate and $s_{SF}^2 = (500 \times 0.01)^2$ was the variance of the spar feed rate and

$$s_{x_B}^2 = 1.21 \times 10^{-3} \quad (\text{fraction conversion})^2$$

$s_{x_B}^2$ was the estimate of the variance of the conversions calculated from one sample. However, the conversion for each run was based on the average of six samples and $s_{\bar{x}_B}^2$, the variance of the average conversion calculated using six samples, was

$$s_{\bar{x}_B}^2 = s_{x_B}^2 / 6 = 2.02 \times 10^{-4}$$

and $S_{x_B} = 0.0142$ (fractional conversion)

The variance of the observed conversions having been estimated to be 2.02×10^{-4} , it can now be compared with the variance of errors of Table VI.17. In this table the largest variance of errors obtained is 1.545×10^{-4} which is smaller than the $S_{x_B}^2$ value.

An examination of the errors ($x_{Bi} - \hat{x}_{Bi}$) does not indicate a correlation between these errors and the corrected acid:spar ratio.

From this analysis it may be concluded that there was no lack of fit of models 9, 10 and 11 to the data and a comparison of the variances (F ratio test) of table VI-17 indicated that none of the models could be assumed superior to the others.

F. The Factorial Experimental Design.

The objective in the factorial experiments was to establish the effects of mixing speed, CaCO_3 content, and the fineness of the spar on the reaction. Factorial design was preferred over the classical one at a time experimental design, as the former is generally more efficient. The classical design is not readily applicable to situations where large interactions between factors are possible. An orthogonal experimental design is more practical because it not only allows the experimenter to obtain an estimate of

the effect of each factor but also to estimate the effect of the interactions between the factors.

1. Planning the design

The form of the orthogonal experimental design chosen is dependent on the degree of the equation which one chooses to estimate the response surface. (8,17) To start with, one may assume that the response surface, in this case, can be adequately described by the equation

$$k = k_0 C^c M^m S^s \exp \left\{ -\frac{E}{R} \left(\frac{1}{T} - \overline{\left(\frac{1}{T} \right)} \right) \right\} \quad (\text{VI-36a})$$

where $C = \text{wt. \% CaCO}_3$ content of the spar, $M = \text{mixing rate (r.p.m.)}$, $T = \text{temperature (}^\circ\text{R)}$, $S = \text{mean partial diameter of the spar}$, $R = \text{gas constant (Btu/lb. mole }^\circ\text{R)}$, $E = \text{activation energy Btu/lb.mole}$ and k_0 , c , m , and s are constants. Equation (VI-36a) may be linearized by taking the natural logarithm of both sides

$$\ln k = \ln k_0 + c \ln C + m \ln M + s \ln S$$

$$- \frac{E}{R} \left\{ \frac{1}{T} - \overline{\left(\frac{1}{T} \right)} \right\} + (\text{INTERACTION}) \quad (\text{VI-36b})$$

and one could obtain estimates of k_0 , m , c , s and E by use of a 2^{4-1} fractional factorial design requiring only 8 experiments. The resulting equation will be, of course, highly empirical but at the same time provide for a linear

approximation of the response surface.

Due to the fact that each experiment was expensive, requiring a significant amount of time and effort on the part of the experimenter, and costly analysis of the samples by the lab at Arvida, it was decided to carry out the least number of experiments possible. The 2^{4-1} fractional factorial design seemed to be a good choice.

Originally, the factorial design was constructed about the base point

$T = 830^{\circ}\text{R}$, $M = 10$ r.p.m. and $C = 5\%$ and the coded factors X_1 , X_2 , X_3 , and X_4 were chosen such that

$X_1 = -1$	$M = 5$ r.p.m.
$X_1 = +1$	$M = 20$ r.p.m.
$X_2 = -1$	$C = 3.5\%$
$X_2 = +1$	$C = 7.14\%$
$X_3 = -1$	spar of normal fineness
$X_3 = +1$	spar ground to a greater fineness
$X_4 = -1$	$T = 760^{\circ}\text{R}$
$X_4 = +1$	$T = 910^{\circ}\text{R}$

However, at 760°R (360°F) the reactor could not be operated much higher than 10 r.p.m. because the slightly

shorter residence times at the higher mixing rate caused the exiting solids to be too wet to be properly handled by the solids out auger. Furthermore, reactor operation at 5 r.p.m. was thought undesirable because, as was observed in run 2F, the solids out flow rate fluctuated very badly. In this run, little or no flow of solids for significant time periods was observed.

Subsequent analysis of the scrubber liquor samples from run 2F indicated no unduly high fluctuations of the fluorine content. Furthermore, there were no undue irregularities in the tracer curve. However, by the time the lab data was made available, the decision to change the levels of the factorial runs had been made and the experimentation had already been completed.

The new base point chosen for the 2^{4-1} factorial experimental design was $T = 868^{\circ}\text{R}$, $M = 19.8\text{r.p.m.}$ and $C = 5\%$. The base point for temperature was chosen so that the low temperature level was 830°R (370°F) and the upper level was 910°R (450°F), and the base point for mixing rate was chosen so that 25 r.p.m. was the highest mixing speed and the lower mixing rate was the log mean of 10 and 25 r.p.m..

$$X_1 = -1 \quad M = 15.8 \text{ r. p. m.}$$

$$X_1 = +1 \quad M = 25 \text{ r. p. m.}$$

$$X_2 = -1 \quad C = 3.5 \%$$

$$X_2 = +1 \quad C = 7.14 \%$$

$$X_3 = -1 \quad \text{regular spar (Newfluor A and B)}$$

$$X_3 = +1 \quad \text{reground spar (Newfluor Af and BF)}$$

$$X_4 = -1 \quad T = 830 \text{ }^\circ\text{R}$$

$$X_4 = +1 \quad T = 910 \text{ }^\circ\text{R}$$

$$\text{with } X_1 = \frac{\ln(M/19.8)}{\ln(25/19.8)} \quad (\text{VI-37})$$

$$X_2 = \frac{\ln C/5.0}{\ln(5.0/3.5)} \quad (\text{VI-38})$$

$$X_4 = \frac{-(1/T - 1/868)}{\left| \frac{1}{830} - \frac{1}{868} \right|} \quad (\text{VI-39})$$

The factorial design was as follows.

NOTATION	X_1	X_2	X_3	X_4	$= X_1 X_2 X_3$
1	-1	-1	-1	-1	
a d	+1	-1	-1	+1	
b d	-1	+1	-1	+1	
a b	+1	+1	-1	-1	
c d	-1	-1	+1	+1	
a c	+1	-1	+1	-1	
b c	-1	+1	+1	-1	
a b c d	+1	+1	+1	+1	

The approach used for the design of the experimental scheme was discussed thoroughly by Box and Hunter (7) and the method of analysis of the factorial design experiments may be found in most applied statistics tests. (2,7,11,14,17,35)

In the above experimental design the effects of factors X_1 , X_2 , X_3 , and X_4 may clearly be determined but the interaction effects i.e. $X_1 X_2$, $X_2 X_3$ etc, are confounded with one another. This point will become more apparent as the analysis of the experimental scheme is discussed.

The equation which was to be fitted to the data was

$$(\ln k)_i = \ln k_0 + m \ln M + c \ln C + s \ln S$$

$$- \frac{E}{R} \left\{ \frac{1}{T_i} - \left(\frac{\bar{1}}{\bar{T}} \right) \right\} + (\text{ERROR}) \quad (\text{VI-40})$$

2. Analysis of Factorial Runs Data

The apparent rate constants for runs 1F - 10F were determined by the method outlined in Appendix I. Table VI.18 contains the variables and the coded variables, the average conversions, and the apparent rate constants for the runs 1F - 10 F.

In Table VI.19 are shown the coded variables with the natural logarithm of the apparent rate constants.

Before considering the analysis of the factorial

experiments it may be recalled that in the A runs there was a measure of the variance of the natural logarithm of the apparent rate constants due to pure error. These $S_{E, \ln(k)}^2$ values were reported in Tables VI.10 and VI.11.

Details of the analysis of the factorial design experiments are not included in this thesis to conserve space.

In Table (VI.20) are shown the results of the factorial experimental design analysis. (Recall that runs 1F and 2F were not part of the factorial experimental design). The mean difference values or mean effect of the factor is the average change of the $\ln k$ value with a change in the factor level from -1 to +1

eg. for the factor $X_1 + X_2 X_3 X_4$ the mean effect is

$$\frac{(ad + ab + ac + abcd) - (l + bd + c + bc)}{4} \quad (\text{VI-41})$$

The change in the $\ln k$ value is, at least in theory, due to the effect of change in X_1 plus the interaction effect $X_2 X_3 X_4$. In practice however, it is very unlikely that a three factor interaction would have an effect on the system (2,7,8,11,14,17). But, for the case where the mean effect

is due to a two factor interaction such as $X_1 X_2 + X_2 X_3$ the statistical analysis of the data must often be fused with the judgement of the experimenter.

In any case, it must first be determined whether the mean effect of the factors is greater than that expected by pure chance i.e. significant. Although this can most directly be accomplished by conducting t tests on each mean effect to determine if it is significantly larger than zero ⁽¹⁴⁾, it is more expedient to use the Analysis of Variance method. (2,11,14,17)

The Analysis of Variance Table is shown as Table VI.21. The mean square values are easily calculated as

$$MS = \frac{(\text{MEAN EFFECT})^2}{2} \quad (\text{VI-41})$$

and are the contributions to the total variance by the effect.

The F test or variance ratio test is a test to determine if the variance of $\ln k$ due to a factor is significantly larger than that expected by chance alone.

$F(1,6,0.95) = 5.99$, $F(1,6, 0.975) = 8.81$ and $F(1,6,0.99) = 13.75$.

The results in Table VI.21 indicate that, as expected, temperature has a very strong influence on the apparent rate constant. It also turns out that the calcite content

of the fluorspar also has a very significant favourable influence. Although the effect of increasing the mixing rate is slightly favourable the analysis of variance indicates that it is not statistically significant at the 5% level of significance. At the same time, the spar fineness, within the range studied, does not have any significant effect on the apparent rate constant. The interaction effect $X_1 X_2 + X_3 X_4$ may be classified as statistically marginally significant and will be explored further by grouping the data as shown in Table VI.22.

In this table the data are grouped according to the calcite content of the spar and temperature, bearing in mind that the spar fineness does not significantly influence the apparent rate constants observed. By grouping the data in this fashion one notes that the apparent rate constants do not vary to any large degree with increased mixing when the CaCO_3 content of the spar is 7.14 %. With the CaCO_3 content at 3.5%, however, the apparent rate constants increase very sharply when the mixing rate is 25 r.p.m.

One may hypothesize the reasons for this result on the basis of the physical phenomenon.

When the CaCO_3 content of the fluorspar is relatively low (3.5 %) the blending action produced by the foaming may be insufficient to produce homogenous mixing of the

reactants. At the same time, the stirrers may not have served to enhance the blending unless they rotated at relatively high speeds i.e. 25 r.p.m.. At rotation speeds lower than 25 r.p.m. the stirrers may well have served only to agitate the macroscopic mass rather than blend the reactants. If the CaCO_3 content of the spar is augmented, the resulting blending action is more extensive and the higher rotation of the stirrers is unnecessary.

The above hypothesis would explain why the interaction term $X_1 X_2 + X_3 X_4$ is statistically marginally significant. It can be ascribed as due to the contribution of $X_1 X_2$ (mixing X CaCO_3 content). There is no reason to expect an interaction effect due to spar fineness and temperature, since the effect due to spar fineness is negligible.

At this point it would seem logical to attempt to fit the data to an equation of the form

$$\begin{aligned}
 (\ln k)_i = & \ln(k_0) + c \ln(C_i) - \frac{E}{R} \left[\frac{1}{T_i} - \left(\frac{1}{T} \right) \right] \\
 & + I \cdot m + \epsilon_i \qquad \qquad \qquad \text{(VI-42)}
 \end{aligned}$$

where $I = 0$ if $C = 7.14\%$ or $M < 25$ r.p.m., and $I = 1$ if $C = 3.5\%$ and $M = 25$ r.p.m.. The coefficient m attempts to account for the increase in the $\ln(k)$ values when the mixing

rate is at 25 r.p.m. and the calcite content of the spar is 3.5 %. Equation (VI-12) is not continuous with respect to the mixing parameters because as was noted in Table VI.22 an increase in mixing did not alter the apparent rate constant until the mixing rate was raised to 25 r.p.m.

Use of least squares to estimate the non-linear model parameters is inappropriate because the factorial experimental design is useful only for approximation of parameters of inherently linear equations.

Table VI.23 shows the least squares estimate of the linear model parameters with the data of the factorial experiments only. The parameter estimates in Table VI.24 were obtained by least squares fit of all the apparent rate constant values (continuous and batch reactor).

The results show that the apparent activation energy estimates in Table VI.23 were not significantly different from those in Table VI.12 and Table VI.24. This indicates that the estimation of the parameters is quite accurate by use of only eight experiments in which four factors are varied.

The final equations correlating the apparent rate constants to the temperature, CaCO_3 content of the spar, and mixing, are model 9; $\hat{k}_9 = 0.0644 c^{1.012} .M^{I \cdot 0.122}$

$$\exp \left\{ - \frac{17410}{R} \left[\frac{1}{T} - \frac{1}{809.9} \right] \right\} \quad (\text{VI-43})$$

$$\text{model 10; } \hat{k}_{10} = 0.0514c^{0.888} \cdot M^{I \cdot 0.116} \exp \left\{ \frac{-15810}{R} \left[\frac{1}{T} - \frac{1}{8099} \right] \right\}$$

(VI-44)

$$\text{model 11; } \hat{k}_{11} = 0.115c^{0.964} \cdot M^{I \cdot 0.120} \exp \left\{ \frac{-16770}{R} \left[\frac{1}{T} - \frac{1}{809.9} \right] \right\}$$

(VI-45)

where $I = 0$ if $C = 7.14 \%$ or $M < 25$ r p m
and $I = 1$ if $C = 3.5 \%$ and $M = 25$ r. p. m..

The variance of residuals S_R^2 values in Table VI.23 and VI.24 are smaller than the $S_{E, \ln(k)}^2$ values indicating that the errors are not significant, and examination of the residuals of Table VI.25 indicated that they were randomly distributed and not correlated to corrected acid: spar ratio or the size of the apparent rate constants.

As was done for the A runs, the predicted conversions were calculated using the reaction rate models combined with equations (VI-43), (VI-44) and (VI-45). The predicted conversions obtained are shown in Table VI.26. The standard deviations of the errors are 0.00875, 0.00934 and 0.00892 (fractional conversion) for models 9, 10 and 11 respectively. These standard deviations are lower than the $S_{\bar{x}_B}$ (the standard deviation of the observed fractional conversion based on an average from six samples) value of 0.0142

previously evaluated. This indicates that no lack of fit of the models is detected. Furthermore, because the standard deviation of the errors in Table VI.26 are not significantly different from one another (F ratio test), there is no basis for assuming that any one of the models is better than the others.

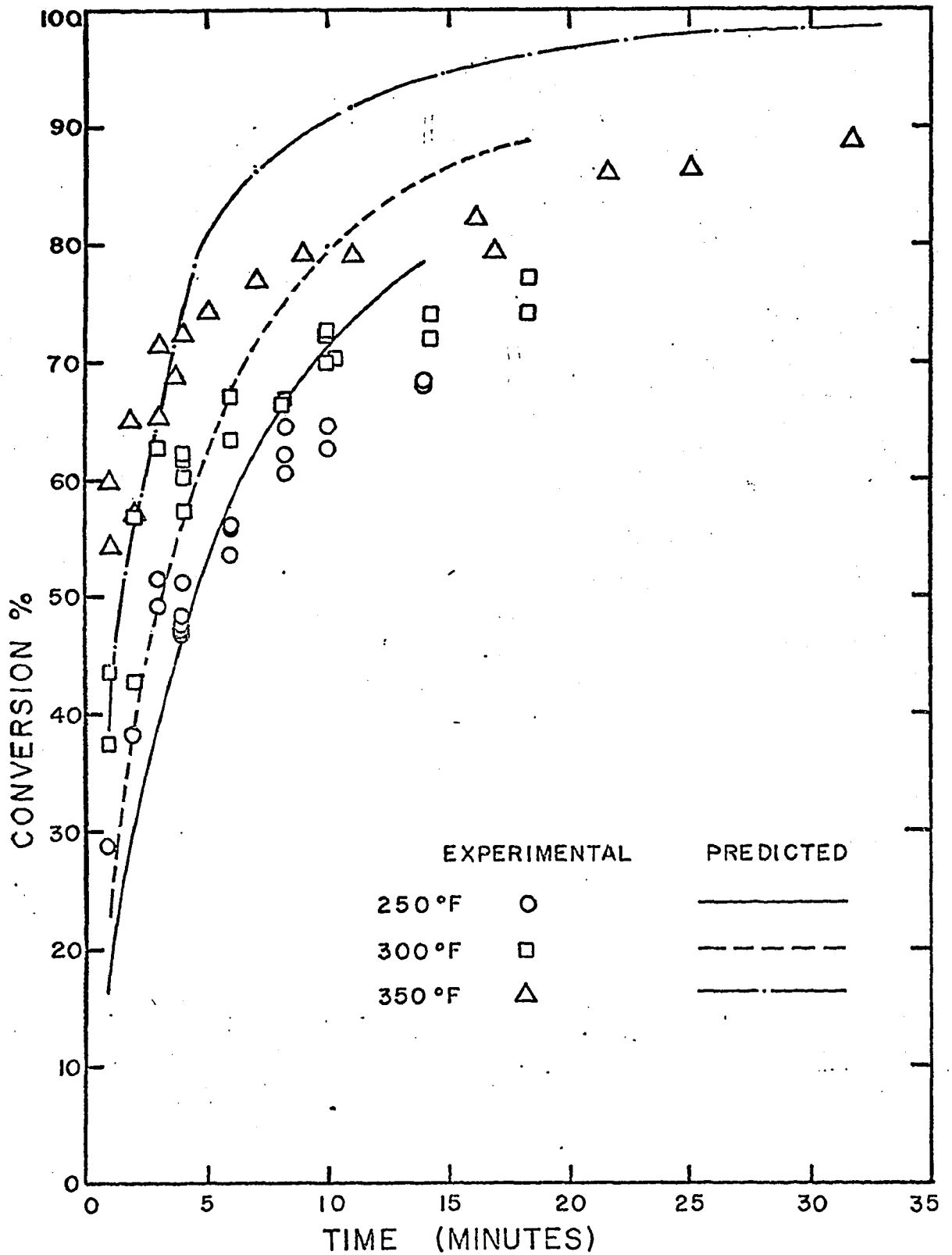


FIG. VI.1 Batch Reactor Conversion - Time Data and Conversion Curves Predicted by the Least Squares Fit of Model 6.

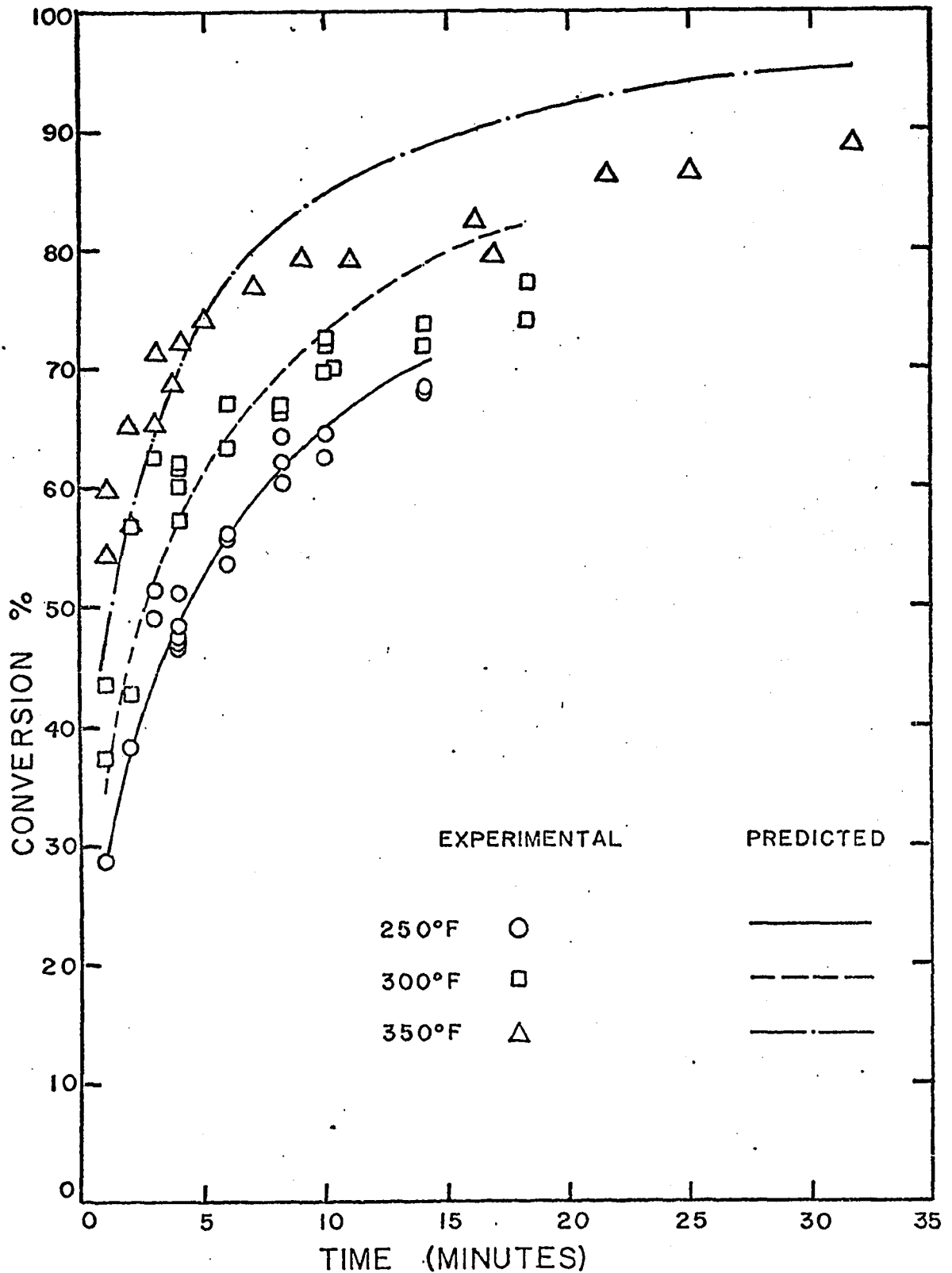


FIG. VI.2 Batch Reactor Conversion - Time Data and Conversion Curves Predicted by Least Squares fit of Model 7

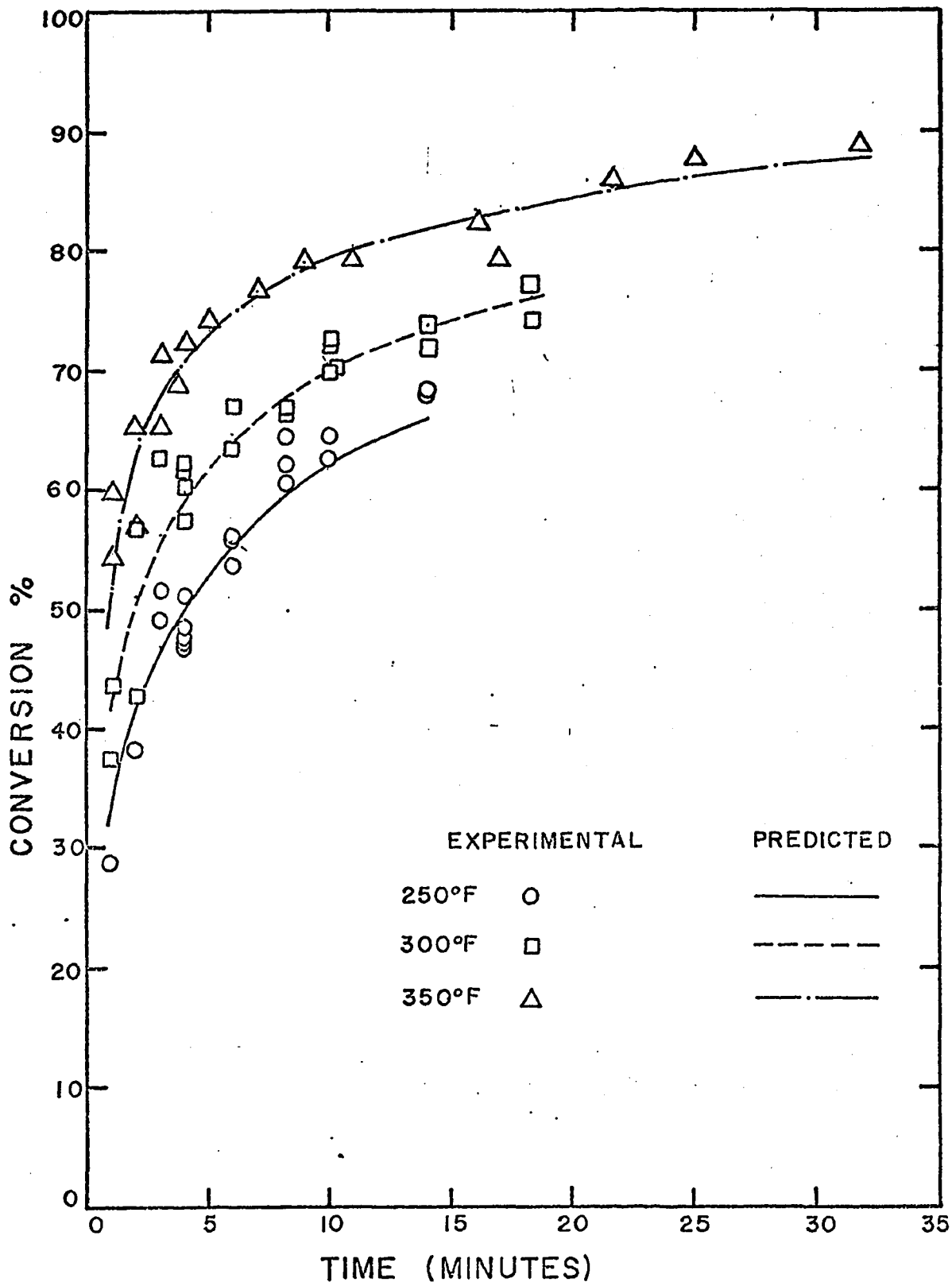


FIG. VI.3 Batch Reactor Conversion-Time Data and Predicted Conversion Curves from the Least Squares Fit of Model 9.

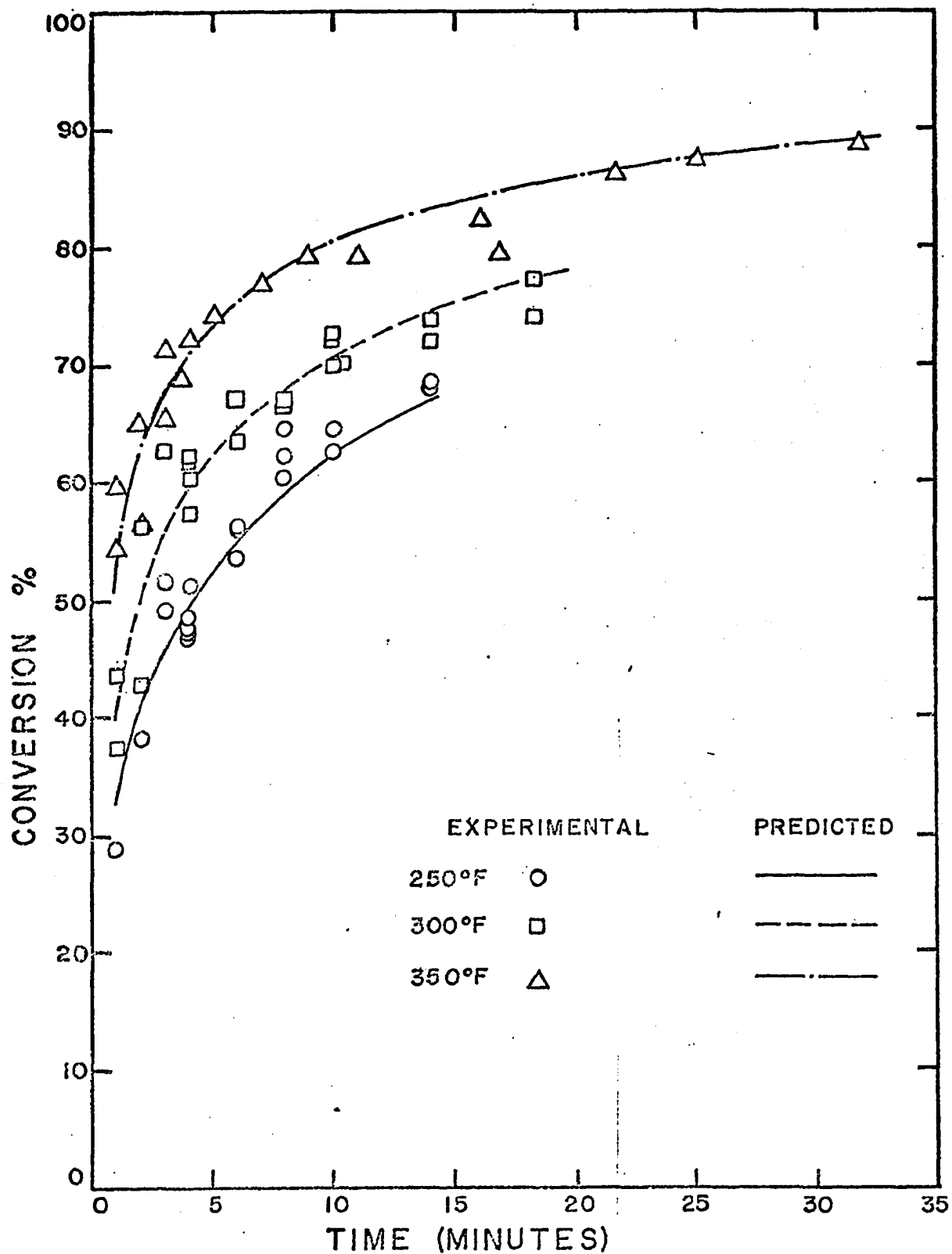


FIG. VI.4 Batch Reactor Conversion-Time Data and Conversion Curves Predicted by the Least Squares fit of Model 10.

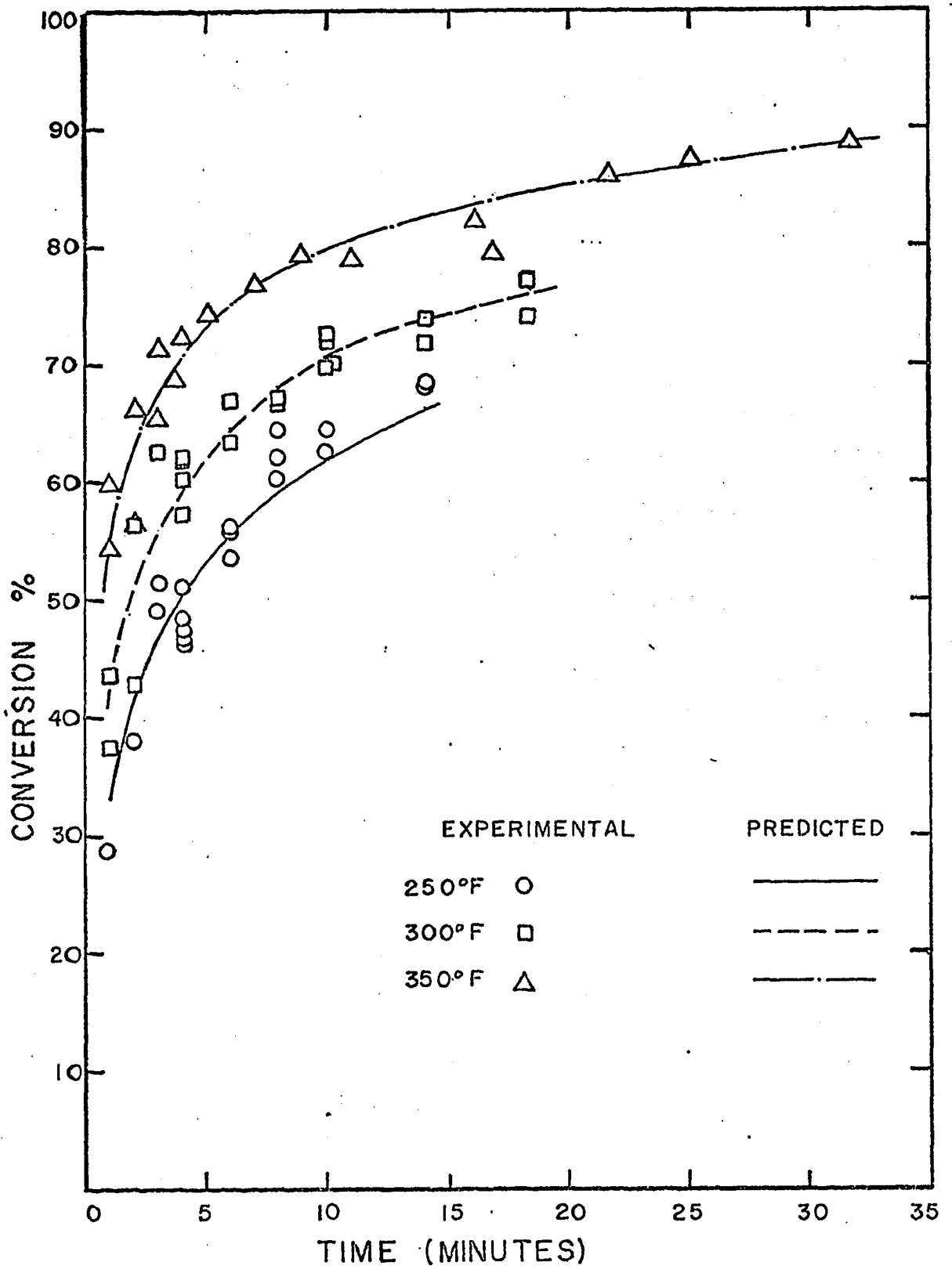


FIG. VI.5 Batch Reactor Conversion-Time Data and Conversion Curves Predicted by the Least Squares fit of Model 11.

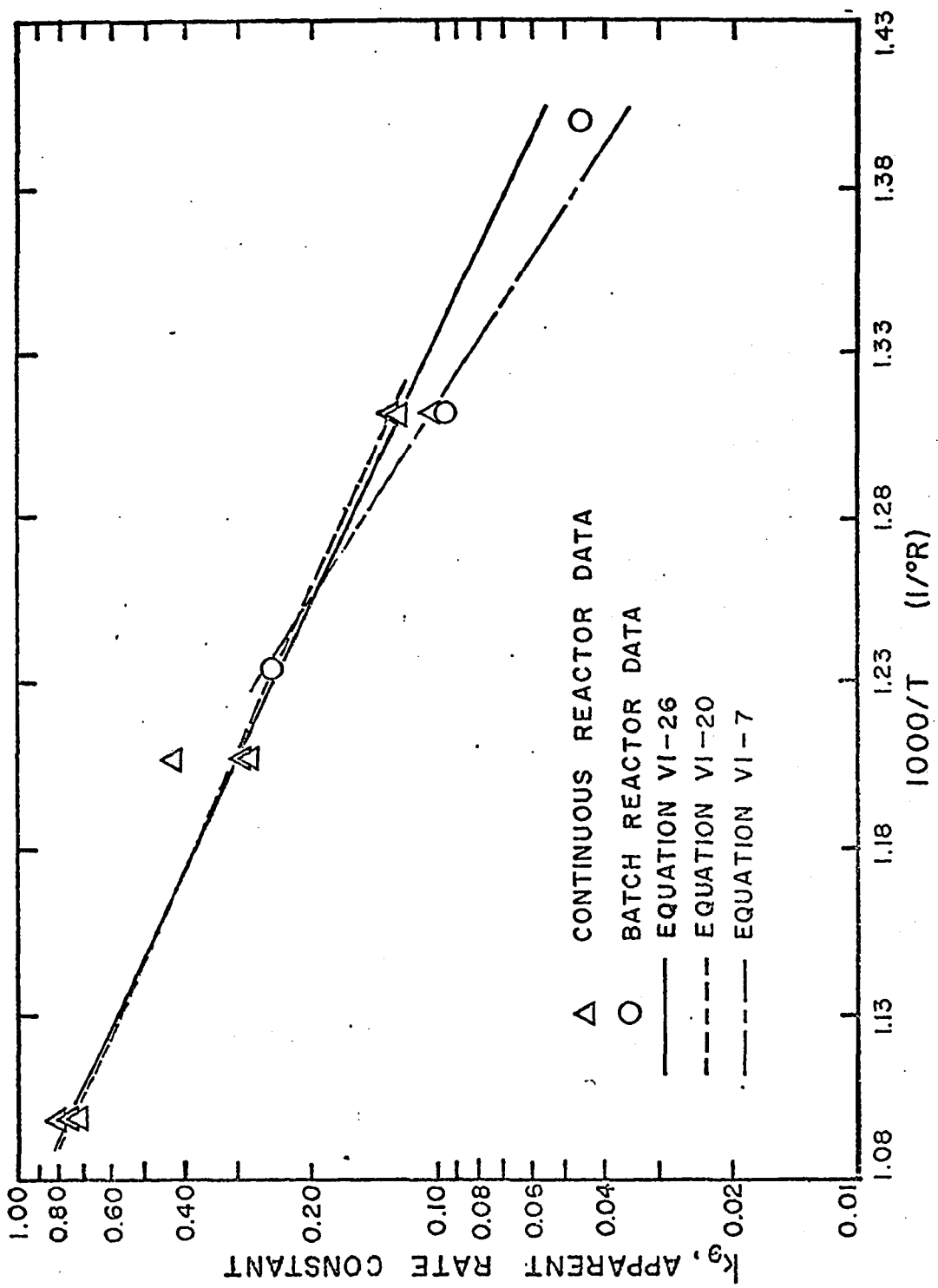


FIG. VI.6 Arrhenius Plot of Apparent Rate Constants of Model 9 with Non-Linear Equation Lines of Best Fit

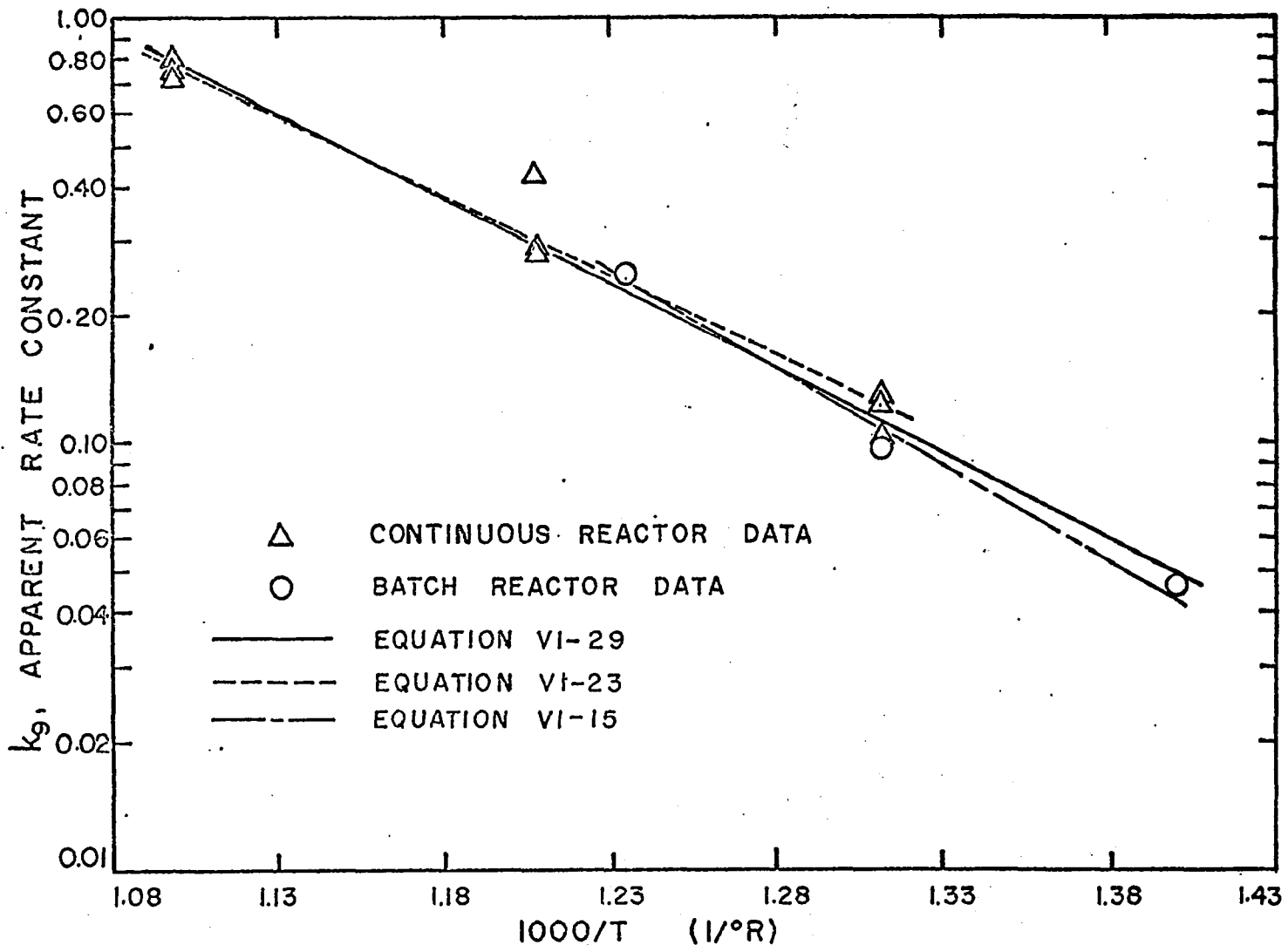


FIG. VI.7 Arrhenius Plot of Apparent Rate Constants of Model 9 with Linearized Equation Lines of Best Fit.

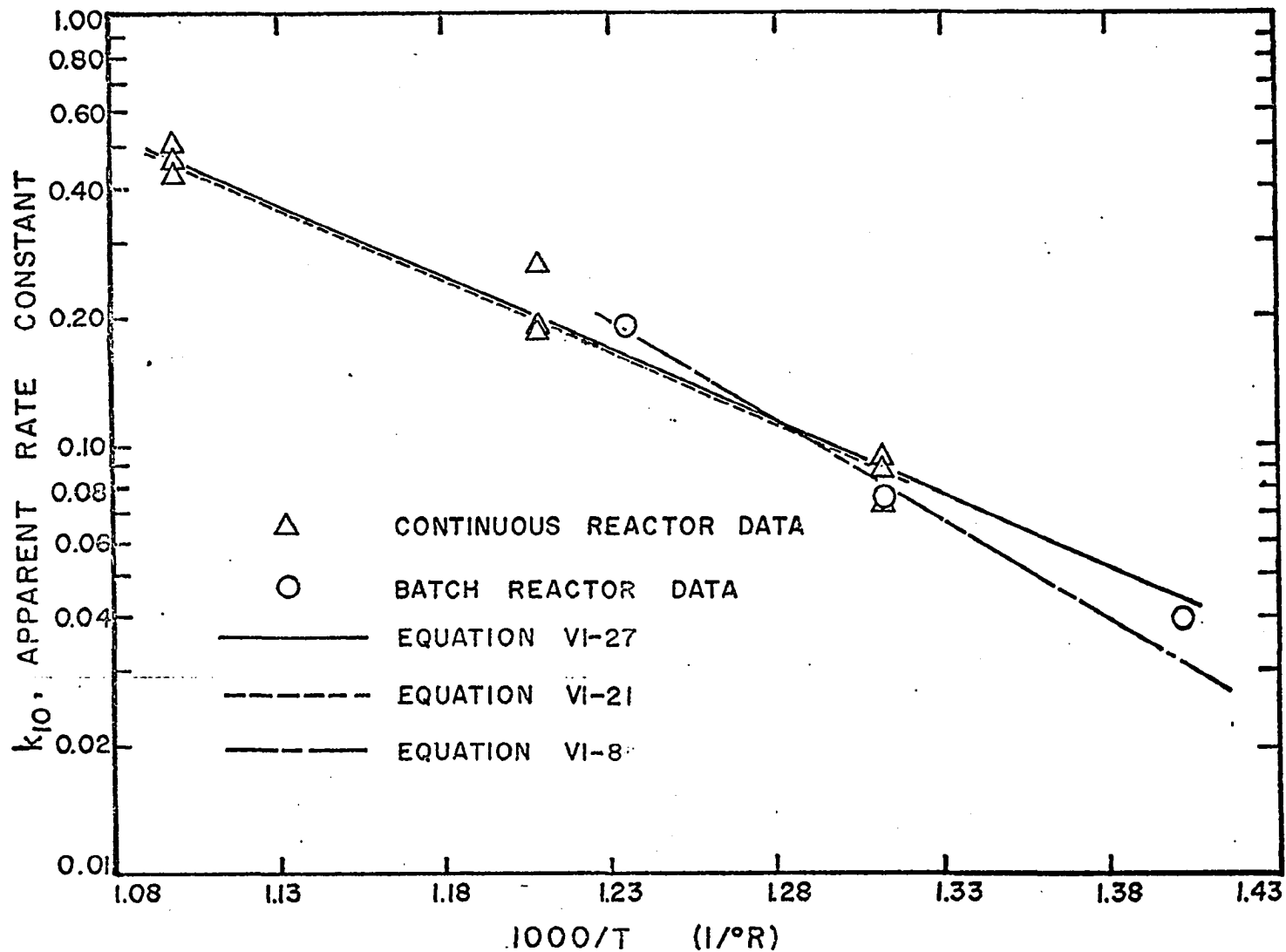


FIG. VI.8 Arrhenius Plot of Apparent Rate Constants of Model 10 with Non-Linear Equation Lines of Best Fit.

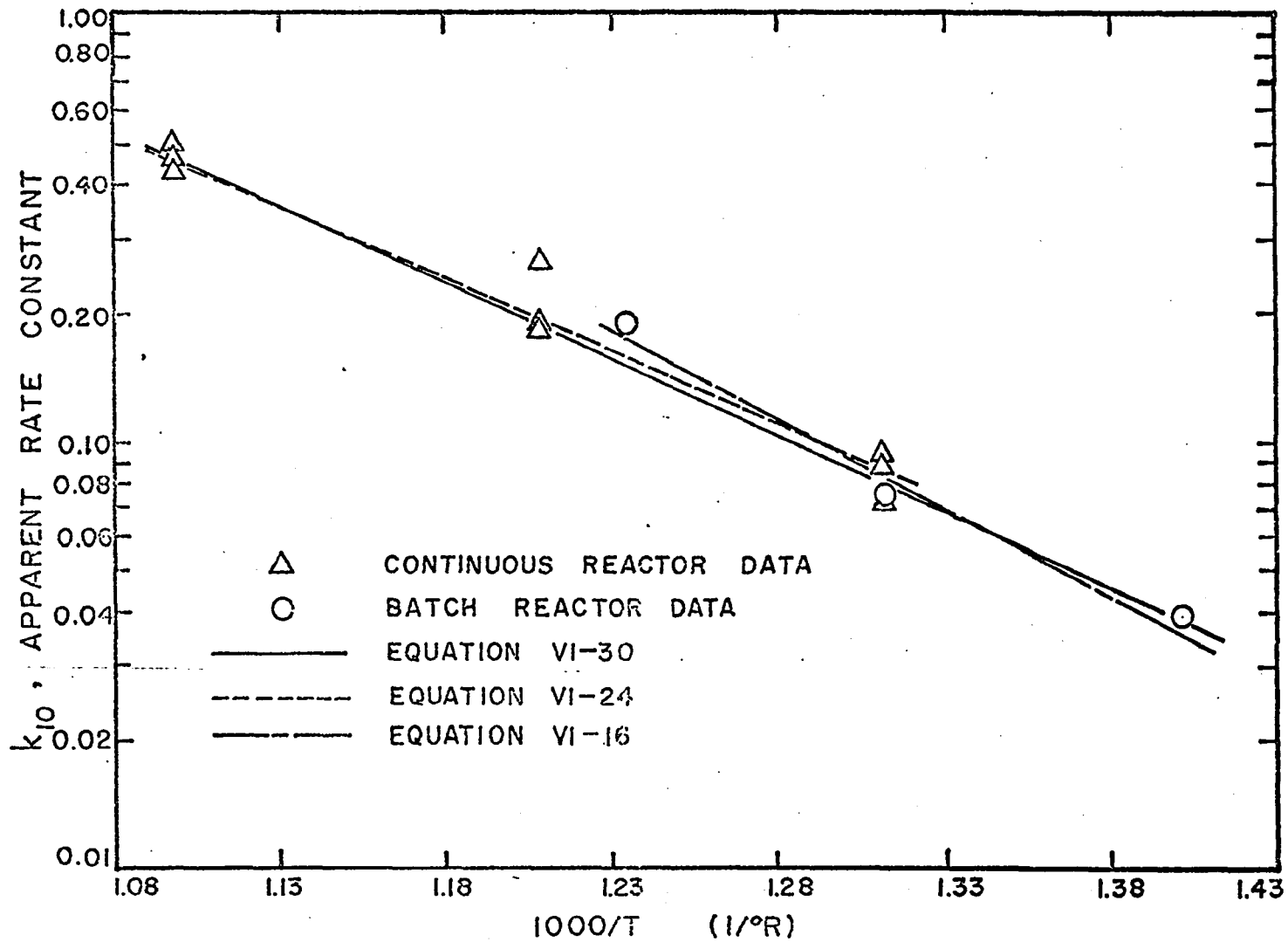


FIG. VI.9 Arrhenius Plot of Apparent Rate Constants of Model 10 with Linearized Equation Lines of Best Fit.

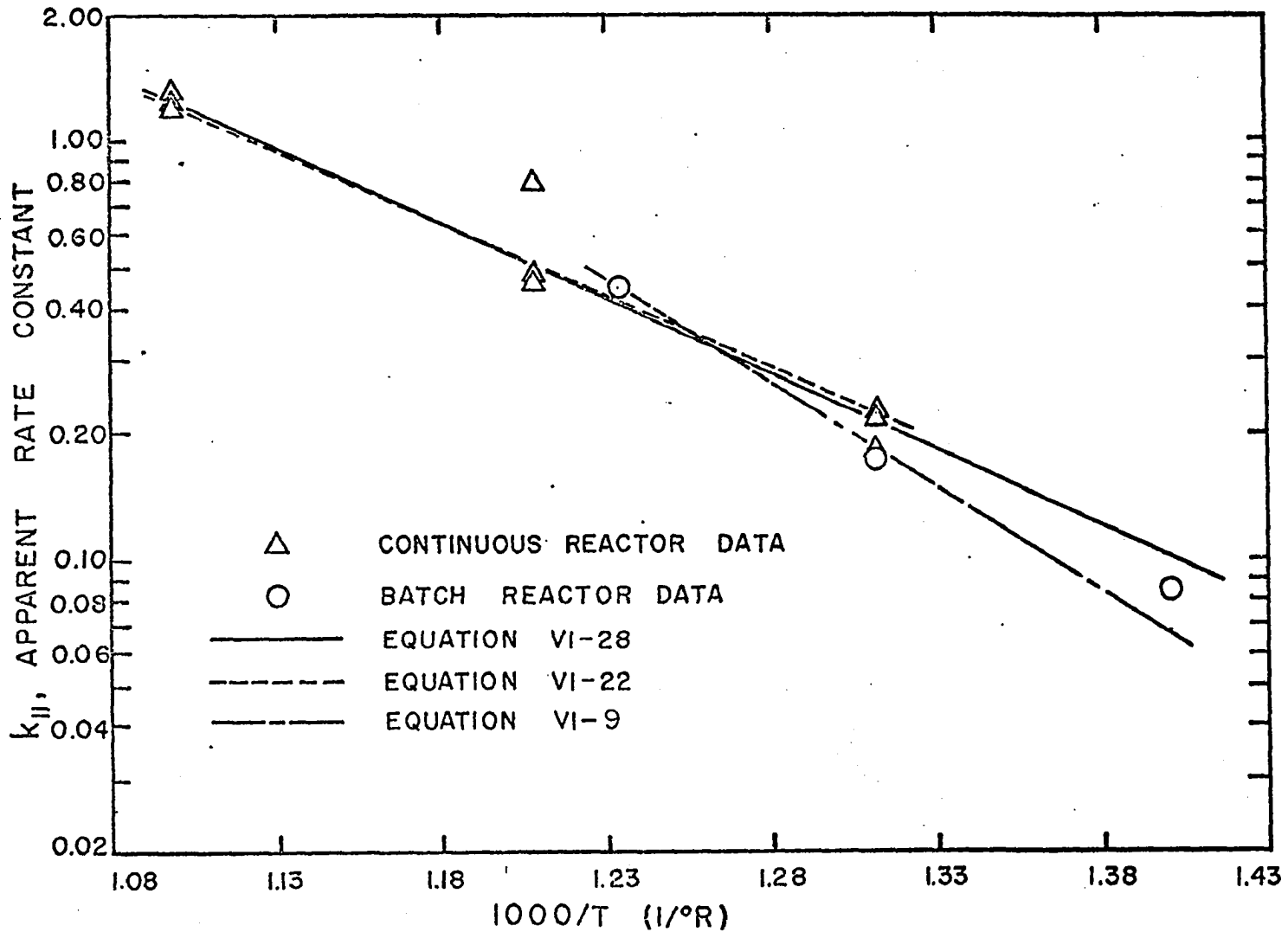


FIG. VI.10 Arrhenius Plot of Apparent Rate Constants of Model 11 with Non-Linear Equation Lines of Best Fit.

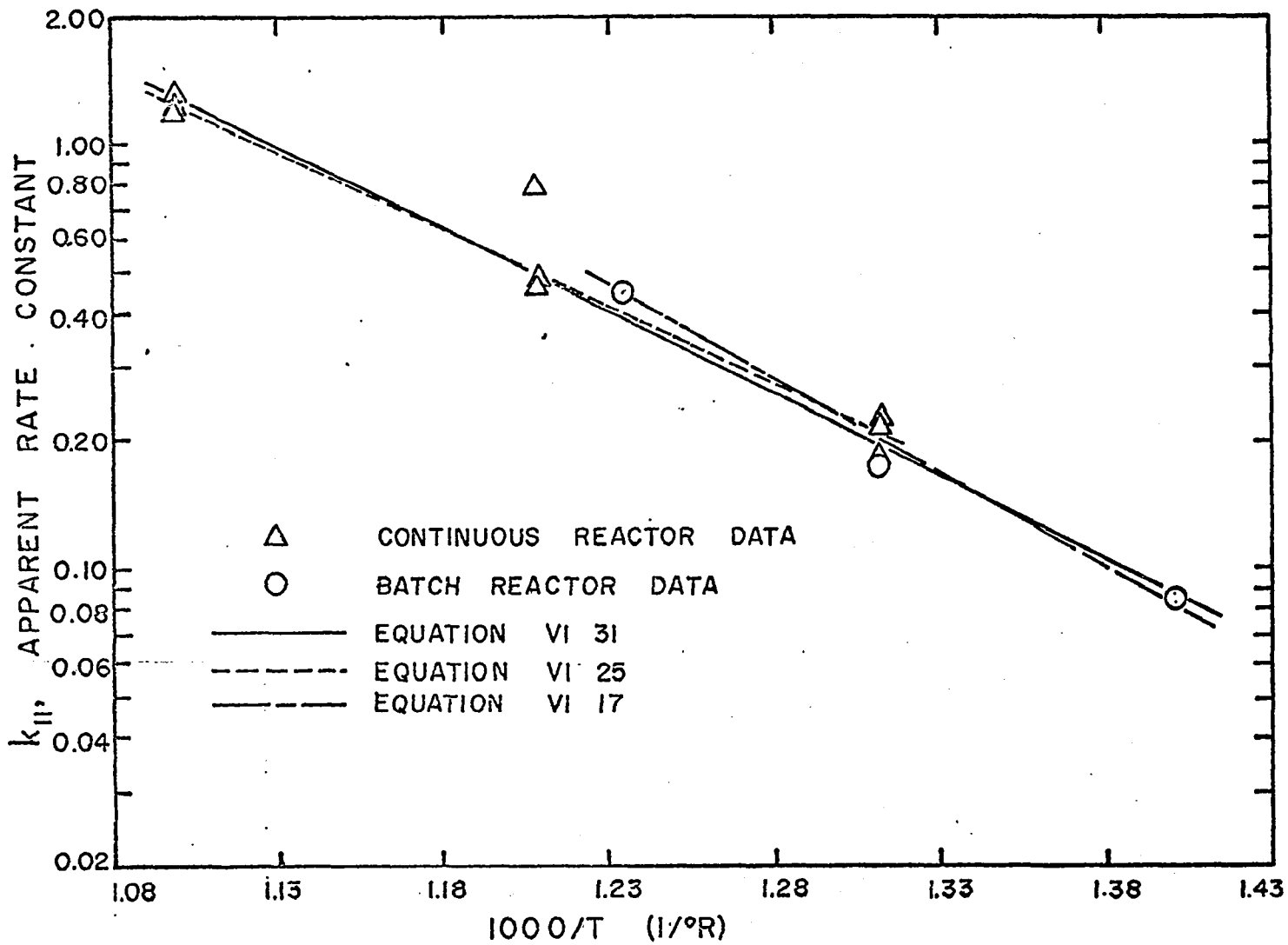


FIG. VI.11 Arrhenius Plot of Apparent Rate Constants of Model 11 with Linearized Equation Lines of Best Fit.

TABLE VI.1 Fluorspar Compositions

	% by wgt.	
	NEWFLUOR	NEWFLUOR
	A	B
CaF ₂	93.9	90.36
CaCO ₃	3.5	7.14
SiO ₂	1.44	1.38
R ₂ O ₃	0.1	0.096
Mean Particle Size	27μ	27μ

NEWFLUOR AF - Newfluor A Reground to A Mean Particle
size of 8μ

NEWFLUOR BF - Newfluor B Reground to a Mean Particle
size of 8μ

TABLE VI.2 Run Parameters for the Continuous Reactor Runs with Mixers at 10 r.p.m.
Using Fluorspar Newfluor - A

Run No.	Acid Feed Rate (g/hr.)	Spar Feed Rate (g/hr.)	Temperatures ($^{\circ}\text{F}$)			Acid:Spar Ratio As Fed	Per Cent Acid Boiloff	Caustic Liquor Feed Rate (l/hr.)	Solids Out Flow Rate (g/hr.)	Transfer Line Sludge Flow Rate (g/l.)
			Inlet	Centre	Outlet					
11A	575	463	290	300	300	1.0096	1.15	57.0	816	0
12A	582	470	360	370	370	1.0079	2.00	70.5	822	0
13A	648	496	300	300	300	1.0632	0.90	70.5	916	0
14A	592	507	300	300	300	0.9502	1.01	70.5	890	0
15A	579	495	370	375	375	0.9519	2.33	70.5	832	0
16A	619	504	450	450	450	0.9995	12.79	70.5	816	62.5
17A	642	495	450	450	450	1.0555	8.24	70.5	852	32.1
18A	642	496	370	370	370	1.0533	4.28	70.5	879	14.45
19A	580	494	450	450	450	0.9547	8.22	70.5	821	31.82

TABLE VI.3

Run Parameters for the Continuous Reactor Factorial Runs

Run No.	Acid Feed Rate (g/hr.)	Spar Feed Rate (g/hr.)	Temperatures ($^{\circ}$ F)			Acid Spar Ratio As Fed	Per Cent Acid Boiloff	Caustic Liquor Feed Rate (Litres/hr.)	Solids Out Rate (g/hr.)	Transfer Line Sludge Flow Rate (g/hr.)
			Inlet	Centre	Outlet					
1F	617	500	370	370	370	1.004	2.71	70.5	882	2.4
2F	614	501	450	450	450	1.004	7.04	70.5	773	25.04
3F	615	502	450	450	450	1.007	8.80	70.5	832.9	33.78
4F	612	500	370	370	370	1.002	2.56	70.5	872	2.36
5F	610	499	450	450	450	0.994	4.36	70.5	821	14.68
6F	611	499	370	370	370	0.9957	2.20	70.5	863	0
7F	615	500	450	450	450	1.008	7.14	70.5	825	33.1
8F	614	502	370	370	370	1.005	1.63	70.5	853	0
9F	610	497	365	365	365	0.998	2.80	70.5	844	6.56
10F	620	498	450	450	450	1.006	11.42	70.5	810	48.66

TABLE VI.3 Con't

Run No.	Mixing Rate (r. p. m.)	Spar Calcite Content % by wt.	Mean Particle Diameter of Spar (In Microns)	Temperature (°F)	Fluorspar Type
1F	20	3.5	27	370	Newfluor A
2F	5.05	7.14	27	450	Newfluor B
3F	15.8	7.14	27	450	Newfluor B
4F	25	7.14	27	370	Newfluor B
5F	15.8	3.5	8	450	Newfluor AF
6F	25	3.5	8	370	Newfluor AF
7F	25	7.14	8	450	Newfluor BF
8F	15.8	7.14	8	370	Newfluor BF
9F	15.8	3.5	27	365	NewFluor A
10F	25	3.5	27	450	NewFluor A

TABLE IV.4, Fractional Age Distribution of Solids
Leaving Reactor $(E(t)\Delta t)_i$

Time Interval (min)	$(E(t)(\Delta t))_i$ Values	
	Run 11A	Run 12A
0-5	0.1221	0.08268
5-10	0.2798	0.22774
10-15	0.1918	0.23075
15-20	0.1042	0.17607
20-25	0.0633	0.09187
25-30	0.0599	0.03003
30-40	0.0386	0.07713
40-50	0.0232	0.02688
50-60	0.0244	0.03126
60-70	0.0169	0.01561
70-80	0.0129	0.00747
80-100	0.0201	0.00250
100-120	0.0059	0
120-140	0.0059	0
140-160	0.0108	0
160-180	0.0097	0
180-200	0.0083	0
200-220	0.0063	0
220-240	0	0

TABLE IV.4 Con't

Time Interval (min)	$(E(t)\Delta t)_i$ Values					
	Run 13A	Run 14A	Run 15 A	Run 16A	Run 17A	Run 18A
0-3	0.0068	0.0638	0.0008	0.0035	0.0008	0.0219
3-6	0.2211	0.2778	0.0668	0.0264	0.0791	0.1745
6-9	0.1214	0.1152	0.0648	0.1003	0.1322	0.1441
9-12	0.0709	0.1029	0.0805	0.2699	0.1512	0.1313
12-15	0.0944	0.0760	0.0910	0.1670	0.0698	0.0710
15-20	0.1434	0.0991	0.1449	0.1365	0.1611	0.1216
20-25	0.0695	0.0712	0.1274	0.0923	0.0790	0.0601
25-30	0.0811	0.0597	0.10967	0.0516	0.0485	0.0546
30-40	0.0763	0.0427	0.1116	0.0796	0.1058	0.0989
40-50	0.0344	0.0281	0.0677	0.0363	0.0564	0.0424
50-60	0.0265	0.0511	0.0251	0.0181	0.0361	0.0338
60-70	0.0127	0.0123	0.0241	0.0121	0.0187	0.0169
70-80	0.0072	0	0.0373	0.0068	0.0154	0.0177
80-100	0.0217	0	0.0457	0	0.0222	0.0059
100-120	0.0080	0	0.0026	0	0.0193	0.0053
120-140	0.0046	0	0	0	0.0069	0
140-160	0	0	0	0	0.0126	0
160-180	0	0	0	0	0.0054	0
180-200	0	0	0	0	0.0084	0
200-220	0	0	0	0	0.0018	0
220-240	0	0	0	0	0.0052	0

TABLE IV.4 Con't

Time Interval (min)	$(E(t)(\Delta t))_i$ Values					
	Run 19A	Run 1F	Run 2F	Run 3F	Run 4F	Run 5F
0-3	0.0142	0.0179	0.0	0.0197	0.0097	0.0237
3-6	0.0594	0.1041	0.0179	0.0949	0.0836	0.0532
6-9	0.1338	0.1414	0.1265	0.0715	0.1401	0.1442
9-12	0.1381	0.1157	0.1220	0.0803	0.1877	0.1475
12-15	0.1045	0.1022	0.0838	0.0826	0.1099	0.0934
15-20	0.1237	0.1899	0.1222	0.1893	0.1152	0.1447
20-25	0.0953	0.1056	0.1090	0.0975	0.08501	0.0763
25-30	0.0854	0.0595	0.0849	0.0864	0.1061	0.0796
30-40	0.1265	0.0623	0.1240	0.1051	0.0766	0.0697
40-50	0.0663	0.0350	0.0960	0.0423	0.0370	0.0356
50-60	0.0247	0.0165	0.0276	0.0391	0.0161	0.0262
60-70	0.0649	0.0247	0.0243	0.0224	0.0096	0.0209
70-80	0.0171	0.0136	0.0134	0.0143	0.0067	0.01802
80-100	0.0046	0.0116	0.0222	0.0146	0.0094	0.0113
100-120	0		0.0097	0.0196	0.0035	0.0142
120-140	0		0.0065	0.0088	0.0038	0.0139
140-160	0		0.0048	0.0055	0	0.0114
160-180	0		0.0051	0.0059	0	0.0089
180-200	0			0	0	0.0073
200-220	0			0	0	0
220-240	0			0	0	0

TABLE VI.4 Con't

Time Interval (min)	$(E(t)\Delta t)_i$ Values				
	Run 6F	Run 7F	Run 8F	Run 9F	Run 10F
0-3	0.0363	0.0779	0.0044	0.0237	0.0288
3-6	0.1267	0.1703	0.0564	0.0589	0.1506
6-9	0.1784	0.1874	0.1219	0.0925	0.1751
9-12	0.1074	0.1471	0.1107	0.0878	0.0996
12-15	0.0948	0.1089	0.1412	0.1486	0.1022
15-20	0.1149	0.1062	0.1303	0.1222	0.1119
20-25	0.0868	0.0768	0.1131	0.1015	0.0756
25-30	0.0599	0.0646	0.0676	0.0614	0.0591
30-40	0.0834	0.0223	0.1228	0.1131	0.0806
40-50	0.0459	0.0258	0.0398	0.0482	0.0552
50-60	0.0254	0.0126	0.0307	0.0256	0.0291
60-70	0.0184	0	0.0198	0.0480	0.0226
70-80	0.0094	0	0.0223	0.0215	0.0057
80-100	0.0071	0	0.0141	0.0085	0.0038
100-120	0.0049	0	0.0047	0.0076	0.00
120-140	0	0	0	0.0129	0.0
140-160	0	0	0	0.0082	0
160-180	0	0	0	0.0050	0
180-200	0	0	0	0.0045	0
200-220	0	0	0	0	0
220-240	0	0	0	0	0

TABLE VI.5 Batch Conversion - Time Data

250°F		300°F		350°F	
Time of Sampling (minutes)	Fractional Conversion of CaF ₂	Time of Sampling (minutes)	Fractional Conversion of CaF ₂	Time of Sampling (minutes)	Fractional Conversion of CaF ₂
1	0.2871	1	0.3747	1	0.5426
2	0.3826	1	0.4358	1	0.5989
3	0.5148	2	0.4274	2	0.5621
3	0.4903	2	0.5627	2	0.6604
4	0.4703	3	0.6256	3	0.6548
4	0.4736	4	0.5724	3	0.7132
4	0.4681	4	0.6001	3 2/3	0.6877
4	0.4847	4	0.6178	4	0.7221
4	0.5119	4	0.6193	5	0.7418
6	0.5351	6	0.6690	7	0.7686
6	0.5609	6	0.6339	9	0.7913
6	0.5634	8	0.6694	11	0.7919
8	0.6046	8	0.6614	16	0.8219
8	0.6205	10	0.6982	16 2/3	0.7947
8	0.6433	10	0.7202	21 2/3	0.8607
10	0.6437	10	0.7238	25	0.8741
10	0.6234	10 1/3	0.7019	31 2/3	0.8891
14	0.6796	14	0.7372		
14	0.6822	14	0.7196		
		18	0.7709		
		18	0.7394		

TABLE VI.6 Least Squares Analysis of Models Using Batch Data

Model	Temp. °F	95% Confidence Interval of Apparent Rate Constant	Correlation Coefficient of I vs. t	Mean Square About Regression $MS_{AR}^{(a)}$	ν	F ^(b) Ratio
9	250	0.0459 \pm 11%	0.9748	0.000904	18	1.01
	300	0.0955 \pm 12%	0.9602	0.001030	20	1.14
	350	0.2558 \pm 14%	0.9603	0.000804	16	< 1
10	250	0.0381 \pm 9.6%	0.9748	0.000739	18	< 1
	300	0.0748 \pm 12%	0.9597	0.001081	20	1.21
	350	0.188 \pm 8.9%	0.9762	0.001006	16	1.12
11	250	0.084 \pm 11%	0.9749	0.000824	18	< 1
	300	0.171 \pm 12%	0.9602	0.001032	20	1.14
	350	0.444 \pm 14%	0.9721	0.000857	16	< 1
6	250	0.0880 \pm 13%	0.9573	0.00518	18	5.78 ^(a)
	300	0.130 \pm 22%	0.9276	0.01203	20	13.41 ^(d)
	350	0.273 \pm 24%	0.9722	0.01171	16	13.05 ^(d)
7	250	0.0211 \pm 7.4%	0.9693	0.000699	18	< 1
	300	0.0348 \pm 14%	0.9452	0.002705	20	3.02 ^(a)
	350	0.0747 \pm 22%	0.9772	0.004275	16	4.76 ^(c)

$$(a) \quad MS_{AR} = \frac{\sum_i (x_{Bi} - \hat{x}_{Bi})^2}{\nu}$$

$$(b) \quad F = \frac{MS_{AR}}{S_E^2}$$

$$S_E^2 = 0.000897 \quad \text{with 23 degrees of freedom}$$

(c) significant at the 5% level of significance

(d) significant at the 1% level of significance

TABLE VI.7A Least Squares fit of the batch data apparent
rate constants to the non-linear Arrhenius equation

Model	E (Btu/lb mole) $\times 10^{-3}$	k_T ($\text{min}^{-1} \times -2$)	S_R^2 Variance of Residuals $\sum_i (k_i - \hat{k}_i)^2 / (n-p)$
9	22.19	0.102	1.431×10^{-4}
10	20.52	0.0775	8.61×10^{-5}
11	21.48	0.176	4.544×10^{-4}

TABLE VI.7B Least squares fit of the batch data
apparent rate constants to the Linearized
Arrhenius equation

Model	E (Btu/lb mole) $\times 10^{-3}$	k_T ($\text{min}^{-1} \times^{-2}$)	Correlation Coefficient	S_R^2 Variance of Residuals $\sum_i (\ln k_i - \ln \hat{k}_i)^2 / (n - p)$
9	19.53	0.104	-0.9924	0.02235
10	18.15	0.0812	-0.9920	0.02044
11	18.94	0.185	-0.9922	0.02158

TABLE VI.8 Average Conversion of Spar and Apparent Rate Constants for A runs

Run No.	Temperature OF	Observed Average Conversion of CaF ₂	Corrected Acid:Spar Ratio	Apparent Rate Constant Values		
				Model 9	Model 10	Model 11
11A	300	0.7463	0.9982	0.123	0.0874	0.211
13A	300	0.7683	1.0551	0.105	0.0731	0.178
14A	300	0.6919	0.9403	0.127	0.0948	0.222
12A	370	0.8431	0.9873	0.428	0.266	0.698
15A	370	0.7886	0.9308	0.283	0.188	0.471
18A	370	0.8249	1.0080	0.281	0.1812	0.464
16A	450	0.8026	0.8728	0.798	0.508	1.306
17A	450	0.8766	0.9654	0.749	0.432	1.185
19A	450	0.8019	0.8749	0.726	0.469	1.195
BATCH	250	-	1	0.0459	0.0381	0.0840
BATCH	300	-	1	0.0955	0.0748	0.171
BATCH	350	-	1	0.256	0.188	0.444

TABLE VI.9

Least squares fit of the continuous reactor data apparent rate constants to the non-linear Arrhenius equation

Model	95% Confidence Interval of Parameters		s_R^2 Variance of Residuals $\sum_i \frac{(k_i - \hat{k}_i)^2}{n - p}$	$s_{E,k}^2$ Variance Due to Pure Error
	E (Btu/lb mole) $\times 10^{-3}$	k (min ⁻¹ $\times 10^{-2}$)		
9	16.2 \pm 3.37	0.317 \pm 0.0537	2.559 $\times 10^{-3}$	2.868 $\times 10^{-3}$
10	15.27 \pm 3.35	0.206 \pm 0.0344	1.09 $\times 10^{-3}$	1.26 $\times 10^{-3}$
11	15.8 \pm 3.28	0.524 \pm 0.0860	6.66 $\times 10^{-3}$	7.60 $\times 10^{-3}$

TABLE VI.10

Least square fit of the continuous reactor data apparent rate constants to the Linearized Arrhenius equation

Model	95% Confidence Interval of Parameters E (Btu/lb mole) $\times 10^{-3}$	k (min ⁻¹ \times 10^{-2})	Correlation Coefficient	S_R^2 Variance of Residuals $\sum_i \frac{(\ln k_i - \ln \hat{k}_i)^2}{n - p}$	$S_{E, \ln k}^2$ Variance Due to Pure Error
9	17.02 \pm 2.58	0.307 \pm 0.0339	-0.9860	0.02121	0.02358
10	15.68 \pm 2.50	0.202 \pm 0.0216	-0.9845	0.01990	0.0215
11	16.50 \pm 2.53	0.5104 \pm 0.0554	-0.9856	0.02048	0.02310

TABLE VI.11 Least squares fit of the continuous reactor and batch reactor data apparent rate constants to the non-linear Arrhenius equation

Model	95% Confidence Interval of Parameters		S_R^2	$S_{E,k}^2$
	E (Btu/lb mole) $\times 10^{-3}$	k_T ($\text{min}^{-1} \cdot \text{X}^{-2}$)	Variance of Residuals $\frac{\sum_i (k_i - \hat{k}_i)^2}{n - p}$	Variance Due to Pure Error
9	16.4 \pm 2.41	0.247 \pm 0.0371	1.92 $\times 10^{-3}$	2.87 $\times 10^{-3}$
10	15.2 \pm 2.35	0.166 \pm 0.0239	8.314 $\times 10^{-4}$	12.6 $\times 10^{-4}$
11	15.9 \pm 2.32	0.414 \pm 0.0595	5.004 $\times 10^{-3}$	7.60 $\times 10^{-3}$

TABLE VI.12 Least squares fit of the continuous reactor and batch reactor data apparent rate constants to the linearized Arrhenius equation.

Model	95% Confidence Interval of Parameters		Correlation Coefficient	S_R^2 Variance of Residuals $\frac{\sum_i (\ln k_i - \hat{\ln k}_i)^2}{n - p}$	$S_{E, \ln k}^2$ Variance Due to Pure Error
	E (Btu/lb.mole) $\times 10^{-3}$	k_T^{-1} (min $^{-1}$ X $^{-2}$)			
9	17.9 \pm 1.87	0.234 \pm 0.0206	-0.9891	2.121 $\times 10^{-2}$	2.36 $\times 10^{-2}$
10	16.1 \pm 1.75	0.161 \pm 0.0133	-0.9883	1.990 $\times 10^{-2}$	2.15 $\times 10^{-2}$
11	17.2 \pm 1.79	0.396 \pm 0.0335	-0.9892	2.048 $\times 10^{-2}$	2.31 $\times 10^{-2}$

TABLE VI.13, TABLE OF RESIDUALS FOR THE LEAST SQUARES FIT OF THE
 APPARENT RATE CONSTANTS OF THE A-RUNS OF THE CONTINUOUS
 REACTOR TO THE NON-LINEAR ARRHENIUS EQUATION

MODEL 9				
TEMP. DEG.R	ACID-SPAR RATIO	OBSERVED RATE CONSTANT	PREDICTED RATE CONSTANT	ERROR IN LINEAR TERMS
760.0	9.9820E-01	1.2344E-01	1.3037E-01	-6.9357E-03
760.0	1.0551E+00	1.0523E-01	1.3037E-01	-2.5145E-02
760.0	9.4030E-01	1.2723E-01	1.3037E-01	-3.1457E-03
830.0	9.8730E-01	4.2835E-01	3.2127E-01	1.0707E-01
830.0	9.3080E-01	2.8306E-01	3.2127E-01	-3.8212E-02
830.0	1.0080E+00	2.8140E-01	3.2127E-01	-3.9872E-02
910.0	8.7280E-01	7.9799E-01	7.5983E-01	3.8154E-02
910.0	9.6540E-01	7.4924E-01	7.5983E-01	-1.0595E-02
910.0	8.7490E-01	7.2607E-01	7.5983E-01	-3.3765E-02

Reproduced with permission of the copyright owner. Further reproduction prohibited without permission.

TABLE VI.13, CONTD.

MODEL 10

TEMP. DEG.R	ACID-SPAR RATIO	OBSERVED RATE CONSTANT	PREDICTED RATE CONSTANT	ERROR IN LINEAR TERMS
760.0	9.9820E-01	8.7400E-02	8.8866E-02	-1.4664E-03
760.0	1.0551E+00	7.3100E-02	8.8866E-02	-1.5766E-02
760.0	9.4030E-01	9.4800E-02	8.8866E-02	5.9335E-03
830.0	9.8730E-01	2.6591E-01	2.0848E-01	5.7426E-02
830.0	9.3080E-01	1.8800E-01	2.0848E-01	-2.0483E-02
830.0	1.0080E+00	1.8120E-01	2.0848E-01	-2.7283E-02
910.C	8.7280E-01	5.0750E-01	4.7048E-01	3.7012E-02
910.0	9.6540E-01	4.3187E-01	4.7048E-01	-3.8617E-02
910.0	8.7490E-01	4.6925E-01	4.7048E-01	-1.2371E-03

TABLE VI.13. CONTD.

MODEL 11

TEMP. DEG.R	ACID-SPAR RATIO	OBSERVED RATE CONSTANT	PREDICTED RATE CONSTANT	ERROR IN LINEAR TERMS
760.0	9.9820E-01	2.1068E-01	2.1976E-01	-9.0833E-03
760.0	1.0551E+00	1.7827E-01	2.1976E-01	-4.1493E-02
760.0	9.4030E-01	2.2203E-01	2.1976E-01	2.2666E-03
830.0	9.8730E-01	6.9757E-01	5.3076E-01	1.6680E-01
830.0	9.3080E-01	4.7095E-01	5.3076E-01	-5.9803E-02
830.0	1.0080E+00	4.6419E-01	5.3076E-01	-6.6573E-02
910.0	8.7280E-01	1.3057E+00	1.2314E+00	7.4258E-02
910.0	9.6540E-01	1.1850E+00	1.2314E+00	-4.6441E-02
910.0	8.7490E-01	1.1949E+00	1.2314E+00	-3.6541E-02

TABLE VI.14, TABLE OF RESIDUALS FOR THE LEAST SQUARES FIT OF THE APPARENT RATE CONSTANTS OF THE A-RUNS OF THE CONTINUOUS REACTOR TO THE LINEARIZED ARRHENIUS EQUATION

MODEL 9

TEMP. DEG.R	ACID-SPAR RATIO	RATE CONSTANT	LN(K)	LN(K) PREDICTED	ERROR IN LOG TERMS
760.0	9.9820E-01	1.2344E-01	-2.0920E+00	-2.1790E+00	8.7090E-02
760.0	1.0551E+00	1.0523E-01	-2.2516E+00	-2.1790E+00	-7.2516E-02
760.0	9.4030E-01	1.2723E-01	-2.0617E+00	-2.1790E+00	1.1733E-01
830.0	9.8730E-01	4.2835E-01	-8.4781E-01	-1.1815E+00	3.3369E-01
830.0	9.3080E-01	2.8306E-01	-1.2620E+00	-1.1815E+00	-8.0591E-02
830.0	1.0080E+00	2.8140E-01	-1.2679E+00	-1.1815E+00	-8.6473E-02
910.0	8.7280E-01	7.9799E-01	-2.2565E-01	-2.2933E-01	3.6761E-03
910.0	9.6540E-01	7.4924E-01	-2.8869E-01	-2.2933E-01	-5.9360E-02
910.0	8.7490E-01	7.2607E-01	-3.2010E-01	-2.2933E-01	-9.0773E-02

TABLE VI.14, CONTD.

MODEL 1U

TEMP. DEG.R	ACID-SPAR RATIO	RATE CONSTANT	LN(K)	LN(K) PREDICTED	ERROR IN LOG TERMS
760.0	9.9820E-01	8.7400E-02	-2.4372E+00	-2.4612E+00	2.3979E-02
760.0	1.0551E+00	7.3100E-02	-2.6159E+00	-2.4612E+00	-1.5468E-01
760.0	9.4030E-01	9.4800E-02	-2.3559E+00	-2.4612E+00	1.0525E-01
830.0	9.8730E-01	2.6591E-01	-1.3245E+00	-1.5853E+00	2.6073E-01
830.0	9.3080E-01	1.8800E-01	-1.6713E+00	-1.5853E+00	-8.5976E-02
830.0	1.0080E+00	1.8120E-01	-1.7081E+00	-1.5853E+00	-1.2281E-01
910.0	8.7280E-01	5.0750E-01	-6.7825E-01	-7.4931E-01	7.1051E-02
910.0	9.6540E-01	4.3187E-01	-8.3963E-01	-7.4931E-01	-9.0320E-02
910.0	8.7490E-01	4.6925E-01	-7.5661E-01	-7.4931E-01	-7.3092E-03

TABLE VI.14, CONTD.

MODEL 11

TEMP.	ACID-SPAR	RATE	LN(K)	LN(K)	PREDICTED	ERROR IN
DEG.R	RATIO	CONSTANT			LOG TERMS	
760.0	9.9820E-01	2.1068E-01	-1.5574E+00	-1.5801E+00	2.2705E-02	
760.0	1.0551E+00	1.7827E-01	-1.7244E+00	-1.5801E+00	-1.4433E-01	
760.0	9.4030E-01	2.2203E-01	-1.5049E+00	-1.5801E+00	7.5177E-02	
830.0	9.8730E-01	6.9757E-01	-3.6015E-01	-6.5853E-01	2.9838E-01	
830.0	9.3080E-01	4.7096E-01	-7.5298E-01	-6.5853E-01	-9.4444E-02	
830.0	1.0080E+00	4.6419E-01	-7.6746E-01	-6.5853E-01	-1.0892E-01	
910.0	8.7280E-01	1.3057E+00	2.6673E-01	2.2108E-01	4.5649E-02	
910.0	9.6540E-01	1.1850E+00	1.6974E-01	2.2108E-01	-5.1346E-02	
910.0	8.7490E-01	1.1949E+00	1.7006E-01	2.2108E-01	-4.3026E-02	

TABLE VI.15, TABLE OF RESIDUALS FOR THE LEAST SQUARES FIT OF THE APPARENT RATE CONSTANTS OF THE A-RUNS OF THE CONTINUOUS REACTOR AND THE BATCH REACTOR TO THE NON-LINEAR ARRHENIUS EQUATION

MODEL 9

TEMP. DEG.R	ACID-SPAR RATIO	OBSERVED RATE CONSTANT	PREDICTED RATE CONSTANT	ERROR IN LINEAR TERMS
760.0	9.9820E-01	1.2344E-01	1.2641E-01	-2.9793E-03
760.0	1.0551E+00	1.0523E-01	1.2641E-01	-2.1189E-02
760.0	9.4030E-01	1.2723E-01	1.2641E-01	8.1069E-04
830.0	9.8730E-01	4.2835E-01	3.1678E-01	1.1156E-01
830.0	9.3080E-01	2.8306E-01	3.1678E-01	-3.3726E-02
830.0	1.0080E+00	2.8140E-01	3.1678E-01	-3.5386E-02
910.0	8.7280E-01	7.9799E-01	7.6130E-01	3.6688E-02
910.0	9.6540E-01	7.4924E-01	7.6130E-01	-1.2061E-02
910.0	8.7490E-01	7.2607E-01	7.6130E-01	-3.5231E-02
710.0	1.0000E+00	4.5940E-02	5.8706E-02	-1.2766E-02
760.0	1.0000E+00	9.5500E-02	1.2641E-01	-3.0919E-02
810.0	1.0000E+00	2.5580E-01	2.4763E-01	8.1629E-03

TABLE VI.15 CONTD.

MODEL 10

TEMP. DEG.R	ACID-SPAR RATIO	OBSERVED RATE CONSTANT	PREDICTED RATE CONSTANT	ERROR IN LINEAR TERMS
760.0	9.9820E-01	8.7400E-02	8.9563E-02	-2.1637E-03
760.0	1.0551E+00	7.3100E-02	8.9563E-02	-1.6463E-02
760.0	9.4030E-01	9.4800E-02	8.9563E-02	5.2362E-03
830.0	9.8730E-01	2.6591E-01	2.0941E-01	5.6492E-02
830.0	9.3080E-01	1.8800E-01	2.0941E-01	-2.1417E-02
830.0	1.0080E+00	1.8120E-01	2.0941E-01	-2.8217E-02
910.0	8.7280E-01	5.0750E-01	4.7108E-01	3.6415E-02
910.0	9.6540E-01	4.3137E-01	4.7108E-01	-3.9214E-02
910.0	8.7490E-01	4.6925E-01	4.7108E-01	-1.8341E-03
710.0	1.0000E+00	3.8060E-02	4.4067E-02	-6.0070E-03
760.0	1.0000E+00	7.4780E-02	8.9563E-02	-1.4783E-02
810.0	1.0000E+00	1.8780E-01	1.6677E-01	2.1027E-02

TABLE VI.15, CONTD.

MODEL 11

TEMP. DEG.R	ACID-SPAR RATIO	OBSERVED RATE CONSTANT	PREDICTED RATE CONSTANT	ERROR IN LINEAR TERMS
760.0	9.9820E-01	2.1068E-01	2.1634E-01	-5.6623E-03
760.0	1.0551E+00	1.7827E-01	2.1634E-01	-3.8072E-02
760.0	9.4030E-01	2.2203E-01	2.1634E-01	5.6876E-03
830.0	9.8730E-01	6.9757E-01	5.2719E-01	1.7037E-01
830.0	9.3080E-01	4.7096E-01	5.2719E-01	-5.6231E-02
830.0	1.0080E+00	4.6419E-01	5.2719E-01	-6.3001E-02
910.0	8.7280E-01	1.3057E+00	1.2336E+00	7.2072E-02
910.0	9.6540E-01	1.1850E+00	1.2336E+00	-4.8628E-02
910.0	8.7490E-01	1.1949E+00	1.2336E+00	-3.8728E-02
710.0	1.0000E+00	8.4040E-02	1.0283E-01	-1.8794E-02
760.0	1.0000E+00	1.7050E-01	2.1634E-01	-4.5842E-02
810.0	1.0000E+00	4.4440E-01	4.1521E-01	2.9189E-02

TABLE VI.16, TABLE OF RESIDUALS FOR THE LEAST SQUARES FIT OF THE
 APPARENT RATE CONSTANTS OF THE A-RUNS OF THE CONTINUOUS
 REACTOR AND THE BATCH REACTOR TO THE LINEARIZED
 ARRHENIUS EQUATION

MODEL 9

TEMP. DEG.R	ACID-SPAR RATIO	RATE CONSTANT	LN(K)	LN(K) PREDICTED	ERROR IN LOG TERMS
760.0	9.9820E-01	1.2344E-01	-2.0920E+00	-2.1158E+00	2.3856E-02
760.0	1.0551E+00	1.0523E-01	-2.2516E+00	-2.1158E+00	-1.3575E-01
760.0	9.4030E-01	1.2723E-01	-2.0617E+00	-2.1158E+00	5.4098E-02
830.0	9.8730E-01	4.2835E-01	-8.4781E-01	-1.1652E+00	3.1747E-01
830.0	9.3080E-01	2.8306E-01	-1.2620E+00	-1.1652E+00	-9.6804E-02
830.0	1.0080E+00	2.8140E-01	-1.2679E+00	-1.1652E+00	-1.0268E-01
910.0	8.7280E-01	7.9799E-01	-2.2565E-01	-2.5800E-01	3.2342E-02
910.0	9.6540E-01	7.4924E-01	-2.8869E-01	-2.5800E-01	-3.0694E-02
910.0	8.7490E-01	7.2607E-01	-3.2010E-01	-2.5800E-01	-6.2107E-02
710.0	1.0000E+00	4.5940E-02	-3.0804E+00	-2.9095E+00	-1.7083E-01
760.0	1.0000E+00	9.5500E-02	-2.3486E+00	-2.1158E+00	-2.3277E-01
810.0	1.0000E+00	2.5580E-01	-1.3633E+00	-1.4201E+00	5.6758E-02

TABLE VI.16, CONTD.

MODEL 10

TEMP. DEG.R	ACID-SPAR RATIO	RATE CONSTANT	LN(K)	LN(K) PREDICTED	ERROR IN LOG TERMS
760.0	9.9820E-01	8.7400E-02	-2.4372E+00	-2.4831E+00	4.5913E-02
760.0	1.0551E+00	7.3100E-02	-2.6159E+00	-2.4831E+00	-1.3275E-01
760.0	9.4030E-01	9.4800E-02	-2.3559E+00	-2.4831E+00	1.2718E-01
830.0	9.8730E-01	2.6591E-01	-1.3245E+00	-1.5840E+00	2.5949E-01
830.0	9.3080E-01	1.8800E-01	-1.6713E+00	-1.5840E+00	-8.7217E-02
830.0	1.0080E+00	1.8120E-01	-1.7081E+00	-1.5840E+00	-1.2405E-01
910.0	8.7280E-01	5.0750E-01	-6.7825E-01	-7.2594E-01	4.7690E-02
910.0	9.6540E-01	4.3187E-01	-8.3963E-01	-7.2594E-01	-1.1368E-01
910.0	8.7490E-01	4.6925E-01	-7.5661E-01	-7.2594E-01	-3.0670E-02
710.0	1.0000E+00	3.8060E-02	-3.2685E+00	-3.2339E+00	-3.4678E-02
760.0	1.0000E+00	7.4780E-02	-2.5932E+00	-2.4831E+00	-1.1003E-01
810.0	1.0000E+00	1.8780E-01	-1.6723E+00	-1.3251E+00	1.5274E-01

TABLE VI.16, CONTD.

MODEL 11

TEMP. DEG.R	ACID-SPAR RATIO	RATE CONSTANT	LN(K)	LN(K) PREDICTED	ERROR IN LOG TERMS
760.0	9.9820E-01	2.1068E-01	-1.5574E+00	-1.6249E+00	6.7540E-02
760.0	1.0551E+00	1.7827E-01	-1.7244E+00	-1.6249E+00	-9.9500E-02
760.0	9.4030E-01	2.2203E-01	-1.5049E+00	-1.6249E+00	1.2001E-01
830.0	9.8730E-01	6.9757E-01	-3.6015E-01	-6.6718E-01	3.0703E-01
830.0	9.3080E-01	4.7096E-01	-7.5298E-01	-6.6718E-01	-8.5795E-02
830.0	1.0090E+00	4.6419E-01	-7.6746E-01	-6.6718E-01	-1.0027E-01
910.0	8.7280E-01	1.3057E+00	2.6673E-01	2.4697E-01	1.9760E-02
910.0	9.6540E-01	1.1850E+00	1.6974E-01	2.4697E-01	-7.7236E-02
910.0	3.7490E-01	1.1949E+00	1.7806E-01	2.4697E-01	-6.8916E-02
710.0	1.0000E+00	8.4040E-02	-2.4764E+00	-2.4247E+00	-5.1759E-02
760.0	1.0000E+00	1.7050E-01	-1.7690E+00	-1.6249E+00	-1.4406E-01
810.0	1.0000E+00	4.4440E-01	-8.1103E-01	-9.2394E-01	1.1291E-01

TABLE VI.17, PREDICTED CONVERSIONS

MODEL 9

RUN NO.	CORRECTED ACID-SPAR RATIO	OBSERVED CONVERSIONS	PREDICTED CONVERSIONS ^①			
			1	2	3	4
11A	0.9982	0.7463	0.7516	0.7444	0.7487	0.7392
13A	1.0551	0.7683	0.7888	0.7816	0.7862	0.7762
14A	0.9403	0.6819	0.6941	0.6868	0.6913	0.6814
12A	0.9873	0.8431	0.8235	0.8216	0.8227	0.8204
15A	0.9308	0.7886	0.7973	0.7953	0.7963	0.7938
18A	1.0080	0.8249	0.8347	0.8324	0.8335	0.8310
16A	0.8728	0.8026	0.8004	0.8011	0.8007	0.8020
17A	0.9654	0.9766	0.8772	0.8781	0.8774	0.8786
19A	0.8749	0.8019	0.8036	0.8046	0.8036	0.8051
VARIANCE OF ERRORS X 1.0E 04			1.452	1.106	1.256	1.167
STANDARD DEVIATION OF ERRORS			0.0121	0.0105	0.0112	0.0108

① REFER TO PAGE 80

TABLE VI.17, CONTD.

MODEL 10		PREDICTED CONVERSIONS				
RUN NO.	CORRECTED ACID-SPAR RATIO	OBSERVED CONVERSIONS	1	2	3	4
11A	0.9982	0.7463	0.7481	0.7437	0.7491	0.7415
13A	1.0551	0.7683	0.7891	0.7853	0.7902	0.7828
14A	0.9403	0.6819	0.6852	0.6812	0.6861	0.6790
12A	0.9173	0.8431	0.8246	0.8232	0.8250	0.8233
15A	0.9308	0.7886	0.7962	0.7949	0.7965	0.7949
18A	1.0080	0.8249	0.8363	0.8350	0.8368	0.8352
16A	0.8728	0.8026	0.7991	0.7992	0.7992	0.8001
17A	0.9654	0.8766	0.8808	0.8811	0.8808	0.8820
19A	0.8749	0.8019	0.8021	0.8023	0.8022	0.8034
VARIANCE OF ERRORS X 1.0E 04			1.505	1.40	1.545	1.393
STANDARD DEVIATION OF ERRORS			0.0123	0.0118	0.0124	0.0118

TABLE VI.17, CONTU.

MODEL 11

P/JN NO.	CORRECTED ACIU-SPAR RATIO	OBSERVED CONVERSIONS	PREDICTED CONVERSIONS			
			1	2	3	4
11A	0.9982	0.7463	0.7504	0.7442	0.7487	0.7399
13A	1.0551	0.7683	0.7893	0.7829	0.7876	0.7784
14A	0.9403	0.6819	0.6908	0.6847	0.6895	0.6802
12A	0.9873	0.8431	0.8241	0.8222	0.8234	0.8215
15A	0.9308	0.7886	0.7970	0.7952	0.7963	0.7946
18A	1.0080	0.8249	0.8352	0.8334	0.8348	0.8329
16A	0.8728	0.8026	0.8000	0.8004	0.8003	0.8017
17A	0.9554	0.8766	0.8784	0.8790	0.8786	0.8802
19A	0.8749	0.8019	0.8031	0.8036	0.8032	0.8048
VARIANCE OF ERRORS X 1.0E 04			1.440	1.251	1.342	1.402
STANDARD DEVIATION OF ERRORS			0.0120	0.0112	0.0116	0.0118

TABLE VI.18 Observed Conversion of CaF_2 and Apparent Rate Constants for Runs 1F-10F.

Run No.	Temperature $^{\circ}\text{F}$ (coded value)	Mixing Rate r.p.m. (coded value)	Per Cent CaCO_3 Content of Spar (coded value)	Fluorspar Used (Newfluor) (Fineness Coded value)	Corrected Acid:Spar Ratio	Observed Conversion of CaF_2	Apparent Rate Constants		
							Model 9	Model 10	Model 11
1 F	370	20	3.5	A (-1)	0.9762	0.8117	0.279	0.1820	0.4603
2 F	450	5.05	7.14	B (-1)	0.9329	0.8827	1.579	0.876	2.453
3 F	450(+1)	15.8(-1)	7.14(+1)	B (-1)	0.9190	0.8669	1.637	0.938	2.581
4 F	370(-1)	25 (+1)	7.14(+1)	B (-1)	0.9766	0.8594	0.611	0.364	0.975
5 F	450(+1)	15.8(-1)	3.5 (-1)	AF(+1)	0.9510	0.8582	0.714	0.426	1.140
6 F	370(-1)	25 (+1)	3.5 (-1)	AF(+1)	0.9736	0.8399	0.487	0.303	0.792
7 F	450(+1)	25 (+1)	7.14(+1)	BF(+1)	0.9366	0.8507	1.417	0.857	2.285
8 F	370(-1)	15.8(-1)	7.14(+1)	BF(+1)	0.9904	0.8787	0.616	0.356	0.971
9 F	370(-1)	15.8(-1)	3.5 (-1)	A (-1)	0.9682	0.8155	0.251	0.163	0.413
10 F	450(+1)	25 (+1)	3.5 (-1)	A (-1)	0.8925	0.8182	1.005	0.637	1.648

TABLE VI.19 Natural Logarithm of the Apparent Rate Constants with the Coded Factors

Run No.	Design Code No.	Observed Conversion of CaF ₂	Corrected Acid:Spar Ratio	Factors				Natural Logarithm of Apparent Rate Constant		
				X ₁	X ₂	X ₃	X ₄	Model 9	Model 10	Model 11
9F	1	0.8155	0.9682	-1	-1	-1	-1	-1.3823	-1.814	-0.884
10F	ad	0.8182	0.8925	+1	-1	-1	+1	0.00499	-0.451	0.4996
3F	bd	0.8669	0.9190	-1	+1	-1	+1	0.49286	-0.0640	0.94818
4F	ab	0.8594	0.9766	+1	+1	-1	-1	-0.4927	-1.0106	-0.0253
5F	c	0.8582	0.9510	-1	-1	+1	+1	-0.3369	-0.8533	+0.13103
6F	ac	0.8399	0.9737	+1	-1	+1	-1	-0.7195	-1.194	-0.2332
8F	bc	0.8787	0.9904	-1	+1	+1	-1	-0.4845	-1.0328	-0.0294
7F	abcd	0.8507	0.9366	+1	+1	+1	+1	+0.3485	-0.1543	0.8264
1F		0.8177	0.9762	-	-	-	-	-1.2765	-1.704	-0.7765
2F		0.8827	0.9329	-	-	-	-	+0.4568	-0.1324	0.8973

Table VI.20 Mean Differences of $\ln k$

Factors	Mean Effect of Factor		
	Model 9	Model 10	Model 11
mean $\ln k$	-0.3389	-0.82176	0.15411
$x_1 + x_2 x_3 x_4$	0.21054	0.2377	0.2107
$x_2 + x_1 x_3 x_4$	0.574467	0.5119	0.5516
$x_3 + x_1 x_2 x_4$	0.046187	0.0257	0.03909
$x_4 + x_1 x_2 x_3$	0.8971	0.8819	0.8943
$x_1 x_2 + x_3 x_4$	-0.28931	-0.2718	-0.2842
$x_1 x_4 + x_2 x_3$	-0.11427	-0.0824	-0.10203
$x_1 x_3 + x_2 x_4$	+0.01216	0.0304	0.02036

Table VI.21 Analysis of Variance

Source of Variance	Degrees of Freedom	Mean Square MS			F Ratio $\frac{MS}{S^2_{E, \ln k}}$		
		Model 9	Model 10	Model 11	Model 9	Model 10	Model 11
X_1 (MIXING)	1	0.08865	0.1130	0.0888	3.76	5.26	3.84
X_2 (SPAR CaCO ₃ CONTENT)	1	0.6600	0.524	0.6086	27.97 ^c	24.37 ^c	26.34 ^c
X_3 (SPAR FINENESS)	1	0.00427	0.00132	0.00306	>1	>1	>1
X_4 (TEMPERATURE)	1	1.6096	1.556	1.5995	68.20 ^c	72.37 ^c	69.24 ^c
$X_1X_2 + X_3X_4$ (INTERACTIONS)	1	0.1674	0.14775	0.1616	9.336 ^b	6.87 ^a	6.996 ^a
$X_1X_4 + X_2X_3$ (INTERACTIONS)	1	0.02611	0.0137	0.02081	1.106	>1	>1
$X_1X_3 + X_2X_4$ (INTERACTIONS)	1	0.0003	0.00185	0.0008	>1	>1	>1
TOTAL SUM OF SQUARES ABOUT MEAN	7	2.7447	2.3572	2.483	a Significant at the 5% Level of Significance		
VARIANCE OF PURE ERROR (ESTIMATED FROM A RUNS)	6	0.0236	0.0215	0.0231	b Significant at the 2.5% level of Significance		
					c Significant at the 1% level of significance		

TABLE VI.22 Regrouping the F Runs

Run No.	Mixing Rate RPM	Apparent Rate Constant		
		Model 9	Model 10	Model 11
$\text{CaCO}_3 = 3.5\%$ $T = 370^\circ\text{F}$				
A runs	10	0.312	0.205	0.513
9 F	15.8	0.251	0.1630	0.413
1 F	20	0.279	0.1820	0.460
6 F	25	0.487	0.3027	0.792
$\text{CaCO}_3 = 3.5\%$ $T = 450$				
A runs	10	0.772	0.484	1.280
5 F	15.8	0.714	0.426	1.140
10 F	25	1.005	0.637	1.648
$\text{CaCO}_3 = 7.14\%$ $T = 370^\circ\text{F}$				
8 F	15.8	0.616	0.355	0.971
4 F	25	0.611	0.364	0.975
$\text{CaCO}_3 = 7.14\%$ $T = 450$				
2 F	5.05	1.579	0.876	2.453
3 F	15.8	1.637	0.938	2.581
7 F	25	1.417	0.857	2.285

THE APPARENT RATE CONSTANT FOR THE A RUNS WAS TAKEN FROM THE VALUE OF K PREDICTED BY THE LINEAR LEAST SQUARES FIT OF THE ARRHENIUS EQUATION TO THE CONTINUOUS REACTOR AND BATCH REACTOR DATA.

Table VI.23

Least Squares Estimate of the Parameters of Equation (VI-42)
from the Factorial Experiments Apparent Rate Constants.

Model	95% Confidence Interval of Parameters				Correlation Coefficient	S_R^2	$S_{E, \ln k}^2$
	k_o	c	$E \cdot 10^{-3}$	m		$\nu = 4$	$\nu = 6$
9	0.0492	$1.158^{\pm 0.322}$	$16.83^{\pm 3.52}$	$0.502^{\pm 0.265}$	0.9928	0.00912	0.0236
10	0.0343	$1.077^{\pm 0.226}$	$16.55^{\pm 2.47}$	$0.511^{\pm 0.186}$	0.9962	0.00450	0.0215
11	0.0826	$1.131^{\pm 0.283}$	$16.78^{\pm 3.09}$	$0.510^{\pm 0.233}$	0.9943	0.00705	0.0231

Table VI.24 Least Squares Estimate of the Parameters of Equation (VI-42)
 Using the Apparent Rate Constants of the A and F runs as
 well as the Batch Reactor Data.

Model	k_o	95% Confidence Interval of Parameters			Correlation Coefficients	S_R^2 $\nu = 17$	$S_{E, \ln k}^2$ $\nu = 6$
		c	$E \cdot 10^{-3}$	m			
9	0.0644	$1.012^{\pm} 0.206$	$17.41^{\pm} 1.35$	$0.393^{\pm} 0.204$	0.9930	0.0158	0.0236
10	0.0514	$0.888^{\pm} 0.196$	$15.81^{\pm} 1.29$	$0.374^{\pm} 0.195$	0.9922	0.0143	0.0215
11	0.115	$0.964^{\pm} 0.199$	$16.77^{\pm} 1.30$	$0.386^{\pm} 0.198$	0.9929	0.0148	0.0231

Table VI.25 Analysis of Residuals For Least Squares fit of Equation

(VI-42) to all the Apparent Rate Constants

Model 9														
Temp. T_R	% CaCO_3 in Spar	r.p.m. of Stirrers	Corrected Acid:Spar Ratio	Observed Rate Constant k	Predicted Rate Constant \hat{k}	Residual $k - \hat{k}$	Residual $\ln k - \ln \hat{k}$							
760	3.5	10	0.9982	0.123	0.112	0.011	0.0902							
760	3.5	10	1.0551	0.105	0.112	-0.007	-0.0680							
760	3.5	10	0.9403	0.127	0.112	0.015	0.122							
830	3.5	10	0.9873	0.428	0.297	0.131	0.3652							
830	3.5	10	0.9308	0.283	0.297	-0.014	-0.0485							
830	3.5	10	1.008	0.281	0.297	-0.016	-0.0556							
910	3.5	10	0.8720	0.798	0.752	0.046	0.0604							
910	3.5	10	0.9654	0.749	0.752	-0.003	-0.0151							
910	3.5	10	0.8749	0.726	0.752	-0.026	-0.0342							
710	3.5	BATCH	1.0	0.0459	0.0499	-0.004	-0.0838							
760	3.5	BATCH	1.0	0.0955	0.112	-0.0165	-0.1628							
810	3.5	BATCH	1.0	0.256	0.2291	0.027	0.1118							
830	3.5	20	0.9762	0.279	0.297	-0.018	-0.0627							
910	7.14	5.05	0.9329	1.579	0.547	0.032	0.0215							
910	7.14	15.8	0.9190	1.637	1.547	0.090	0.0576							
830	7.14	25.0	0.9766	0.611	0.612	-0.001	-0.00022							
910	3.5	15.8	0.9510	0.714	0.752	-0.038	-0.05082							
830	3.5	25	0.9737	0.487	0.440	0.047	0.1016							
910	7.14	25	0.9366	1.417	1.547	-0.130	-0.0868							
830	7.14	15.8	0.9904	0.616	0.612	0.004	0.0079							
830	3.5	15.8	0.9682	0.251	0.297	-0.046	-0.1685							
910	3.5	25.0	0.8925	1.005	1.114	-0.109	-0.1016							

Table VI. 25 Con't

Model 10

Temp. °R	% CaCO ₃ in Spar	r. p. m. of Stirrers	Corrected Acid:Spar Ratio	Observed Rate Constant k	Predicted Rate Constant \hat{k}	Residual k - \hat{k}	Residual ln k - ln \hat{k}
760	3.5	10	0.9982	0.0874	0.0820	0.0054	0.0637
760	3.5	10	1.0551	0.0731	0.0820	0.0089	-0.115
760	3.5	10	0.9403	0.0948	0.0820	0.0128	0.1450
830	3.5	10	0.0973	0.266	0.1983	0.068	0.2936
830	3.5	10	0.9308	0.188	0.1983	-0.0103	-0.04919
830	3.5	10	1.008	0.181	0.1983	-0.0173	-0.09138
910	3.5	10	0.8720	0.508	0.4607	0.0473	0.09772
910	3.5	10	0.9654	0.432	0.4607	-0.0287	-0.06434
910	3.5	10	0.8749	0.469	0.4607	0.0093	0.01784
710	3.5	BATCH	1.0	0.0381	0.0392	-0.011	-0.0292
760	3.5	BATCH	1.0	0.0748	0.0820	-0.0072	-0.092
810	3.5	BATCH	1.0	0.188	0.156	0.032	0.1833
830	3.5	20	0.9762	0.1820	0.1983	-0.0163	-0.0859
910	7.14	5.05	0.9329	0.876	0.868	-0.008	-0.00927
910	7.14	15.8	0.9190	0.938	0.868	0.070	0.0777
830	7.14	25.0	0.0766	0.364	0.374	0.010	-0.02605
910	3.5	15.8	0.9510	0.426	0.461	-0.035	-0.07832
830	3.5	25	0.9737	0.303	0.288	0.015	0.04991
910	7.14	25	0.9366	0.857	0.868	-0.011	-0.01265
830	7.14	15.8	0.9904	0.356	0.374	-0.018	-0.0483
830	3.5	15.8	0.9682	0.163	0.198	-0.035	-0.1961
910	3.5	25.0	0.8925	0.637	0.669	-0.032	-0.0499

TABLE VI.25 Con't

Model 11

Temp. °R	% CaCO ₃ in Spar	r.p.m. of Stirrers	Corrected Acid:Spar	Observed Rate Constant k	Predicted Rate Constant \hat{k}	k - \hat{k}	ln k - ln \hat{k}
760	3.5	10	0.9982	0.211	0.195	0.016	0.0793
760	3.5	10	1.0551	0.178	0.195	-0.017	-0.0876
760	3.5	10	0.9403	0.222	0.195	0.027	0.1316
830	3.5	10	0.9873	0.698	0.497	0.201	0.3399
830	3.5	10	0.9308	0.471	0.497	-0.026	-0.0528
830	3.5	10	1.008	0.464	0.497	-0.033	-0.0678
910	3.5	10	0.8720	1.305	0.214	0.091	0.0731
910	3.5	10	0.9654	1.185	1.214	-0.029	-0.0242
910	3.5	10	0.8749	1.194	1.214	-0.020	-0.0166
710	3.5	BATCH	1.0	0.0840	0.0890	-0.050	-0.0582
760	3.5	BATCH	1.0	0.171	0.195	-0.024	-0.1323
810	3.5	BATCH	1.0	0.444	0.386	0.058	0.1392
830	3.5	20	0.9762	0.460	0.497	-0.037	-0.0765
910	7.14	5.05	0.9329	2.453	2.415	0.038	0.0163
910	7.14	15.8	0.0190	2.581	2.415	0.166	0.0672
830	7.14	25	0.9766	0.975	0.988	-0.013	-0.0123
910	3.5	15.8	0.9510	1.140	1.215	-0.075	-0.0629
830	3.5	25	0.9737	0.792	0.731	0.061	0.0806
910	7.14	25	0.0366	2.285	2.415	-0.130	-0.0546
830	7.14	15.8	0.9904	0.971	0.988	-0.017	-0.0165
830	3.5	15.8	0.9682	0.413	0.497	-0.084	-0.1842
910	3.5	25.0	0.8925	1.648	1.788	-0.140	-0.0806

TABLE VI.26 Predicted Conversions

Run No.	Temp. °R	%CaCO ₃ in Spar	r. p. m. of Stirrers	Corrected Acid:Spar Ratio	Observed Conversion	Predicted Conversions		
						Model 9	Model 10	Model 11
11A	760	3.5	10	0.9982	0.7463	0.7376	0.7397	0.7386
13A	760	3.5	10	1.0551	0.7683	0.7752	0.7808	0.7773
14A	760	3.5	10	0.9404	0.6919	0.6803	0.6773	0.6788
12A	830	3.5	10	0.9873	0.8431	0.8181	0.8209	0.8192
15A	830	3.5	10	0.9308	0.7886	0.7920	0.7925	0.7925
18A	830	3.5	10	0.008	0.8249	0.8289	0.8324	0.8305
16A	910	3.5	10	0.8728	0.8026	0.8002	0.7978	0.7995
17A	910	3.5	10	0.9654	0.8766	0.8768	0.8797	0.8777
19A	910	3.5	10	0.8749	0.8019	0.8035	0.8012	0.8023
1 F	830	3.5	20.0	0.9762	0.8117	0.8163	0.8185	0.8172
2 F	910	7.14	5.05	0.9329	0.8827	0.8820	0.8824	0.8822
3 F	910	7.14	15.8	0.9190	0.8669	0.8650	0.8640	0.8647
4 F	830	7.14	25.0	0.9766	0.8594	0.8597	0.8608	0.8602
5 F	910	3.50	15.8	0.9510	0.8582	0.8605	0.8621	0.8612
6 F	830	3.5	25.0	0.9737	0.8399	0.8335	0.8362	0.8348
7 F	910	7.14	25.0	0.9366	0.8507	0.8545	0.8514	0.8535
8 F	830	7.14	15.8	0.9904	0.8787	0.8786	0.8816	0.8796
9 F	830	3.5	15.8	0.9682	0.8154	0.8267	0.8298	0.8280
10F	910	3.5	25.0	0.8925	0.8182	0.8225	0.8205	0.8220
VARIANCE OF ERRORS X 10 ⁴ (SS ERRORS/15)						0.7657	0.87193	0.7958
STANDARD DEVIATION OF ERRORS X 10 ²						0.875	0.934	0.892

VII DISCUSSION OF RESULTS

A. The Results

1. The Batch Reactor

In section VI of this thesis, a thorough statistical treatment of the batch data established the following three rate models as satisfactory correlations for the entire range of the conversion-time data.

$$\text{Model 9} \quad \frac{dx_B}{dt} = \frac{k_9 X_{B_0}^2 (A - x_B)^2 (1 - x_B)^{2/3}}{1 - (1 - x_B)^{1/3}} \quad (\text{VII-1})$$

$$\text{Model 10} \quad \frac{dx_B}{dt} = \frac{k_{10} X_{B_0}^2 (A - x_B)^2 (1 - x_B)^{1/3}}{1 - (1 - x_B)^{1/3}} \quad (\text{VII-2})$$

$$\text{Model 11} \quad \frac{dx_B}{dt} = \frac{k_{11} X_{B_0}^2 (A - x_B)^2 (1 - x_B)^{2/3}}{1 - (1 - x_B)^{2/3}} \quad (\text{VII-3})$$

where X_{B_0} = moles of CaF_2 per mole of calcium in the feed, A = acid:spar ratio, x_B = fractional conversion of CaF_2 , t = time (minutes), and k_9 , k_{10} , and k_{11} are rate constants ($\text{min}^{-1} X^{-2}$) where X is the molar concentration in moles per mole of calcium.

The statistical treatment of the data, also indicated that none of the three models can be considered as better than the others.

It should be noted that the pseudo steady state solution for a heterogeneous reaction the rate of which is controlled by the diffusion of the liquid reactant through the ash layer to the unreacted core, did not adequately fit the data. For that model, the concentration of the liquid reactant on the ash perimeter is assumed to decrease in proportion to the amount of conversion of CaF_2 . The model equation is.

$$\text{Model 7 } \frac{dx_B}{dt} = \frac{k_7 X_{B_0} (A - x_B)(1 - x_B)^{1/3}}{1 - (1 - x_B)^{1/3}} \quad (\text{VII-4})$$

2. The Continuous Reactor

The statistical treatment in section VI also established that the following equations satisfactorily correlated all the apparent rate constants obtained from the batch and continuous reactor data.

$$k_9 = 0.0644 C^{1.012} M^{1.0122} \exp \left\{ \frac{-17410}{R} \left(\frac{1}{T} - \frac{1}{809.9} \right) \right\} \quad (\text{VII-6})$$

$$k_{10} = 0.0514 C^{0.888} M^{I \cdot 0.166} \exp \left\{ \frac{-15810}{R} \left(\frac{1}{T} - \frac{1}{809.9} \right) \right\} \quad (\text{VII-7})$$

$$k_{11} = 0.115 C^{0.964} M^{I \cdot 0.120} \exp \left\{ \frac{-16770}{R} \left(\frac{1}{T} - \frac{1}{809.9} \right) \right\} \quad (\text{VII-8})$$

where $I = 0$ when $C = 7.14\%$ or $M < 25$ r.p.m.

and $I = 1$ when $C = 3.5\%$ and $M = 25$ r.p.m.

$C = \text{CaCO}_3$ content of the fluorspar (wht%), $M =$ mixing speed (r. p.m.), $R =$ gas constant (1.987 Btu/lb mole $^{\circ}\text{R}$) and $T =$ temperature ($^{\circ}\text{R}$).

The three rate models, 9, 10, and 11, along with the appropriate correlations of their apparent rate constants (equations (VII-5)(VII-6) and (VII-7) respectively), were used to predict the conversions in the continuous reactor runs. All three models yielded very good results, and none of them could be considered as providing a better fit than the others.

Analysis of the experimental data has demonstrated the following;

(1) The factorial experimental design was very efficient in yielding a great deal of information with a minimum of effort. In particular, with only 8 runs, in

which 4 parameters were varied, an estimate of the activation energy was obtained which was as accurate as that obtained with 9 runs, in which only 2 parameters were varied.

(2) The activation energy values were in the order of 16,000 Btu/lb mole, and were indicative of a diffusion controlled mechanism.

(3) The rate of CaF_2 disappearance is proportional to the square of the fraction of acid unconverted.

(4) Calcium carbonate plays a very important role in enhancing the reactivity of the spar. The reaction velocity is approximately linearly proportional to the CaCO_3 content of the fluorspar.

(5) In the range of 5 to 20 r.p.m., the variation in the mixing speed did not alter the reaction velocity. However, when the CaCO_3 content was 3.5% by wt., at 25 r.p.m. an enhancement of approximately 50% was observed in the apparent rate constant. This enhancement did not occur when the CaCO_3 content of the fluorspar was 7.14%, by wt.

(6) Fluorspar which was ground to approximately thrice the fineness of the normally ground spar did not

react with a greater velocity than the normally ground spar.

In the discussions that follow an attempt is made to explain the above results on the basis of the observed phenomena.

B. Interpretation of Results

1. Mixing in the Continuous Reactor.

a. The effect of calcium carbonate content.

One needs only to refer to any one of the many patents on the manufacture of HF from acid grade fluorspar, to appreciate the difficulties encountered with the formation of large lumps within the reactors. But, aside from the run in which pure synthetic CaF_2 was used as the fluorspar feed, the formation of large lumps did not occur in the continuous reactor used in this study. However, the solids leaving the reactor were quite coarse (1/4 inch to 1/16 inch with some powder), so that lumping or conglomeration, per se, was not completely eliminated.

To understand how these lumps or granules formed one must first consider what the situation could be if

no CaCO_3 is present.

When no CaCO_3 is present, the acid, on contact with the cold spar, does not easily penetrate, but rather surrounds, a large conglomerate of unreacted fluorspar particles. As the particles on the conglomerate perimeter begin to react, CaSO_4 crystals precipitate and bond the particles together to form a lump. Further reaction causes further binding of the mass. If the resistance to diffusion is also significantly high, the mass interior is largely void of acid, and the reaction proceeds only with the particles on the perimeter of the conglomerate. As the reaction continues, the diffusional resistance increases.

When CaCO_3 is present in the fluorspar, it reacts vigorously with the sulfuric acid to evolve CO_2 gas bubbles, which, as they rise, cause agitation of the mass and penetration paths in their wake. The gas evolution occurs quite rapidly and creates good mixing before a significant amount of CaSO_4 crystalizes out to bind the solids together into a large impenetrable lump. Thus, the blending action enhances the formation of smaller conglomerates, in which the diffusion path is shorter.

One may argue that HF evolution should also produce the same effect described above. The reason why this is not the case is that CaF_2 does not react with sulfuric acid with the same vigor as CaCO_3 . Consider, that the spar coming into contact with the hot acid is very close to room temperature. At this temperature CaF_2 , unlike CaCO_3 , reacts slowly with the acid. Two experiments to prove this hypothesis were carried out.

In the first experiment, 24 g. of sulfuric acid at 200°F were added to 20 g. of pure synthetic CaF_2 powder. Although some bubbles of HF were evolved, no appreciable frothing ensued. The acid, rather than penetrating into the spar, lay on the surface for some time. In the second experiment the conditions were the same as above but the fluorspar was a composite of 95% by wht. pure CaF_2 and 5% by wht. pure CaCO_3 . In this case appreciable frothing followed the acid addition and penetration of the acid into the powder began almost immediately.

The amount of CO_2 evolution at initial contact of the reactants would likely be proportional only to the CaCO_3 content, and the mixing effect may be expected to be directly proportional to the CO_2 evolution. An

approximately first order dependence on the apparent rate constant on the per cent CaCO_3 content, as observed, was perhaps not an anticipated result, but it can be easily explained as above.

b. Effect of mixing rate.

One might have expected that the mixing rate would play a prominent role in the reaction.

However, while mixing does always play an important role in aiding the contact between the reactants as they enter, and in enhancing heat transfer by maintaining the wall deposits to a minimum, there is some question as to the effect the mixing rate has at reducing the lump formation. In the run in which pure CaF_2 was fed to the reactor, lump formation was so prominent so as to render the reactor inoperable. This indicated that mixing at 10 r.p.m. was of little consequence in reducing lump formation.

However, when the CaCO_3 content was 3.5% and the mixing speed was increased to 25 r.p.m. there was an abrupt increase in the reaction velocity (or the apparent rate constant). This enhancement did not occur in the 25 r.p.m. runs, in which the CaCO_3 content was 7.14% by weight.

The conclusion one may draw from these observations is that a 3.5% CaCO_3 content results in a significant degree of micromixing, and further micromixing can only be effected by application of a high shearing action at 25 r. p. m.. With the CaCO_3 content raised to 7.14%, micromixing is more extensive and only a much greater shearing action than that produced at 25 r. p. m. would further enhance the blending.

The reaction scheme which arises out of the above discussions is illustrated in the Figure VII.1 .

2. Effect of Fluorspar Size Reduction.

In the discussion entered into in the above, one concluded that the size of the conglomerates can be reduced by the presence of CaCO_3 in the fluorspar. It is unlikely that the micromixing is sufficiently efficient to eliminate all conglomerate formation. If conglomerate formation had been eliminated the finer spar should have reacted with a greater velocity than the regular spar, since the mean path through which the acid would have been required to diffuse to reach the unreacted core, would have been shorter. However, with

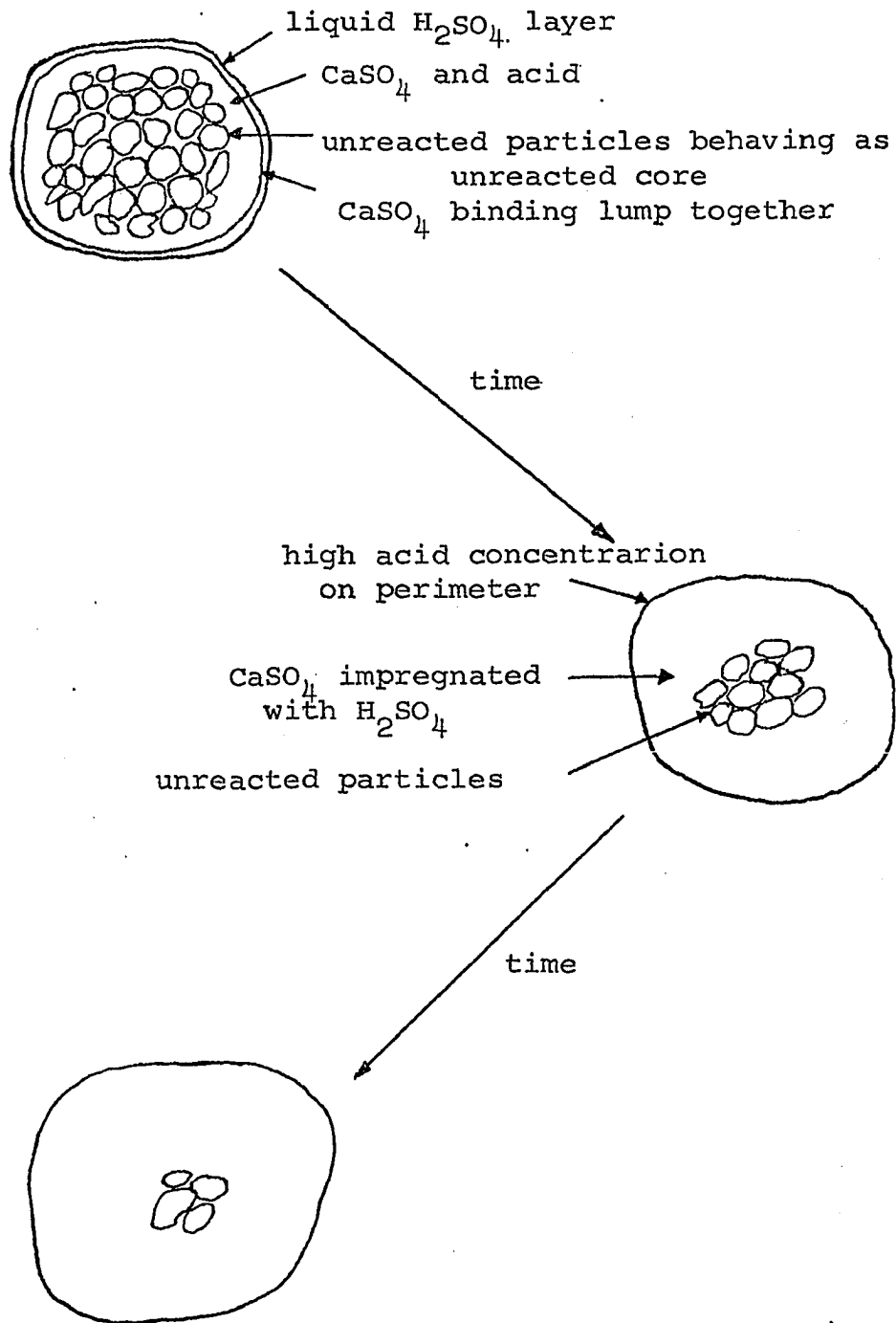


FIG. VII.1 Reacting Scheme of Lumps

the formation of conglomerates, whose sizes were determined not by spar fineness but by the CaCO_3 mixing effect, the spar fineness, in the range studied, was not a determining factor on the reactivity of the fluorspar.

C. Interpretation of Rate Equations

Budnikov and Ginstling ⁽⁹⁾ in their studies of crystalline reactions, found that when diffusion controls the rate of reaction, the reaction velocity changes by 10 - 40% with a 10°C temperature change, but, if the reaction is controlled by the chemical step, the reaction velocity increases 2 - 4 times with a 10°C rise in temperature. The rate constants for the three models found acceptable in this investigation, did not vary by more than 40% per 10°C rise, in the temperature region studied. In light of the discussion in section B, one might expect diffusion control to refer to the diffusion of sulfuric acid to the unreacted core, or, in this case, the unreacted core of the conglomerate.

The pseudo steady state solution of a diffusion controlled unreacted core mechanism was considered in the THEORY section. The equation arrived at, in that section was

$$\frac{dx_B}{dt} = \frac{3aD_{eA} C'_{SO}}{C_{SO} R_p^2} \frac{(A - x_B)(1 - x_B)^{1/3}}{1 - (1 - x_B)^{1/3}} \quad (\text{VII-8})$$

The $(A - x_B)$ term was brought about by assuming that the bulk phase concentration of the fluid reactant, was proportional to the amount unconverted. By grouping the constants of equation (VII-8) and using molar rather than volumetric concentrations, the equation

$$\frac{dx_B}{dt} = \frac{k_7 X_{B_0} (A - x_B)(1 - x_B)^{1/3}}{1 - (1 - x_B)^{1/3}} \quad (\text{VII-4})$$

is obtained. However, the three models which were found acceptable in section VII are not linearly dependent on the fraction of acid unconverted. In particular, equation (VII-2) below

$$\frac{dx_B}{dt} = k_{10} \frac{X_{B_0}^2 (A - x_B)^2 (1 - x_B)^{1/3}}{1 - (1 - x_B)^{1/3}} \quad (\text{VII-2})$$

is dependent on the square of the molar concentration of unreacted acid.

Derivation of equation (VII-2) from equation (III-5)

of the theory, may be easily accomplished by assuming that, in this case, the molar concentration of the acid on the ash perimeter is dependent on the square of the amount of acid unconverted. i.e.

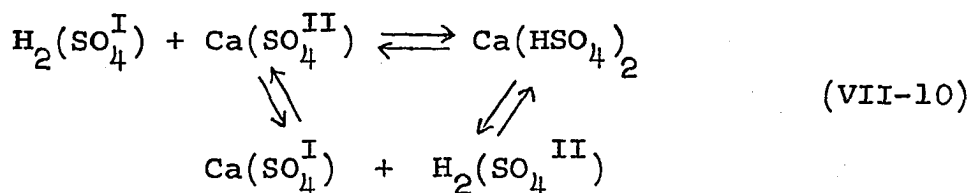
$$x_{AR} \approx \beta x_{BO}^2 (A - x_B)^2 \quad (\text{VII-9})$$

where β is a proportionality constant. Because we are dealing with a rather complex reaction mass in which no liquid bulk phase exists, per se, the above assumption may not be totally unwarranted. However, this approach makes no attempt to consider the physical phenomena which may be occurring.

It has already been mentioned that the reactor contents are, for the most part, incompletely reacted dry granules which, are found to contain a significant amount of acid. The acid may be present within the solid phase in the form of precipitated $\text{CaSO}_4 \cdot \text{H}_2\text{SO}_4$ (as suggested by Ostrovskii and Amirova ⁽²⁴⁾) or as entrained liquid. Diffusion of the acid toward the unreacted solid may occur by capillary action, but as the liquid content decreases the capillaries would also tend to retain the fluid rather than transport it. Yet overall conversions

of 97% or better are quite common in industrial reactors with acid:spar ratio addition close to unity.

A possible explanation for these observations is a migration of sulfuric acid through the solid phase by way of the following scheme.



The ion exchange (H^+ and Ca^{++} ion migration) would be from an area of high concentration to one of low concentration, and using the analogy to diffusion of electrolytes in concentrated solutions, the diffusivity could be proportional to the acid concentration at that point (23).

With the above assumption, the Fick's law equation would take on the following modified form.

$$N_{A,\text{ash}} = -\rho_{\text{Ca}} k_D X_A \frac{\partial X_A}{\partial r} \quad (\text{VII-11})$$

X_A = molar concentration of acid as a diffusing species in the ash (moles of acid per mole of calcium)

$\frac{\partial x_A}{\partial r}$ = molar concentration gradient in the radial direction (moles of acid per mole of calcium/cm)

ρ_{Ca} = moles of calcium per cm^3 of the ash layer

k_D = coefficient (cm^2/min . moles of acid per mole of calcium)

$N_{A,ash}$ = molar flux of acid (moles of acid/ cm^2 min.)

A pseudo steady state mass balance on the ash layer gives

$$\rho_{Ca} \cdot k_D \frac{d}{dr} \left(r^2 x_A \frac{dx_A}{dr} \right) = 0 \quad (\text{VII-12})$$

with the boundary conditions

$$\left. \begin{array}{ll} r = R & x_A = x_{AR} \\ r = r_c & x_{Ac} = 0 \end{array} \right\} \quad (\text{VII-13})$$

Equation (VII-12) may be solved, using the boundary conditions, to obtain the concentration profile and the rate of change in the radius of the unreacted core (or the conglomerate), as

$$-\frac{dr_c}{dt} = \frac{\rho_{Ca} k_D x_{AR} R}{c_{So} r_c} \left/ \left\{ 1 - \frac{r_c}{R} \right\} \right. \quad (\text{VII-14})$$

where R is the radius of the conglomerate, and C_{So} is the molar density of CaF_2 in the unreacted conglomerate core (moles/cm³).

If, one now makes the further assumption that the acid is largely trapped within the ash perimeter, and that its concentration (on a mole per mole of calcium basis) at the ash perimeter is linearly proportional to the fraction of acid unconverted, then

$$x_{AR} \approx \alpha x_{Bo} \cdot (A - x_B) \quad (\text{VII-15})$$

where α is a proportionality constant. Equation (VII-14) may now be expressed in terms of the fractional conversion as

$$\frac{dx_B}{dt} = \frac{3 \rho_{Ca} k_D \alpha^2}{C_{So} R^2} \frac{x_{Bo}^2 (A - x_B)^2 (1 - x_B)^{1/3}}{1 - (1 - x_B)^{1/3}} \quad (\text{VII-16})$$

If ρ_{Ca} , k_D , α , C_{So} and R may all be assumed to be constants, equation (VII-16) may be altered to the form

$$\frac{dx_B}{dt} = k_{10} \frac{x_{Bo}^2 (A - x_B)^2 (1 - x_B)^{1/3}}{1 - (1 - x_B)^{1/3}} \quad (\text{VII-17})$$

where
$$k_{10} = 3 \rho_{Ca} k_D \alpha^2 / C_{SO} R^2 \quad (\text{VII-18})$$

Equation (VII-17) is model 10, and is typical of the three models found to acceptably fit the data.

It must be stressed at this point, that the above discussion was only an attempt to explain the phenomena, and does not alter the fact that the three acceptable models are basically empirical in nature.

D. Comparison of Results to Previous Works.

1. The Work of Ostrovskii and Amirova

Ostrovskii and Amirova ⁽²⁴⁾ found that their data could be correlated by a chemical reaction controlled mechanism with the activation energy values of 37,400 (Btu/lb mole) in the 85 - 100°C range, and 16,560 (Btu/lb mole) in the 105-145°C range. They attributed the change in activation energy as being due to the lack of formation of FSO₃H above 100°C. Formation of FSO₃H would impede HF boiloff, and since they determined the extent of conversion by weight loss, with time, the rate would appear to be lower at the lower temperatures, and increase rapidly as the temperature increased, due to the dual effect of a higher surface reaction rate and a decreased

formation of FSO_3H .

While one cannot discount the rationality of such an argument, one can question whether it sufficiently explains a 50% decrease in the activation energy. The decrease in activation energy is more characteristic of a change in the reaction mechanism from surface reaction control to ash diffusion control. Indeed, their activation energy in the 105-145°C range is very close to the values found in this work.

There is also some question as to the validity of the experimental approach used by Ostrovskii and Amirova. By using very small reacting mixtures (0.1185 grams), which were well mixed prior to being introduced into the furnace, they eliminated the possible nonhomogeneity of the initial mix, and the lumping which seems to be a characteristic of the reaction mass. Extrapolation of their results to industrial conditions is, therefore, in question.

2. The Works of Gnyra and Menard and Whicher.

The results obtained in this work on the effect of calcite content of the fluorspar, are in substantial agreement with the qualitative observations made by

Gnyra (15). Menard and Whicher, (22) on the other hand, had suggested that due to the enhanced setting rates in the presence of calcite, calcite should have the effect of reducing mixing. This is not observed to be the case, so it might be concluded that the "needed" mixing is already accomplished, and that this mixing is helped by the presence of calcite, Prior to the setting.

E. Thermal Effects

Aside from efforts to maintain the batch reactor and continuous reactor at constant temperatures, no attempts were made in this study to consider thermal effects within the reacting solid. Qualitatively, however, because the reaction of CaF_2 with H_2SO_4 is endothermic, cooling of the reacting core can be expected. The magnitude of the temperature drop can be influenced by

- (1) The diameter of the reacting conglomerate
- (2) The amount of H_2SO_4 entrained within the product ash layer
- (3) The thickness of the product ash layer (degree of conversion)

Although one could estimate a thermal conductivity coefficient, it would be highly dependent on the degree of conversion. Furthermore, the diameters of the lumps

are difficult to establish.

However, at this point one can foresee that CaCO_3 played another positive role in the reaction. If the hypothesis previously considered can be deemed acceptable, the CaCO_3 enhances good heat transfer by inhibiting large lump formation. It further enhances reactant heating by generating heat in its reaction with acid at the time when heat is most required.

F. The Silica Reaction

Silica reacts with HF to produce SiF_4 and water. This important side reaction is detrimental to the economics of the process as it results in loss of HF and contamination of the HF stream.

During the investigation, it was hoped that the necessary data to establish the kinetics of the silica reaction would be obtained from the analysis of the product streams. However, the silica content of the fluorspar was very low (1.31% by weight) and small errors in the analysis in either the fluorspar or the product streams resulted in very poor mass balances on silica. Often the mass balance indicated

more silica leaving in the solids out than entering with the fluorspar.

Although not shown in the mass balances of Appendix IV, the extent of silica conversion, calculated on the basis of SiO_2 in the scrubber effluent, was usually 20%, and varied by only 1% from one run to the next. If one accepts this result as representative one must conclude that silica must react very slowly.

VIII CONCLUSIONS

A. On the basis of the experimental runs varying the temperature in the range of 250 - 450°F, and the per cent theoretical acid added in the range of 95 - 105, the following equations were seen to fit the experimental data with acceptable accuracies

$$\frac{dx_B}{dt} = 0.234 \exp \left\{ - \frac{17900}{R} \left[\frac{1}{T} - \frac{1}{809.9} \right] \right\} \frac{x_{B_0}^2 (A-x_B)^2 (1-x_B)^{2/3}}{1 - (1-x_B)^{1/3}} \quad (\text{VIII-1})$$

$$\frac{dx_B}{dt} = 0.161 \exp \left\{ - \frac{16100}{R} \left[\frac{1}{T} - \frac{1}{809.9} \right] \right\} \frac{x_{B_0}^2 (A-x_B)^2 (1-x_B)^{1/3}}{1 - (1-x_B)^{1/3}} \quad (\text{VIII-2})$$

$$\frac{dx_B}{dt} = 0.396 \exp \left\{ - \frac{17200}{R} \left[\frac{1}{T} - \frac{1}{809.9} \right] \right\} \frac{x_{B_0}^2 (A-x_B)^2 (1-x_B)^{2/3}}{1 - (1-x_B)^{2/3}} \quad (\text{VIII-3})$$

B. On the basis of experimental runs varying the mixing in the range of 5 - 25 r.p.m., the CaCO₃ content of the fluorspar in the range of 3.5 - 7.14% by weight, the temperature in the range of 370 - 450°F, and varying the spar fineness by a factor of 3, the following conclusions were arrived at:

- (1) The dependence of the reaction velocity on the temperature was quite pronounced and the activation energy values were in agreement with the results of Section A.
- (2) The CaCO_3 in the fluorspar appreciably enhances the reaction velocity.
- (3) The degree of the fluorspar fineness does not seem to alter its reactivity.
- (4) Mixing rate affects the reactivity in a discontinuous fashion.

On the basis of A and B above the following equations are recommended for scale-up and design.

$$\frac{dx_B}{dt} = 0.0644C^{1.012} M^{I \cdot 0.122} \exp \left\{ \frac{-17410}{R} \left[\frac{1}{T} - \frac{1}{809.9} \right] \right\}$$

$$\frac{x_{B_0}^2 (A-x_B)^2 (1-x_B)^{2/3}}{1 - (1-x_B)^{1/3}} \quad (\text{VIII-4})$$

$$\frac{dx_B}{dt} = 0.0514C^{0.888} M^{I \cdot 1.116} \exp \left\{ \frac{-15810}{R} \left[\frac{1}{T} - \frac{1}{809.9} \right] \right\}$$

$$\frac{x_{B_0}^2 (A-x_B)^2 (1-x_B)^{1/3}}{1 - (1-x_B)^{1/3}} \quad (\text{VIII-5})$$

$$\frac{dx_B}{dt} = 0.115c^{0.964} M^I \cdot 0.120 \exp \left\{ - \frac{16770}{R} \left[\frac{1}{T} - \frac{1}{809.9} \right] \right\}$$

$$\frac{x_{B_0}^2 (A-x_B)^2 (1-x_B)^{2/3}}{1 - (1-x_B)^{2/3}} \quad (\text{VIII-6})$$

where $I = 0$ if $C = 7.141$ or $M < 25$ r.p.m.

and $I = 1$ if $C = 3.5\%$ and $M = 25$ r.p.m.

and $x_B =$ fractional conversion of CaF_2 ,

$M =$ mixing speed (r.p.m.), $C =$ wnt % CaCO_3 in spar,

$T =$ temperature ($^{\circ}\text{R}$), $A =$ acid:spar ratio corrected for
boiloff and reaction with CaCO_3 ,

$x_{B_0} =$ moles of CaF_2 per mole of calcium in the fluorspar
and $t =$ time in minutes.

In section VI statistical analysis of the data indicated that all three of the models above equally fit the data. However, on the basis of the analysis considered in section VII, and also because it most resembles the theoretically derived equation VII-20 of the Theory section, one is apt to prefer model 10 (equation VII-2 and VII-6 above).

BIBLIOGRAPHY

1. Arsdel, W. B., Trans A.I. Ch. E., 43, No. 1
13 (1947).
2. Bennett, C. A., Franklin, N. L., Statistical
Analysis in Chemistry and the Chemical Industry,
John Wiley and Sons Inc., New York, 1954.
3. Bischoff, K. B., Chem. Eng. Sci., 18, 711 (1963).
4. Blumberg, A. A., J. Phys. Chem., 63, 1129 (1959).
5. Blumberg, A. A., Starvinou, S.C., J. Phys. Chem.,
64, 1438 (1960).
6. Boden, H., Report No. A-RR-69-09, Aluminum Laboratories
Ltd., Arvida P.Q. March, 1969.
7. Box, G.E.P., Hunter, J.S. Technometrics 3, No. 3,
311 (1961).
8. Box, G.E.P., Wilson, K.B., J.R. Statist. Soc. B,
13, No. 1, 1 (1951).
9. Budnikov, P.P., Ginstling, A.M., Principles of Solid
State Chemistry, Translated by K. Shaw, Maclaren
and Sons, London, 1968.
10. Cannon, K. J., Denbigh, K. G., Chem. Eng. Sci, 6, No.
4-5, 145 (1957).
11. Davies, O. L., The Design and Analysis of Industrial
Experiments, 2nd ed., Oliver and Boyd, London, 1956.
12. Dervedde, E., Private Communications, Aluminum
Co. of Canada, 1967-1971.
13. Draper, N. R., Smith, H., Applied Regression Analysis,
John Wiley and Sons Inc., New York, 1966.

14. Duckworth, W. E., Statiscal Techniques in Technological Research, Methuen and Co. Ltd., London, 1968.
15. Gnyra, B., Report No. AW-108-5, Aluminum Co. of Canada Ltd., Arvida, P.Q., Aug., 1961.
16. Gnyra, B., Whicher, C.H., Report No. AW-248-TM-23, Aluminum Co. of Canada Ltd., Arvida P.Q., Dec., 1965.
17. Himmelblau, D. M., Process Analysis by Statistical Analysis, John Wiley and Sons, New York, 1970.
18. Levenspiel, O. L., Chemical Reaction Engineering, John Wiley and Sons, New York, 1962.
19. Levenspiel, O. L., Bischoff, K. B., Ind. Eng. Chem., 51, 1431 (1959).
20. Levenspiel, O. L., Smith, W. K., Chem. Eng. Sci., 6, 227 (1957).
21. Meeter, D. A., Program GAUSCHAUS, Numerical Analysis Laboratory, University of Wisconsin, Madison, Wisconsin, 1964 (Revised 1966).
22. Menard, W., Whicher, C. H., Report No. AW-248-TM-3, Aluminum Co. of Canada Ltd., Arvida P. Q., Dec. 1955.
23. Moore, W. J., Physical Chemistry, 3rd ed., pp.340, Prentice-Hall Inc., Englewood Cliffs, N. J., 1962.
24. Ostrovskii, S. V., Amirova, S. M., Zhurnal Prikladnoi Khimii, 42, No. 11, 2405 (Nov. 1969).
25. Palmer, W. G., J. Chem. Soc., 1630 (1930).
26. Puxley, P. A., Woods, E. A., Report No. A-RR-74-48-20, Aluminum Laboratories Ltd., Arvida, P.Q., March, 1948.
27. Rowe, E. L., Report No. AW-248-TM-2, Aluminum Co. of Canada Ltd., Arvida, P.Q., Sept. 1955.

28. Shen, J., Smith, J. M., *Ind. Eng. Chem., Fundamentals*, 4, 293 (1965).
29. Standard Methods for Chemical Analysis, Aluminum Laboratories Ltd., (1947).
30. Sood, R., Ph. D. Thesis, Part IV, University of Windsor, Windsor, Ont., 1968.
31. Traube, W., Lange, E., *Ber.* 57, 1038 (1924).
32. Traube, W., Reubke, E., *Ber.* 54, 1618 (1921).
33. Volk, W., Applied Statistics for Engineers, McGraw Hill Co. Inc., New York, 1958.
34. Wen, C. Y., *Ind. Eng. Chem.*, 60, No. 9, 34 (1968).
35. Youden, W. J., Statistical Methods for Chemists, John Wiley and Sons Inc., New York, 1961.

Some Patents Dealing with HF Production

U.S.	2,846,290	Aug. 5, 1958
U.S.	3,071,437	Aug.19, 1959
U.S.	1,748,735	Feb.25, 1930
U.S.	2,932,557	Apr.12, 1960
U.S.	2,967,759	Jan.10, 1961
U.S.	3,063,815	Nov.13, 1962
U.S.	3,218,125	Nov.16, 1965
Br.	995,843	Aug. 6, 1965
Br.	940, 289	Nov.28, 1963
Br.	554,127	Nov.18, 1941
Fr.	923,102	Jan. 30, 1963

Fr.	958,456
Swiss	319,931

Dec. 26, 1963

April 3, 1957

NOMENCLATURE

- L = length θ = time
- A = acid:spar ratio corrected for acid boiloff and reaction with CaCO_3 , ((moles of H_2SO_4 in - correction)/(moles of CaF_2 in)).
- a = stoichiometric coefficient
- C = CaCO_3 content in the fluorspar, (% by wht.)
- C_A, C_{AC} ,
 C_{Ao} C_{AS} = concentration of the fluid reactant as shown in Figure III.1, (moles/ L^3)
- C_{Ao} = initial concentration of the fluid reactant in the bulk phase in equation (III-18), (Moles/ L^3)
- C_{So} = concentration of the solid reactant in the unreacted core (moles/ L^3).
- C_{So}^I = initial concentration of solid reactant referred to the volume of fluid (moles/ L^3)
- c = a parameter in equation (VI-36a)
- D_{eA} = effective diffusivity of the fluid reactant in the ash layer, (L^2/θ)
- E = activation energy in the Arrhenius equation, (Btu/lb.mole).
- E(t) = residence time distribution of the solid stream leaving the reactor
- $(E(t) \cdot \Delta t)_i$ = fraction of solids out stream consisting of elements of ages between t_i and Δt_i .
- F = ratio of variances

- I = the integral of a rate model defined in equation (AI-4)
- k_1, k_2
 k_{16} = apparent rate constants for models 1-16 in Table V.1, units as shown in table
- k_D = mass transfer coefficient in equation (VII-11), ($\text{cm}^2/\text{min} \cdot (\text{moles of H}_2\text{SO}_4/\text{mole of calcium})$).
- k_{mA} = mass transfer coefficient across the fluid film in equation (III-5), (L/θ)
- k_S = reaction rate constant based on the surface of the unreacted core in equation (III-2), ($L^3(m+n-2)/\text{moles}^{m+n-1} \theta$)
- k_T of k_o = coefficients, ($\text{min}^{-1} \times \text{ }^{-2}$).
- M = mixing speed, (r.p.m.)
- M_A = total flux of liquid reactant toward the unreacted core, (moles/θ)
- M S = mean square as defined in equation (VI-41)
- MS_{AR} = mean square about regression as defined in equation (VI-2)
- m = a coefficient in equations (III-2) and (VI-36a) or the number of levels at which replicate runs or samples were taken
- N_B = moles of CaF_2 in the reacting mass in equation (V-4)
- $N_{A, \text{ash}}, N_{Ac}$,
 N_s = molar flux of fluid reactant A through the ash layer, through the unreacted core, and through the outer particle surface respectively, ($\text{moles}/\theta L^2$)
- N_{Ca} = moles of calcium in the reacting mass in equation (V-4)
- n = order of reaction in equation (III-2) or the total number of data points

- n_j = number of parameters in a regression equation
- R = gas constant, 1.987 (Btu./lb.mole $^{\circ}R$) or 1.987 (cal/gm. mole $^{\circ}K$)
- R = radius of reacting particle or conglomerate in equation (VII-13), (L)
- R_p = radius of reacting particle, (L)
- r = distance from centre of spherical particle or conglomerate, (L)
- r_c = radius of unreacted core of conglomerate or unreacted particle (L)
- S = mean size of fluor spar particles (L)
- S_A^2 = estimate of the variance of the fluorine content in the scrubber samples due to chemical analysis (g/l. fluorine)²
- S_E^2 = estimate of the variance of the fractional conversions of the batch data due to pure error as defined in equation (VI-3)
- $S_{E,k}^2$ = estimate of the variance of k due to pure error, defined in equation (VI-18)
- $S_{E, \ln(k)}^2$ = estimate of the variance of $\ln k$ due to pure error, defined in equation (VI-19)
- S_R^2 = estimate of the variance about regression, it may refer to $S_{R,k}^2$ or $S_{R, \ln(k)}^2$ depending on whether the regression is non-linear or linear, respectively.
- $S_{R,k}^2$ = estimate of the variance of k about regression, defined in equation (VI-6), $(\min^{-1} X^{-2})^2$
- $S_{R, \ln(k)}^2$ = estimate of the variance of $\ln k$ about regression, defined in equation (VI-14) $(\ln(\min^{-1} X^{-2}))^2$

- s_s^2 = estimate of the variance of fluorine content of the scrubber liquor samples due to sampling or fluctuations in the reactor, (g./l. fluorine)²
- s_{SF}^2 = estimate of the variance of the spar feed rate (gm/hr.)²
- s_{SL}^2 = estimate of the variance of the scrubber liquor feed rate, (litres/hr.)²
- $s_{x_B}^2$ = estimate of the variance of the estimate of conversion of CaF₂ from one scrubber liquor samples
- $s_{\bar{x}_B}^2$ = estimate of the variance of the estimate of the conversion of CaF₂ from the average of 6 scrubber liquor samples.
- s = s coefficient in equation (VI-36a)
- T = temperature (°R) or (°K)
- time = time usually in minutes
- X = molar concentration in the reaction mass (moles per mole of calcium)
- X_A = molar concentration of H₂SO₄ in the reaction mass, (moles of H₂SO₄ per mole of calcium)
- X_{Ao} = initial molar concentration of H₂SO₄ in the reacting mass accounting for boiloff and reaction with CaCO₃, (moles of H₂SO₄ in - correction)/(moles of calcium in)⁴
- X_{AR} = molar concentration of H₂SO₄ on the perimeter of the ash of the reacting conglomerate in equation (VII-13), (moles of H₂SO₄ per mole of calcium)
- X_B = molar concentration of CaF₂ in the reaction mass, (moles of CaF₂ per mole of calcium)

- x_1 = coded mixing speed defined in equation (VI-37)
 x_2 = coded CaCO_3 content of the fluorspar defined in equation (VI-38)
 x_3 = coded fineness of fluorspar = -1 for regularly ground = +1 for reground fluorspar
 x_4 = coded temperature defined in equation (VI-39)
 x_B = fractional conversion of fluorspar
 \bar{x}_B = average fractional conversion in solids out stream in equation (V-2)
 $x_B(\bar{t}_i)$ = average fractional conversion of CaF_2 for stream elements of ages between t_i and $t_i + \Delta t_i$

Greek Symbols

- α = a proportionality constant in equation (VII-15)
 β = a proportionality constant in equation (VII-9)
 ϵ = void fraction in ash layer in equation (III-4)
 ϵ_{1i} = random error in equation (VI-5), $(\text{min}^{-1} \text{X}^{-2})$
 ϵ_{2i} = random error in equation (VI-11) $\ln(\text{min}^{-1} \text{X}^{-2})$
= number of degrees of freedom
 ρ_{Ca} = molar density of calcium in the ash layer in equation (VII-11), (moles of calcium cm^3)
 $\hat{\sigma}_k$ = standard deviation of k about the true regression equation $(\text{min}^{-1} \text{X}^{-2})$
 $\hat{\sigma}_{\ln(k)}$ = standard deviation of $\ln k$ about the true regression equation $\ln(\text{min}^{-1} \text{X}^{-2})$

ϕ

= a random factor by which the rate constant k_i differs from the predicted rate constant k_i , for the inherently linear equation of equation (VI-10)

Superscripts

 \wedge

= denotes predicted value

APPENDIX I.

MODEL DISCRIMINATION AND DETERMINATION OF RATE CONSTANTS

A. Using Batch Data.

The batch data consisted of conversion of fluorspar at various points in time.

The data was analysed by the Integral Method of Analysis (18). The procedure may be summarized as follows.

1. The reaction rate models listed in Table V.1 of section V were written in the form

$$\frac{dx_B}{dt} = f(k, A, x_B) \quad (\text{AI-1})$$

However, since A was always unity in the batch data, it was not a factor to be considered here.

Also, the rate constant of each of the models could be separated from the conversion - dependent terms so that

$$\frac{dx_B}{dt} = k \cdot f(x_B) \quad (\text{AI-2})$$

2. Equation (AI-2) was rearranged to the form

$$\frac{dx_B}{f(x)} = k dt \quad (\text{AI-3})$$

Now the left hand side of equation(AI-3) may be integrated to the form

$$I = \int_{x=0}^{x_B} \frac{dx_B}{f(x_B)} = kt \quad (\text{AI-4})$$

The integral for all the models listed in Table V-1 was easily obtained for the case when A=1.

3. The value of I was determined for each conversion versus time point and plotted versus time(t).

4. If the plot of I versus t was not linear the model was discarded.

5. If the plot of I versus t was fairly linear the line of best fit passing through the origin was determined by linear least squares and the slope was equated to the apparent rate constant value k.

6. The initial estimate of the rate constant was refined by least squares regression of x_B onto t. The criterion being to minimize

$$\sum_i (x_{Bi} - \hat{x}_{Bi})^2 = \sum_i (x_{Bi} - f(k, t_i))^2 \quad (\text{AI-5})$$

Because \hat{x}_{Bi} could not be expressed as an analytical function of k and t , the \hat{x}_{Bi} values were determined by the Newton-Raphson root seeking technique. The program GAUSHAUS (21) employing the method of steepest descent was used to determine the best estimate of the rate constant.

B. The Continuous Reactor Data

The method employed was best illustrated by way of an example. Consider Run 9F Data.

Average fractional conversion of $\text{CaF}_2 = 0.8154$

$X_{Ao} = 0.9408$ g moles of H_2SO_4 /g. mole of Ca^{++} in feed

$X_{Bo} = 0.9717$ g moles of CaF_2 /gm. mole of Ca^{++} in feed

The X_{Ao} value above accounted for acid fuming

$AA = 0.9682 =$ acid:spar ratio corrected for fuming and reaction with CaCO_3

The residence time distribution for the run was tabulated in section VI of the thesis.

The rate constant of the rate model

$$\frac{dx_B}{dt} = \frac{kx_{Bo}^2 (A - x_B)^2 (1 - x_B)^{1/3}}{1 - (1 - x_B)^{1/3}} \quad (\text{AI-6})$$

was to be evaluated. For simplification let $AK = k \cdot X_{Bo}^2$.

As an initial estimate of AK let $AK(1) = 0.10$

Because the rate model was not easily integrated by direct analytical mathematical techniques the value of $x_B(t_i)$ required in the summation below had to be obtained indirectly

$$(1 - \bar{x}_B) = \sum_{i=1}^n (E(t)(\Delta t))_i (1 - x_B(\bar{t}_i)) \quad (AI-7)$$

where $(E(t)\Delta t)_i$ = fraction of solids out stream which consisted of elements of ages between t_i and $t_i + \Delta t_i$, $x_B(\bar{t}_i)$ = conversion of a stream with an average age of t_i and \bar{x}_B = observed average conversion in the exit stream.

Knowing that

$$\int_0^{x_B} \frac{dx_B}{f(x_B)} = k x_{B_0}^2 t = AK \cdot t \quad (AI-8)$$

and that for this model

$$f(x_B) = \frac{1 - (1 - x_B)^{1/3}}{(A - x_B)^2 (1 - x_B)^{1/3}} \quad (AI-9)$$

The discussion that follows will be in terms of the computer program used for the purpose of calculating the rate constant.

The program begins by evaluating the integral $YI(I)$ for $x_B = 0.001, 0.002$ to $x_B = 0.999$ or $x_B = AA - 0.001$, if $AA < 1.0$.

x_B	$YI(I)$
Fractional Conversion	Integral
0.001	.
0.002	.
⋮	⋮
0.500	⋮
0.501	⋮
⋮	⋮
0.999	⋮

But equation (AI-7) may be rewritten in the form

$$\int_0^{x_B(\bar{t}_i)} \frac{dx_B}{f(x_B)} = AK \cdot \bar{t}_i \quad (\text{AI-10})$$

so that the value of $x_B(\bar{t}_i)$ may be obtained by searching the $YI(I)$ matrix for the integral value equal to $AK \cdot \bar{t}_i$

and equating the corresponding X value to $x_B(\bar{t}_i)$. These $x_B(\bar{t}_i)$ values were stored as the VXB(I) vector.

The $(E(t) \cdot \Delta t)_i$ values were stored as the E(I) vector in the program.

The sum

$$\text{SUM} = \sum_{I=1}^n E(I) \cdot (1 - \text{VXB}(I)) \quad (\text{AI-11})$$

was calculated and compared to $(1 - \bar{x}_B)$ (written in the program as $(1 - \text{XAVG})$). (AI-12)

$$\text{AC}(1) = \text{SUM} - (1 - \text{XAVG})$$

AC(I) was a vector containing all the differences obtained for each estimate of the rate constant AK(I).

If AC(I) was less than 1.0×10^{-5} it was assumed that the rate constant value was accurate so as to satisfy the equation

$$(1 - \text{XAVG}) = \sum E(I) \cdot (1 - \text{VXB}(I)) \quad (\text{AI-13})$$

1. Initialization

For the initial estimate of the rate constant

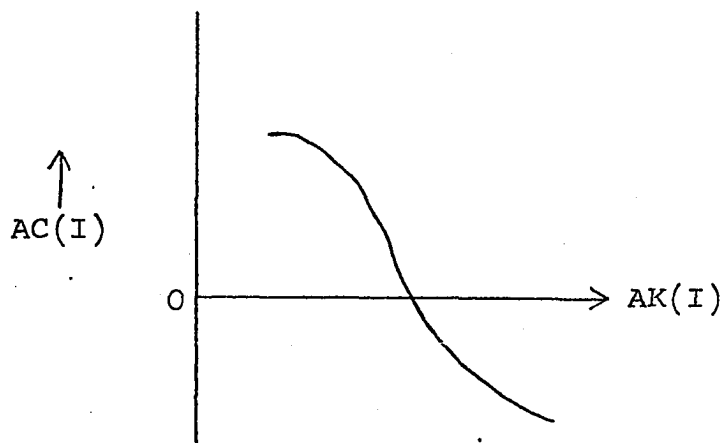
$$\text{AK}(1) = 0.1 \quad \text{AC}(1) = 0.03469.$$

Because AC(1) was positive it indicated that the rate constant estimate was too small since the calculated

amount of CaF_2 leaving the reactor was higher than that measured. A rough second estimate of the rate constant was obtained by letting

$$AK(2) = AK(1) \cdot 2 \quad (AI-14)$$

The figure below shows the expected response of $AC(I)$ to the rate constant $AK(I)$.



The exact nature of the response was not known but it was expected to have only one root.

If $AC(1)$ had been negative, the second estimate $AK(2)$ would have been calculated by letting

$$AK(2) = AK(1)/2 \quad (AI-15)$$

Using the $AK(2)$ value, a value for $VXB(2)$ was calculated and the new SUM value calculated as per equation (AI-10) and $AC(2)$ was calculated as per equation (AI-11) to be -0.01904 .

Note that $AC(2)$ was negative indicating that the true AK value lies between $AK(1)$ and $AK(2)$.

Had the $AC(2)$ value been positive the estimate for $AK(3)$ would again have been obtained by letting $AK(3) = AK(2) \cdot 2$. The successive $AK(M)$ values would have been obtained by letting

$$AK(M) = AK(M-1) \cdot 2 \quad (AI-16)$$

until $AC(M)$ became negative.

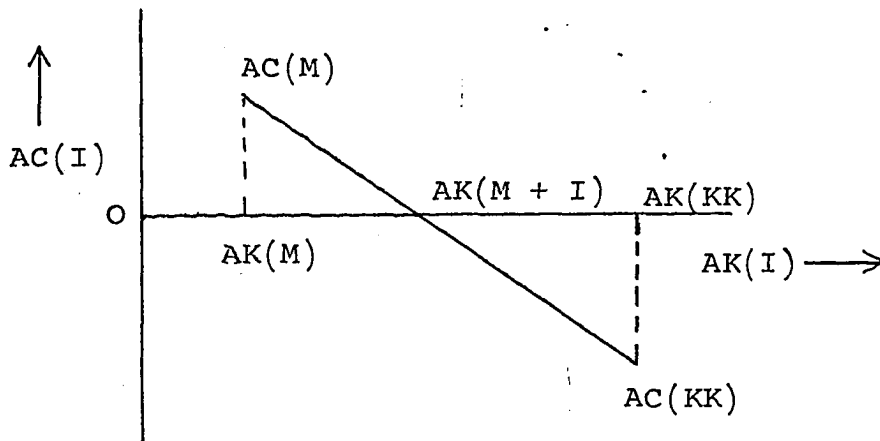
The above was by way of initialization.

Had the initial estimate $AK(1)$ yielded a negative $AC(1)$ value successive estimates of $AK(I)$ would have been obtained by letting $AK(M) = AK(M-1)/2$, until a positive $AC(I)$ value was obtained.

2. Linear Approximation and Steepest Descent

The method of linear approximation was used to determine the next approximation of the rate constant $AK(M+1)$. The method begins by searching the $AC(I)$ vector from $AC(1)$ to $AC(M-1)$ for the smallest absolute value of $AC(I)$ to be designated as $AC(KK)$.

Suppose now that $AC(M)$ was positive while $AC(KK)$ was negative as shown



As shown the best approximation for the rate constant was one which would yield an AC value of 0.

From the geometry of the figure

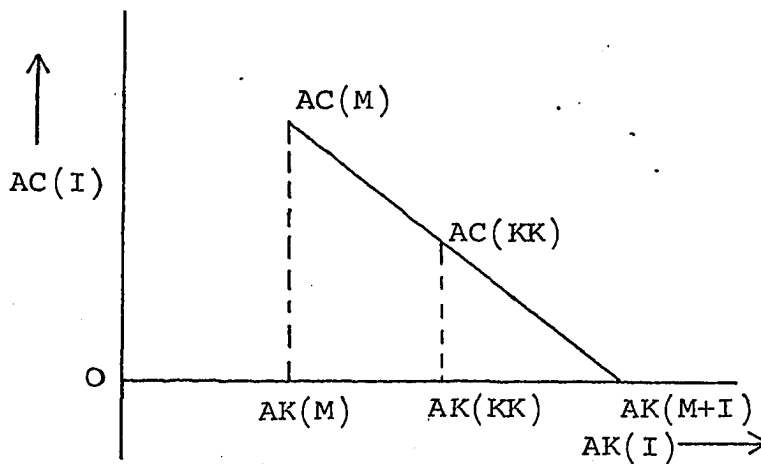
$$|AC(KK)| \cdot (AK(M+1) - AK(M)) = |AC(M)| \cdot (AK(KK) - AK(M+1))$$

which yields

$$AK(M+1) = \frac{|AC(KK)| \cdot AK(M) + |AC(M)| \cdot AK(KK)}{|AC(KK)| + |AC(M)|} \quad (AI-17)$$

The result would be the same if AC(M) were negative and AC(KK) was positive

If on the other hand both AC(M) and AC(KK) were positive as shown



Again from the geometry of the figure

$$|AC(M)| \cdot (AK(M+L) - AK(KK)) = |AC(KK)| \cdot (AK(M+L) - AK(M))$$

and

$$AK(M+1) = \frac{|AC(KK)| \cdot AK(M) - |AC(M)| \cdot AK(KK)}{|AC(KK)| - |AC(M)|} \quad (AI-18)$$

The reader can verify for himself that equation (AI -13) was valid for the cases where $AC(M) < AC(KK)$ and $AC(M) < 0$, $AC(KK) < 0$ where $AC(M) \geq AC(KK)$.

The procedure was simply to test if $AC(M)$ and $AC(KK)$ were both of the same sign. If they were equation(AI-13) was used and if not equation(AI-12) was used. In the program the equation was written as

$$AK(M) = \frac{|AC(KK)| \cdot AK(M-1) - \text{SIGN } 1 \cdot |AC(M-1)| \cdot AK(KK)}{|AC(KK)| - \text{SIGN } 1 \cdot |AC(M-1)|} \quad (AI-18)$$

where $\text{SIGN } 1 = +1.0000$ when $\text{AC}(\text{KK}) \cdot \text{AC}(\text{M}-1) > 0$

and $\text{SIGN } 1 = -1.0000$ when $\text{AC}(\text{KK}) \cdot \text{AC}(\text{M}-1) < 0$

Successive estimates of the rate constant are shown

below

TRIAL	AK	AC
1	0.100	0.0347
2	0.200	-0.019038
3	0.1793	-0.00522
4	0.18572	+0.001223
5	0.1537	0.0000786

This rapid a convergence was rather unusual but convergence was usually accomplished in about 7 iterations.

However, the AK value was equal to $k X_{B_0}^2$ and

$$k = \frac{\text{AK}}{X_{B_0}^2} = 0.163.$$

```

C THIS PROGRAM ATTEMPTS TO FIND THE RATE CONSTANT FOR THE SITUATION
C WHERE THE INTEGRATION OF THE RATE EQUATION IS NOT PRACTICAL BY USE
C OF ANALYTICAL METHODS
C
C INTEGRATION IS ACCOMPLISHED BY SUBDIVIDING THE INTERVAL INTO N
C SECTIONS UTILISING THE SUBROUTINE RQATR
C
C DATA INPUT
C CARD 1$ (1-4) RUN NO. IDENTIFICATION (A4)$ (5-16) AVERAGE CONVERS-
C ION OF SPAR (F11.5)
C CARD 2$ IF THIS REQUIRES A NEW AA VALUE PUT A 1 IN THE FIRST
C COLUMN
C CARD 3$ (1-12) INITIAL ESTIMATE OF THE RATE CONSTANT (E12.5)
C CARD 4$ (1-3) NO. OF DATA POINTS FOR TRACER DATA (I3)
C CARD 5FF $ T(1) 5 POINTS PER CARD (5F11.5)
C E(1) IS PUT INTO THE SUCCEEDING CARDS $ 5 POINTS PER CARD (5F12.8)
C CARD FOLLOWING E(1)$XAO AND XBO (2E14.7)
C
C DIMENSION E(50),T(50),AK(150),AC(150),X(1000),YI(1000),KT(50)
C DIMENSION VXB(50),AKT(50)
50 READ 1,NRUN,XAV
IF(XAV.EQ.0.0)GO TO 51
READ 55,NEW
READ 2,AK(1)
READ 3,N,(T(I),I=1,N)
READ 4,(E(I),I=1,N)
READ 5,XAO,XBO
PRINT 6,NRUN,XAV
PRINT 7,AK(1)
AA=XAO/XBO
PRINT 502,XAO,XBO
PRINT 501,AA
502 FORMAT(1H0,10X,@XAO = @,E14.7/1H0,10X,@XBO = @,E14.7)

```

```

PRINT 8
PRINT 9,(T(I),E(I),I=1,N)
IF(NEW.EQ.0)GO TO 1101
1  FORMAT(A4,F12.8)
55 FORMAT(I2)
2  FORMAT(E12.5)
3  FORMAT(I3/(5F11.5))
4  FORMAT(5F12.8)
5  FORMAT(2E14.7)
6  FORMAT(IH1//IHU,1UX,@RUN NO,@,2X,A4/IHJ,10X,@AVG. FRACTIONAL CONVE
    1RSION OF SPAR = @,F12.8//)
7  FORMAT(IHJ,1UX,@INITIAL VALUE OF THE RATE CONSTANT = @,E12.5)
8  FORMAT(IHJ,16X,@T@,15X,@E(T)@//)
9  FORMAT(IHJ,1UX,F11.5,8X,F12.8)
11 FORMAT(IHJ,1UX,@THE DESIRED ACCURACY IS IMPOSSIBLE TO OBTAIN WITHI
    IN 1000 STEPS@)
501 FORMAT(IHJ,1UX,@ACID TO SPAR RATIO = @,E14.7)
EPS=1.0E-9
NDIM=1000
K=1
XB=0.00000
DELTX=1.000000E-03
YI(K)=0.0
X(K)=0.0
1100 XB=XB+DELTX
IF(XB.GE.0.999.0R.XB.GE.(AA-0.001))GO TO 1101
K=K+1
XL=X(K-1)
XU=XB
Y=0.0
IER=0
CALL ROATR(XL,XU,EPS,NDIM,Y,IER,AA)
IF(IER.EQ.2)PRINT 11
X(K)=XB

```



```

YI(K)=Y+YI(K-1)
GO TO 1100
1101 J=1
PRINT 6,NRUN,XAV
PRINT 2000
2000 FORMAT(1H0,10X,@ITERATION RATE CONSTANT SUMMATION SUM-(1-
1XAV) XAV PREDICTED@1H ,10X,15X,@VALUE@)
M=1
90 BK=A*(M)
I=1
DO 1200 I=1,N
1200 AKT(I)=BK*T(I)
JN=1
DO 1201 JN=1,N
AKTN=AKT(JN)
LL=1
JJ=1
DO 1202 JJ=1,K
S=AKTN-YI(JJ)
SS=AKTN-YI(LL)
1202 IF(ABS(S).LT.ABS(SS))LL=JJ
1201 VXB(JN)=X(LL)
SUMF)=0
I=1
DO 100 I=1,N
Z=1.0-VXB(I)
100 SUM=SUM+Z*E(I)
C=1.0-XAV
SC=SUM-C
SUMI=1.0-SUM
PRINT 102,M,BK,SUM,SC,SUMI
102 FORMAT(1H0,14X,13,6X,E12.5,3X,E12.5,3X,E12.5)
AC(M)=SC
IF(M.EQ.1)GO TO 200

```



```

203 IF(J.EQ.1)GO TO 207
SIGN1=1.000000
KK=M-1
GO TO 302
207 M=M+1
AK(M)=AK(M-1)*2.0
GO TO 90
202 M=M+1
AK(M)=AK(M-1)*2.0
GO TO 90
201 IF(M.EQ.1)GO TO 204
IF(AC(M-1).LT.0.0)GO TO 205.
J=2
KK=M-1
GO TO 303
205 IF(J.EQ.1)GO TO 206
SIGN1=1.000000
KK=M-1
GO TO 302
206 M=M+1
AK(M)=AK(M-1)/2.0
GO TO 90
204 M=M+1
AK(M)=AK(M-1)/2.0
GO TO 90
304 IF(AC(KK))305,306,306
305 SK=AMIN1(AK(KK),AK(M))
SIGN3=1.000000
207 M=M+1
AK(M)=SK-SIGN3*(ABS(AK(KK)-AK(M-1)))/2.0
GO TO 90
306 SK=AMAX1(AK(KK),AK(M))
SIGN3=-1.000000000
GO TO 307

```

```

SUBROUTINE RQATR(XL,XU,EPS,NDIM,Y,IER,AA)
DIMENSION AUX(1000)
C XL = LOWER LIMIT OF THE INTEGRAL
C XU = UPPER LIMIT OF THE INTEGRAL
C EPS = UPPER BOUND OF THE ABSOLUTE ERROR
C FUNC = EXTERNAL FUNCTION REQUIRED
C Y = RESULTING VALUE OF THE INTEGRAL DESIRED
C AUX = INTERNAL ARRAY WITH DIMENSION NDIM OR LARGER
C IER = ERROR PARAMETER
C IER = 0 - DESIRED ACCURACY WAS POSSIBLE NO ERROR
C IER = 1 ROUNDOFF ERROR MAKES DESIRED ACCURACY IMPOSSIBLE
C IER = 2 REQUIRED ACCURACY IMPOSSIBLE WITHIN 1000 STEPS
C
AUX(1)=0.5*(FUNC(XL,AA)+FUNC(XU,AA))
H=XU-XL
IF(NDIM-1)8,8,1
1 IF(H)2,10,2
2 HH=H
E=EPS/ABS(H)
DELT2=0.0
P=1.0
JJ=1
DO 7 I=2,NDIM
DELT1=DELT2
HD=HH
HH=0.5*HH
P=0.5*P
X=XL+HH
SM=0.0
DO 3 J=1,JJ
SM=SM+FUNC(X,AA)
3 X=X+HD
AUX(I)=0.5*AUX(I-1)+P*SM
Q=1.0
JI=I-1

```

```
DO 4 J=1,JI
  II=I-J
  Q=Q+Q
  Q=Q+Q
  4 AUX(II)=AUX(II+1)+(AUX(II+1)-AUX(II))/(Q-1.0)
  DELT2=ABS(Y-AUX(1))
  IF(I-5)7,5,5
  5 IF(DELT2-E)10,10,6
  6 IF(DELT2-DELT1)7,11,11
  7 JJ=JJ+JJ
  8 IER=2
  9 Y=H*AUX(1)
  RETURN
10 IER=0
  GO TO 9
11 IER=1
  Y=H*Y
  RETURN
  END
```

```
FUNCTION FUNC(X,AA)
MODEL 10
Y=AUX(1)
DA=(1.0-X)**(1.0/3.0)
DB=1.0-DA
DC=(AA-X)*(AA-X)
DD=DA*DC
FUNC=DB/DD
RETURN
END
```

```
C
C
C
```

APPENDIX II

THERMODYNAMIC CONSIDERATIONS

The aims here were to establish whether the reactions were predetermined by possible equilibrium. The heats of reaction were also established.

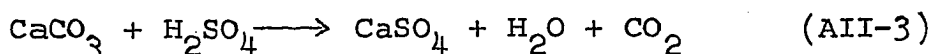
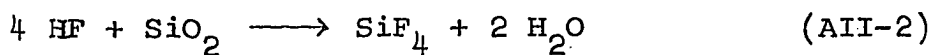
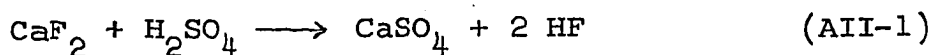


Table AII.1 contains all the thermodynamic data necessary for the determination of ΔF_T and ΔH_T for these three reactions. To determine ΔF_T from the tabled data the following equation was used

$$\frac{\Delta F_T}{T} - \frac{\Delta F_{T_0}}{T_0} = \int_{T_0}^T - \frac{\Delta H_T}{T^2} dT \quad (\text{AII-4})$$

Table AII.2 contains the calculated values of ΔF_T , ΔH_T and K the equilibrium constant. The value of K was obtained by use of the equation

$$RT \ln k = - \Delta F_T \quad (\text{AII-5})$$

Since all the equilibrium constant values are relatively large one may assume that the reactions were essentially irreversible.

Table AIII.1

Thermodynamic Data of Reactants and Products

Material g - gas s - solid l - liquid	$\Delta H_f^\circ, 298.15^\circ\text{K}$ Kcal/gm mole	$\Delta F_f^\circ, 298.15^\circ\text{K}$ Kcal/gm mole	$\Delta H_{f,T} - \Delta H_f^\circ, 298.15$ Kcal/gm mole
CaCO_3 (s)	-288.14	-269.57	$24.98T + 0.00262T^2 + \frac{620000}{T} - 9760.0$
CO_2 (g)	-94.05	-94.26	$10.57T + 0.00105T^2 + \frac{206000}{T} - 39360$
H_2O (g)	-57.80	-54.64	$7.30T + 0.00123T^2 - 2286$
SiF_4 (g)	-385.98	-375.855	$21.95T + 0.00133T^2 + \frac{472000}{T} - 8246.0$
SiO_2 (s)	-217.65	-204.64	$4.28T + 0.01053T^2 - 2212.0$
H_2SO_4 (l)	-193.91	-163.9	$33.2T - 9898.58$
HF (g)	-64.2	-64.7	$6.55T + 0.00036T^2 - \frac{17000}{T} - 1928.0$
CaSO_4 (s)	-343.335	-316.475	$16.78T + 0.0118T^2 - 6052.0$
CaF_2 (s)	-290.3	-277.796	$14.3T + 0.00364T^2 - \frac{47000}{T} - 4429.0$

Table AII.2 Thermodynamic Quantities for the Principle Reactions Occuring in the Reactor

Temp Reaction	298.15°K	400°K	450°R	500°K	550°K
	ΔF_T (Kcal/gm mole)				
1	- 4.179	- 9.688	-12.300	-15.606	-17.303
2	-21.69	-19.69	-18.761	-17.770	-16.742
3	-31.905	-38.122	-40.961	-43.932	-46.749
	ΔH_T (Kcal/gm mole)				
1	12.475	11.3	10.777	10.331	9.931
2	-27.13	-27.555	-27.745	-27.964	-28.178
3	-13.141	-14.100	-14.944	-15.484	-15.984
	K (Equilibrium constant)				
1	1.157×10^3	1.964×10^5	8.583×10^5	6.627×10^6	7.508×10^6
2	7.927×10^{15}	6.288×10^{10}	1.293×10^9	5.851×10^7	4.94×10^6
3	2.447×10^{23}	6.742×10^{20}	7.821×10^{19}	1.595×10^{19}	3.769×10^{18}

APPENDIX III

ANALYSIS OF THE DATA OF PUXLEY AND WOODS

The data of Puxley and Woods (26) were fitted to a zero order reaction of the form

$$-\frac{dN}{dt} = k$$

where $k = \text{gm. moles/min.}$

The equation was valid for conversions up to 50%. Average k values were determined at the 20% and 50% conversion levels and can be found in Table AIII.1.

An Arrhenius plot was drawn to determine the activation energy. Figure (AIII-1) illustrates the $\ln k$ vs. $1/T$ plot for 20% and 50% conversion and an average line was drawn through the points. Approximate values of the activation energy values were determined to be as follows.

20% conversion	$E = 4570 \text{ cal/gm mole CaF}_2$
50% conversion	$E = 5450 \text{ cal/gm mole CaF}_2$
Overall	$E = 5000 \text{ cal/gm mole CaF}_2$

Table AIII.1 Reaction Constants for Puxley's Data Assuming Zero Order Kinetics

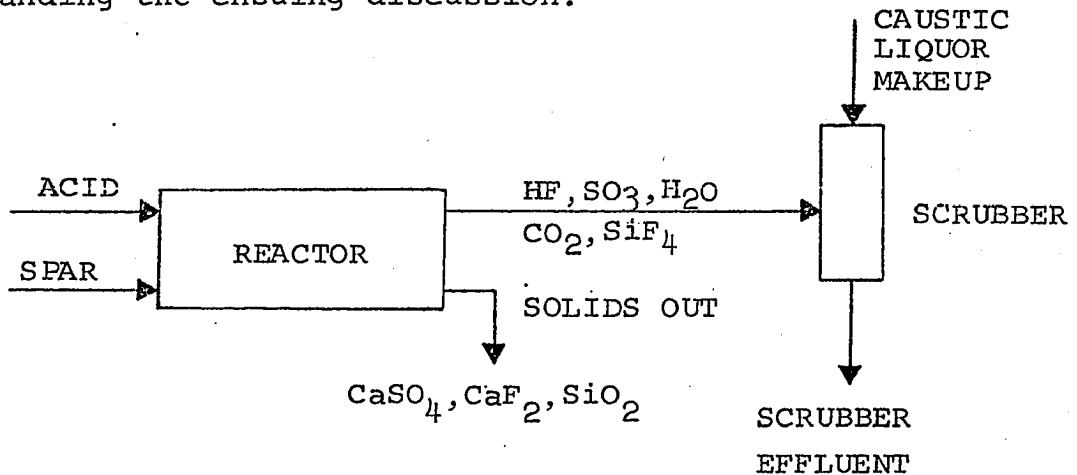
T ^o C	At 20% CaF ₂ Reacted		At 50% CaF ₂ Reacted	
	k (gm.moles/min.)	ln k	k (gm.moles/min.)	ln k
125	1.32 x 10 ⁻⁴	-8.94	1.12 x 10 ⁻⁴	-9.1
175	2.40 x 10 ⁻⁴	-8.34	2.36 x 10 ⁻⁴	-8.355
225	3.47 x 10 ⁻⁴	-7.955	3.653 x 10 ⁻⁴	7.90

APPENDIX IV

SAMPLE TREATMENT AND MASS BALANCES

In analysing the experimental data, the objective was to determine the extent of conversion of CaF_2 or H_2SO_4 in the solids out stream. To establish the accuracy of the conversion determined, it was first necessary to ensure adequate mass balances.

The figure below should aid the reader in understanding the ensuing discussion.



Aside from temperatures, the following parameters were measured.

- (1) Feed rates of acid and spar
- (2) Solids out flow rate
- (3) Caustic liquor makeup flow

- (4) Solids Samples analysis
- (5) Scrubber effluent analysis.

Knowing the caustic liquor flow rate, and the fluorine content of that liquor, one is able to calculate the amount of CaF_2 converted to HF. If, at the same time, the amount of CaF_2 exiting the reactor with the solids is known, one can again calculate the extent of CaF_2 conversion. There were, therefore, two methods available for the determination of the extent of conversion.

In the initial scrubber setup discussed in the Apparatus and Experimental Procedure section, it was impossible to obtain reliable liquor stream data due to the excessive fluctuations in caustic makeup flow rate, and frequent flooding of the column. It was, therefore, necessary to rely solely upon the solids out analysis for the determination of the fractional conversion of the fluorspar. Also, no reliance could be placed upon the fluorine mass balances.

The mass balances were, of course, based upon the premise that if the reactor was operating at steady state so that the following should be true.

$$\text{Ca in} = \text{Ca in solids out}$$

$$F \text{ in} = F \text{ out into scrubber} + F \text{ out in solids out}$$

$$SO_4 \text{ in} = SO_4 \text{ out into scrubber} + SO_4 \text{ out in solids out}$$

$$SiO_2 \text{ in} = SiO_2 \text{ out into scrubber as } SiF_4 + SiO_2 \text{ out in solids out}$$

The silica, entered the scrubber as SiF_4 but it was easier to consider it in terms of SiO_2 , since it was analysed as SiO_2 .

A. Sample Treatment

Figures AIV.1 and AIV.2 illustrate the methods used in handling the solids out samples. The quenching step was done in situ, as the sample was being collected, to ensure reaction termination. In the initial sample handling technique, only about 20 grams of sample were collected, but as the amount of quenching solution was increased from 100c.c. to 500 c.c. the amount of solids sample was also increased to about 80 grams.

When the initial samples handling technique was being used, several discrepancies came to light that caused one to doubt the accuracy of both the handling, and subsequent chemical analysis of the samples. The first discrepancy, was that the volume of the sample

liquor was much lower than the expected 100 or 150cc, originally added to the sample bottles. In addition, the weight of the filtered solids was greater than that expected after accounting for dissolution of H_2SO_4 .

The discrepancy in weight was attributed to the formation of the hydrates of $CaSO_4$ ($CaSO_4 \cdot 1/2H_2O$ and $CaSO_4 \cdot 2H_2O$). The volume discrepancy was attributed partly to the hydrate formation, but more largely to the physical entrainment of liquid within the filtered solids.

It was safe to assume that very little if any of the hydrates of $CaSO_4$ could form within the reactor because there was little or no water present in the reactor. Only 0.6 grams of water per 100 grams of fluor-spar could possibly have been present within the reactor. If one could account for H_2O boiloff this figure would be much lower. Also, above $220^\circ F$, only the $CaSO_4 \cdot 1/2H_2O$ hydrate of gypsum could form.

Nevertheless, subsequent analysis indicated that unless the sample solids were dried at $200^\circ C$ or higher, as much as 5% of the solids could consist of water of hydration. The major error caused by this water content, was its presence as an unaccounted for impurity in the solids. The major portion of this water of hydration

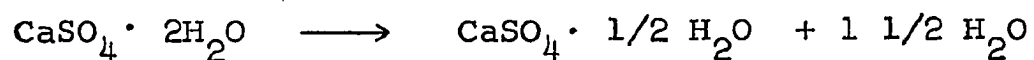
must have formed after the quenching step.

To eliminate the water of hydration, as well as to obtain an accurate measure of the amount of this water, two drying steps were necessary as shown in Figure AIV.2.

Crushing of the solids prior to the filtration step was necessary because the solids set as one large mass upon standing in the quenching liquor. It took a considerable amount of force to crush the solids into fine granules. The crushing step was carried out in the plastic sample bottles prior to decanting the liquid, using a 1 inch diameter 12 inches long glass rod. The crushed solids were easier to wash and did not entrain as much liquor.

To obtain an estimate of the amount of entrained liquid, the solids were weighed while still wet after filtering and drying over night at 90°C.

The drying step at 90°C was critical in that if the solids were not dried for a sufficient period of time incomplete drying was a possibility. On the other hand, prolonged drying could also drive off some of the water of hydration.

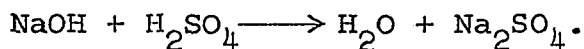


Determination of Water of Hydration: An Example

Consider Sample 8F-16

- (1) Wet filtered solids wgt. = 80.87 g.
- (2) Weight of filtered solids dried at 90°C = 66.19
- (3) Weight of filtered solids dried at 200°C = 60.54
- (4) Volume of liquor measured at filtering = 478 c.c.
- (5) Volume of liquor entrained = (1)-(2) = 14.68 c.c.
- (6) Volume of liquor hydrated = (2)-(3) = 5.65 c.c.
- (7) Total liquor volume at filtration = (4)+(5) = 493 c.c.
- (8) Total accountable liquor = (7)+(6) = 498.33

In the above example, it has been illustrated that all but 1.7 c.c. of the original liquid has been accounted for. However, no correction was attempted for the water formation by the reaction



Nor was any correction attempted to account for density changes due to non-ideal solution behaviour.

To obtain a measure of the accuracy of the analytical work being done at the Alcan labs, synthetic samples were compounded from pure reagents and sent for analysis.

Table AIV.2 contains the results of the analyses and the compositions as prepared. These samples were handled by

the modified sample handling technique of Figure AIV.2. Although the overall results were encouraging the analysis for samples 2 and 3 indicated a 6% error in the CaF_2 analysis.

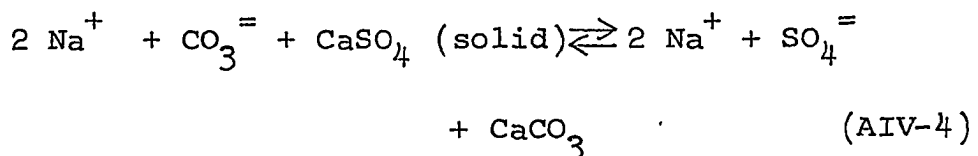
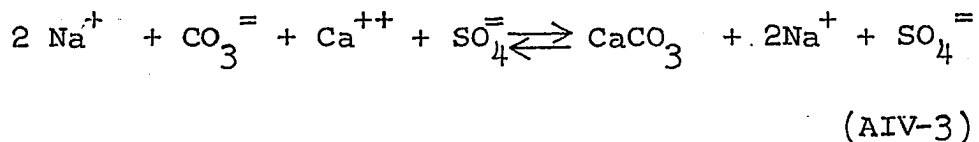
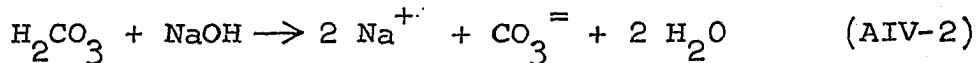
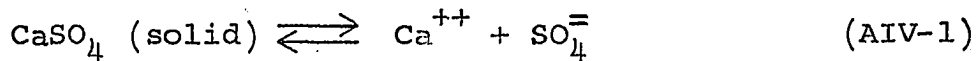
However, some of the problems encountered with the solids out samples did not occur with the synthetically compounded samples. The solids did not set upon standing, nor did they appear to take up any water of hydration. The author was often reminded by the lab people that although synthetic samples could be analysed within a high degree of accuracy, the results often could not be extrapolated to product stream samples. The product stream, may often contain impurities which interfere with the analysis. The determination of the $\text{SO}_4^{=}$ content was especially sensitive to impurities that could promote reduction of BaSO_4 during the fusion step in the $\text{SO}_4^{=}$ determination. (29)

Another discrepancy encountered in some of the solids out samples analyses reported, was that the addition of the compositions of the dried filtered solids failed to add to 100%. Quite often, the summation was lower than 90%. Furthermore, substantial amounts of CaCO_3 were detected in these samples. Often, the CaCO_3 content was

so high that if taken at face value, indicated more CaCO_3 leaving the reactor than entering it:

While modifications in analytical techniques made at the Alcan Works Laboratory eventually corrected the lack of summation to 100%, the results still indicated a high CaCO_3 content in the solids.

A likely explanation of the high CaCO_3 content is that it was being precipitated out of solution or being formed in the solid phase by the following reactions



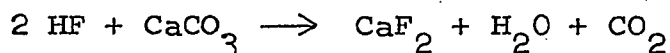
The equilibrium in equations (AIV-3) and (AIV-4) shifted to the right due to the lower solubility of CaCO_3 .

Na_2CO_3 may have been present in the quenching solution or formed by contact of the caustic solution with air during the quenching or filtering steps. Carbon

dioxide dissolved in the distilled water, used for washing the solids after filtering, would also cause CaCO_3 precipitation, but would not alter the $\text{SO}_4^{=}$ content of the mother liquor. On the other hand, the reaction scheme indicated that if the CaCO_3 was formed while the mother liquor was present, it would alter the $\text{SO}_4^{=}$ content of the mother liquor, by the formation of Na_2SO_4 . In any case, the precipitation of CaCO_3 , from what was originally CaSO_4 , must be accounted for.

Although CaCO_3 formation would occur prior to, and after removal of the mother liquor, only the two extremes were subject to analysis.

All the CaCO_3 detected in the samples was assumed to have been formed by way of equations (AIV-1) to (AIV-4). Because the reactor contents were much too reactive to CaCO_3 , it was safe to assume that none of it leaves unreacted. In addition to reacting with H_2SO_4 it will react with HF as follows



If the CaCO_3 was assumed to have been formed after the mother liquor was separated from the solids (CaCO_3 formation after filtration), the $\text{SO}_4^{=}$ content of the mother

liquor needed no correction but the CaSO_4 content of the solids was corrected as follows.

$$\begin{aligned} \text{Corrected \% CaSO}_4 &= \% \text{ CaSO}_4 \text{ detected} \\ \text{in dry solids} &+ \% \text{ CaCO}_3 \text{ detected} \cdot \left(\frac{\text{MW CaSO}_4}{\text{MW CaCO}_3} \right) \end{aligned}$$

- (AIV - 5)

When the CaCO_3 was assumed to have been formed prior to the washing step, while the mother liquor was present, the CaCO_3 present in the solids was considered to be an impurity which must be corrected for.

$$\begin{aligned} \text{Corrected \% CaSO}_4 &= \frac{\% \text{ CaSO}_4 \text{ detected}}{100 - \% \text{ CaCO}_3 \text{ detected}} \end{aligned} \quad (\text{AIV-6})$$

in dry solids

The $\% \text{ CaF}_2$, $\% \text{ SiO}_2$ and $\% \text{ R}_2\text{O}_3$ were also corrected in this manner.

The $\text{SO}_4^{=}$ present in solution as CaSO_4 was determined from the Ca^{++} content of the solution, but further correction was necessary due to the fact that CaCO_3 formation enhances dissolution of the sulfate ion.

$$\text{SO}_4^{=} \text{ present in soluble CaSO}_4 \text{ or put into solution by CaCO}_3 \text{ formation} = \left\{ \begin{array}{l} \text{Ca}^{++} \text{ detected} \\ \text{in g/l.} \end{array} \right. \cdot \left\{ \begin{array}{l} \text{volume} \\ \text{of} \\ \text{liquor} \end{array} \right.$$

$$\left. \frac{\text{MW}_{\text{SO}_4^{=}}}{\text{MW}_{\text{Ca}^{++}}} \right\} + \left\{ \begin{array}{l} \text{grams of CaCO}_3 \\ \text{detected in sample} \end{array} \right. \cdot \left. \frac{\text{MW}_{\text{SO}_4^{=}}}{\text{MW}_{\text{CaCO}_3}} \right\} \quad (\text{AIV-7})$$

Thus far, no mention has been made of the scrubber effluent samples. Treatment of these samples was much simpler, requiring only a filtration to remove any suspended solids present. The liquid was analysed for F^- , $\text{SO}_4^{=}$ and SiO_2 content. (29)

Because the scrubber liquor samples required no elaborate preparation for analysis, they were deemed more accurate. Furthermore, because the analysis was done by an automated technique, replicate analysis was accomplished easily, thus reducing the errors involved.

A summary of the determinations carried out on the samples and their utility is given in Table AIV.1.

In the Table is included the analysis of the sludge collected from the teflon transfer line, conveying the reactor gases to the scrubber. When the reactor was run at 450°F , considerable amount of condensation occurred in

the line to produce a sludge-like material consisting chiefly of condensed H_2SO_4 . At $370^{\circ}F$ the amount of this material was much less, while at $300^{\circ}F$ almost none was formed.

The sludge was removed from the line continuously, and its flow rate noted. At the Alcan lab it was filtered, and analysed as outlined in Table AIV.1.

Tables AIV.3, AIV.4 and AIV.5 show the chemical analysis results for runs 11A through 10F. In some of the solids out samples, the % $CaSO_4$ of the solids was not determined. However, for these cases the % $CaSO_4$ was calculated by difference. In the cases where it was reported, the summation of the percentages were reasonably close to 100%.

In runs 16A to 10F only the scrubber effluent samples were analysed. Analysis of the solids out samples was time consuming and unnecessary once the mass balances had been established. Recalling that the primary aim of the analysis was to establish the extent of conversion, the scrubber effluent samples sufficed for that purpose.

The analysis of the sludge samples was done only for the runs where a significant amount of this sludge was collected.

For the runs where only the scrubber effluent analyses were done, it was also necessary that the SiO_2 content of the solids out samples be determined. The results of these analyses are shown in Table AIV.6

B. Mass Balances

Basically, the solids out sample analyses were used only to establish a mass balance. The scrubber effluent analysis was used to establish a mass balance, and to determine the extent of conversion. In the discussion of sample treatment, the point was raised that in some of the solids out samples the summation of the components failed to add to 100%. Compensation for this error was made by assuming that either the per cent CaF_2 or per cent CaSO_4 of these solids was erroneous. If the % CaF_2 determination is assumed erroneous, it can be corrected by the following equation:

$$\% \text{CaF}_2 = 100 - (\% \text{CaSO}_4 + \% \text{SiO}_2 + \% \text{R}_2\text{O}_3 + \% \text{CaCO}_3)$$

If the % CaSO_4 reported is assumed in error, then the corrected % CaSO_4 can be determined as follows:

$$\% \text{CaSO}_4 = 100\% - (\% \text{CaF}_2 + \% \text{SiO}_2 + \% \text{R}_2\text{O}_3 + \% \text{CaCO}_3)$$

The mass balances using data with the above two alternate correction procedures are not reported here. All that needs to be said about those results is that they were not encouraging. Those mass balances indicated that usually less than 90%, and often less than 80%, of the Ca^{++} and F^- being fed into the reactor could be accounted for in the outlet streams. Accounting for the presence of CaCO_3 improved the results somewhat, but not to the point where the balances could be considered acceptable. Runs 1A - 6A and 1E - 5E were all discarded due to difficulties in obtaining good mass balances.

After modifications were made to the analytical techniques employed at the Alcan Laboratories, the addition of the compositions of the dry solids of the solids out samples was much closer to 100%. If one examines the data of table AIV.3 one notes that although the summations of the solid compositions were not exactly 100%, they were reasonably close to that value.

Tables AIV.7, AIV.8, AIV.9 and AIV.10 show the results of the mass balances for runs 11A to 15A.

Because the solids out flow was rather unstable, due to pulsations of the reactor, there was reason to believe

that an accurate measure of the solids out flow rate was unavailable. To compensate for this, a solids out flow correction was attempted on the basis of an accurate sulfate balance. The solids out flow rate was modified by forcing a sulfate mass balance.

$$\text{Corrected solids out flow rate} = \text{Measured solids out flow rate} \times \left(\frac{100}{100 + \text{SO}_4^{=}\text{ balance error}} \right)$$

And the $\text{SO}_4^{=}$ balance error was

$$\text{SO}_4^{=} \text{ balance error} = \left(\frac{\text{SO}_4^{=} \text{ in} - \text{SO}_4^{=} \text{ out}}{\text{SO}_4^{=} \text{ in}} \right) \times 100$$

If the sulfate balance error was positive or negative, the solids out flow rate was decreased or increased respectively, to compensate for this error.

Similarly

$$\text{Ca}^{++} \text{ balance error} = \left(\frac{\text{Ca}^{++} \text{ in} - \text{Ca}^{++} \text{ out}}{\text{Ca}^{++} \text{ in}} \right) \times 100$$

$$\text{F}^{-} \text{ balance error} = \left(\frac{\text{F}^{-} \text{ in} - \text{F}^{-} \text{ out}}{\text{F}^{-} \text{ in}} \right) \times 100$$

and

$$\text{SiO}_2 \text{ balance error} = \left(\frac{\text{F}^{-} \text{ in} - \text{F}^{-} \text{ out}}{\text{F}^{-} \text{ in}} \right) \times 100$$

The following relations were also used.

$$\text{SO}_4^{\equiv} \text{ out} = (\text{SO}_4^{\equiv} \text{ out in solids out as H}_2\text{SO}_4 \text{ or CaSO}_4) \\ + (\text{SO}_4^{\equiv} \text{ out in Scrubber Effluent}) + \\ (\text{SO}_4^{\equiv} \text{ in sludge})$$

$$\text{Ca}^{++} \text{ out} = (\text{Ca}^{++} \text{ out in solids out as CaF}_2 \text{ or CaSO}_4) \\ + (\text{Ca}^{++} \text{ out as sludge})$$

$$\text{F}^- \text{ out} = (\text{F}^- \text{ out as CaF}_2 \text{ in solids out}) \\ + (\text{F}^- \text{ out in scrubber effluent}) + (\text{F}^- \text{ out in sludge})$$

$$\text{SiO}_2 \text{ out} = (\text{Si})_2 \text{ out in solids out} + (\text{Si}) \text{ out in scrubber} \\ \text{effluent} + (\text{SiO}_2 \text{ out in sludge})$$

$$\% \text{ CaF}_2 \text{ reacted} = \left[\frac{\text{CaF}_2 \text{ in} - \text{CaF}_2 \text{ out in solids}}{\text{CaF}_2 \text{ in}} \right] \times 100$$

$$\% \text{ H}_2\text{SO}_4 \text{ reacted} =$$

$$\text{H}_2\text{SO}_4 \text{ in} - \left(\frac{(\text{H}_2\text{SO}_4 \text{ out in solids} + \text{H}_2\text{SO}_4 \text{ out in scrubber} \\ \text{effluent})}{\text{H}_2\text{SO}_4 \text{ in}} \right) \times 100$$

$$\% \text{ SiO}_2 \text{ reacted} = \left[\frac{\text{SiO}_2 \text{ in} - \text{SiO}_2 \text{ out in solids}}{\text{SiO}_2 \text{ in}} \right] \times 100$$

A computer program was written to do the mass balances on the reactor. A nomenclature is provided for easier understanding of the program.

Mass balances of sorts, using only the scrubber effluent analysis, were also calculated. For these calculations, the following identities were used.

$$(\text{CaF}_2 \text{ reacted}) = \left[\begin{array}{l} (\text{F}^- \text{ in scrubber}) \times (\text{flow of scrubber}) \times \frac{78}{38} \\ \text{effluent} \qquad \qquad \qquad \text{effluent} \end{array} \right]$$

Every 38 grams of F^- in the scrubber effluent required that 78 grams of CaF_2 react

$$(\text{H}_2\text{SO}_4 \text{ reacted}) = \left[\begin{array}{l} (\text{F}^- \text{ in scrubber}) \times (\text{flow of scrubber}) \times \frac{98}{38} \\ \text{effluent} \qquad \qquad \qquad \text{effluent} \end{array} \right] \\ + \left[\begin{array}{l} \text{CaCO}_3 \text{ fed} \times \frac{98}{100} \\ \text{in fluorspar} \end{array} \right]$$

Every 38 grams of F^- in the scrubber effluent required that 98 grams of H_2SO_4 react, and every 100 grams of CaCO_3 in the fluorspar feed reacted with 98 grams of H_2SO_4 .

$$\text{Solids flow out} = (\text{Total feed}) - \left[(\text{CO}_2 + \text{HF} + \text{SiO}_2 + \text{H}_2\text{SO}_4) \right. \\ \left. \text{out into scrubber} \right] - (\text{sludge flow})$$

CO_2 was formed from CaCO_3

Insoluble solids out = (solids out) - (H_2SO_4 left in reactor)

(H_2SO_4 left in reactor) = (H_2SO_4 fed) - (H_2SO_4 out into

scrubber + H_2SO_4 reacted + H_2SO_4 out in sludge)

$$(\text{SiO}_2 \text{ in solids out}) = \left[\text{Insoluble solids out} \right] \times \left[\frac{\% \text{ SiO}_2 \text{ in solids of solids out sample}}{100} \right]$$

This was the only point where a solids sample analysis was required.

$$\text{CaSO}_4 \text{ out in solids out} = \left[\text{Insoluble solids out} \right] - \left[\text{CaF}_2 \text{ unreacted} \right] + \text{SiO}_2$$

$$(\text{Total CaSO}_4 \text{ out}) = \left[\text{CaSO}_4 \text{ out in solids out} \right] + \left[\text{CaSO}_4 \text{ out in sludge} \right]$$

$$\% \text{ CaF}_2 \text{ reacted} = (\text{CaF}_2 \text{ reacted} / \text{CaF}_2 \text{ in}) \times 100$$

The amount of CaF_2 reacted, was calculated on the basis of how much fluorine was detected in the scrubber effluent.

The above calculations, were based on the premise that all the fluorine be accounted for. Whatever part of the fluorine that did not appear in the scrubber effluent must have appeared in the solids out as CaF_2 .

The results obtained by this method of calculation are shown in Table AIV.11. The average conversions shown in this table were the accepted conversion values used in calculating the rate constants for the reaction rate models.

C. Discussion

While fluctuations in the solids out flow rate occurred in most of the runs carried out in the continuous reactor, the mass balances in tables AIV.7 through AIV.11 may be considered to be reasonably good. There was, however, a persisting nagging suspicion that the solids out samples analysis was not entirely satisfactory. This suspicion was based upon the fact that too many things can go wrong in the analyses.

The analyses for fluorine content in the scrubber effluent were considered to be more reliable because replicate analyses were carried out. Without replication of analyses, however, the results could be sometimes misleading, because the error in one analysis could be very high due to instrument error.

At the Alcan Works Laboratory the fluoride analysis was carried out by means of an automatic sample handling apparatus (Technicon). This equipment first carried out a sulfuric acid distillation, to drive all the fluorine from the original sample, and thus separate it from possible interfering ions. The amount of fluorine collected was subsequently determined by photometric analysis, using a

complexing reagent.

This automatic analyser was subject to malfunctions when initially put into operation, which unfortunately was also the time the first analyses of the scrubber liquor samples were being carried out.

However, once the Technicon analyser was functioning properly, the results were quite accurate, as was substantiated by having some of the samples check analysed by the Alcan Research Laboratories. In the research labs, the fluoride determination again required the distillation step but using perchloric acid, and the amount of fluorine distilled out of the sample was determined by a recently developed potentiometric titration with $\text{La}(\text{NO}_3)_3$ or $\text{Th}(\text{NO}_3)_4$ solution, using an Orion Fluoride electrode. (6) The results indicated that there was no bias in the method used by the Alcan Works Laboratory.

The standard error of single analysis was determined to be 0.079 g. per litre in a 2.5 g/l fluorine content, and an overall standard error in the estimate of the average fractional conversion of 0.0142. The average fractional conversion was calculated on the basis six samples for each run. The standard error in the estimate of the fractional conversion accounted for errors in the

scrubber liquor flow rate, the spar feed rate as well as deviations observed from sample to sample within each run. The overall degree of accuracy can be considered as acceptable.

Unfortunately, the analysis of the batch runs solids samples could not be analysed in replicate because of the time and costs involved. However, replicate samples were taken (samples taken at the same reaction time at the same temperature), and analysis of these samples allowed one to determine the pure error due to analysis and chance errors that could occur in any run. The pure error was determined to be 0.03 (fractional conversion). This error was significantly larger than the error in the continuous reactor determination of the fractional conversion.

It had been hoped that rather than relying on chemical analysis of the samples one could determine the degree of chemical conversion in the batch reactor by gravimetric techniques ie. following the weight of the reacting mass with time. However, this proved to be very difficult unless very sophisticated equipment was used. Thermal conversion effects, in particular, could not be adequately controlled.

D. Nomenclature for Mass Balance Program

By order of appearance; All flows in grams per hour

I	=	run no.
ISAMP	=	sample no.
RPM	=	rotation rate of reactor stirrers
SPARF	=	spar feed rate
CAUSTF	=	caustic liquor feed rate to scrubber (litres/hr.)
ACIDF	=	acid feed rate
SOLF	=	solids out flow rate
SSW	=	solids sample weight in grams
DSOLW	=	weight of dried solids from solids out sample (grams)
VSS	=	volume of liquor from solids out sample in litres
FCL	=	fluorine in caustic liquor sample (g./l.)
S04CL	=	sulfate in caustic liquor sample (g./l.)
CACL	=	calcium in caustic liquor sample (g./l.)
SILCL	=	silica in caustic liquor sample (g./l.)
S04SS	=	sulfate in solids out sample liquor (g./l.)
CASS	=	calcium in solids out sample liquor (g./l.)
PCAF2	=	per cent CaF_2 in dried solids of solids out sample.

PCAS04	= per cent CaSO_4 in dried solids of solids out sample
PSIL	= per cent silica in dried solids of solids out sample
PCAC03	= per cent CaCO_3 in dried solids of solids out sample
PR203	= per cent R_2O_3 in dried solids of solids out sample
S	= sludge flow rate out
SL	= fraction of sludge as liquid
SLS04	= fraction of sludge liquor as $\text{SO}_4^{=}$
SLF	= fraction of sludge liquid as fluorine
SLSIL	= fraction of sludge liquid as silica
SS	= fraction of sludge as solids
SSCAS04	= per cent CaSO_4 in sludge solids
SSSIL	= per cent silica in sludge solids
SCA	= calcium out as part of sludge
SF	= fluorine out as part of sludge
SSIL	= silica out as part of sludge
SS04	= sulfate out as part of sludge
SH2S04	= H_2SO_4 out as part of sludge
SHF	= HF out as part of sludge
CAIN	= calcium into reactor
CAF2IN	= CaF_2 into reactor
FIN	= fluorine into reactor
SILIN	= silica into reactor
CO2OUT	= CO_2 out of reactor

SO4IN	= sulfate into reactor
FSO4CL	= sulfate out in caustic liquor
ACIDCL	= H_2SO_4 out in caustic liquor
SOLS04	= soluble sulfate out of reactor in the solids out
SCAS04	= soluble $CaSO_4$ out of reactor in the solids out
ACIDO	= acid out of reactor in solids out
TCAS04	= total $CaSO_4$ out of reactor
SILISO	= silica out in solids out
S04OUT	= total sulfate out of reactor
S04ERR	= error in sulfate balance
CAOUT	= calcium out of reactor
CAERR	= error in calcium balance
FOUT	= fluorine out of reactor
FERR	= error in Fluorine balance
CAF2R	= CaF_2 reacted
PCAF2R	= per cent CaF_2 reacted
ACIDR	= acid reacted
PACIDR	= per cent acid reacted
TSILO	= total Silica out
SILERR	= error in silica balance
PSILR	= per cent silica reacted
A	= solids out flow rate corrected to force a calcium balance
CPCAF2	= corrected per cent CaF_2 content of solids out sample solids.

MASS BALANCES ON HF STILL.

TO CHANGE THE PROGRAM FOR A DIFFERENT SPAR FEED CHANGE CARDS 15,
 16,17,18,18, AND 19
 CARD 15, CAIN = SPARF*((FRACTIONAL CACO3 CONTENT*0.40)+(FRACTIONAL
 CAF2 CONTENT*40.0/78.0)
 CARD 16, FIN = SPARF*(FRACTIONAL CAF2 CONTENT*38.0/78.0)
 CARD 17, CAF2IN = SPARF*(FRACTIONAL CAF2 CONTENT)
 CARD 18, SILIN = SPARF*(FRACTIONAL SILICA CONTENT)
 CARD 19, CO2OUT = SPARF*(FRACTIONAL CACO3 CONTENT*0.44
 LAST DATA CARD MUST BE BLANK

DATA INPUT -

FIR.LF CARD, RUN NO.(ALPHANUMERIC) COLS1-4,SAMPLE NO. (FIXED MODE)
 COLS 5-7, RPM OF STIRRERS F11.5,COLS 9-18
 SUCCEEDING CARDS,SPAR FEED RATE,CAUSTIC FLOW RATE,ACID FEED RATE,
 SOLIDS OUT RATE,SOLIDS SAMPLE WEIGHT,DRY SOLIDS SAMPLE WEIGHT,
 VOL. OF SAMPLE LIQUOR IN LITRES,FLUORINE CONTENT OF CAUSTIC LIQUOR
 SULFATE CONTENT OF CAUSTIC LIQUOR,CALCIUM CONTENT OF CAUSTIC
 LIQUOR,SILICA CONTENT OF CAUSTIC LIQUOR,SULFATE CONTENT OF SOLIDS
 OUT LIQUOR,CALCIUM CONTENT OF SOLIDS OUT LIQUOR,(CAF2 OF DRY
 SOLIDS,(CASO4 OF DRY SOLIDS,(SILICA OF DRY SOLIDS (CACO3 OF DRY
 SOLIDS AND (R2O3 OF DRY SOLIDS , ALL ON SEPARATE CARDS AND IN
 ORDER
 SLUDGE FLOW RATE,FRACTION OF SLUDGE AS LIQUID, SO4 IN SLUDGE LIQUID
 AND FLUORINE IN SLUDGE LIQUID ON THE NEXT CARD (4F11.5)
 SILICA IN SLUDGE LIQUID, FRACTION SOLIDS IN SLUDGE,CASO4 IN SLUDGE
 SOLIDS,AND SILICA IN SLUDGE SOLIDS ARE ON THE NEXT CARD (4F11.5)

50 READ 1,1,1,ISAMP,RPM 1
 IF(RPM)52,52,51 2
 51 READ 2,SPARF,CAUSTF,ACIDF,SOLF,SSW,DSOLW,VSS,FCL,S04CL,CACL,SILCL, 3
 IS04SS,CASS,PCAF2,PCASO4,PSIL,PCACO3,PR2O3 4
 READ 600,S,SL,SLSO4,SLF,SLSIL,SS,SSCASO,SSSIL

```

5 PRINT 3,I,ISAMP
6 PRINT 4,SPARF
7 PRINT 5,ACIDF
8 PRINT 6,SOLF
9 PRINT 7,RPM
10 PRINT 8,CAUSTF
11 PRINT 9,FCL,S04CL,CACL,SILCL
12 PRINT 10,SSW,DSOLW,VSS
13 PRINT 11,PCAF2,PCASO4,PSIL,PCACO3,PR2O3
14 PRINT 12,S04SS,CASS
    PRINT 601
PRINT 602,S,SL,SLSO4,SLF,SLSIL,SS,SSCASO,SSSIL
SCA=(SSCASO/100.0)*S*SS*40.0/136.0
SF=S*SL*SLF
SSIL=S*SS*(SSSIL/100.0)+S*SL*SLSIL
SSO4=S*SS*(SSCASO/100.0)*(96.0/136.0)+(S*SL*SLSO4)
SH2SO4=S*SL*SLSO4*98.0/96.0
SHF=(S*SL*SLF/19.0)-(S*SL*SLSIL/60.1))*84.1
IF(SHF.LT.0.0)SHF=0.0
CAIN=SPARF*((0.0714*0.40)+(0.9036*40.0/78.0))
CAF2IN=SPARF*0.9036
FIN=SPARF*(0.9036*38.0/78.0)
SILIN=SPARF*0.0125
CO2OUT=SPARF*0.0714*0.44
C
C CALCULATIONS ASSUMING CACO3 FORMATION AFTER
C REMOVAL OF SAMPLE LIGUOR
C
A=SOLF
R=0.0
S04IN = ACIDF*(96.0/98.0)
FS04CL = CAUSTF*S04CL
ACIDCL = FS04CL*(98.0/96.0)
PRINT 3,I,ISAMP
23
24
25
26
27
21A

```

```

21B PRINT 13
22 PRINT 14
28 SOLS04 = S04SS*VSS*(A/SSW)
29 SCAS04 = CASS*(136.0/40.0)*VSS*(A/SSW)
30 ACIDO = (SOLS04-(SCAS04*96.0/136.0))*(98.0/96.0)
C
C D = DRY SOLIDS OUT FLOW RATE
30A
C
C D = A-ACIDO
30B
31 TCAS04 = SCAS04+((PCACO3/100.0)*D*1.36)+((PCASO4/100.0)*D)
32 CAF20 = (PCAF2/100.0)*D
33 SILISO = (PSIL/100.0)*D
34 S04OUT = (TCAS04*(96.0/136.0))+FSO4CL+(ACIDO*(96.0/98.0))
34B S04OUT=S04OUT+SSO4
35 S04ERR = ((S04OUT-S04IN)/(S04IN))*100.0
36 CAOUT = (TCAS04*(40.0/136.0))+((CACL*CAUSTF)+CAF20*(40.0/78.0))
36B CAOUT=CAOUT+SCA
37 CAERR = ((CAOUT-CAIN)/(CAIN))*100.0
38 FOUT = (CAF20*38.0/78.0)+(FCL*CAUSTF)
38B FOUT=FOUT+SF
39 FERR = ((FOUT-FIN)/(FIN))*100.0
C
C CALCULATING PER CENT CONVERSIONS
C
CAF2R = CAF2IN-CAF20
40 PCAF2R = (CAF2R/CAF2IN)*100.0
41 ACIDR = ACIDF-(ACIDO+ACIDCL)
42 ACIDR=ACIDR-SH2SO4
42B PACIDR = (ACIDR/ACIDF)*100.0
43 TSIL0 = SILISO+(SILCL*CAUSTF)
44 TSIL0=TSIL0+SSIL
44B SILERR = ((TSIL0-SILIN)/(SILIN))*100.0
45 PSILR = ((SILIN-SILISO)/SILIN)*100.0
46 PRINT 20,CAF2IN
D46B PRINT 21,C02OUT
D46C

```

```

D46J PRINT 22,ACIDCL
D46E PRINT 23,ACIDO
D46F PRINT 24,TCASO4
D46G PRINT 25,CAF2O
D46H PRINT 26,CAF2R
D46I PRINT 27,ACIDR
47 PRINT 15,S04ERR,CAERR,FERR,SILERR
48 PRINT 16,PACIDR,PCAF2R,PSILR
49 IF(R)500,500,501

C SOLIDS OUT FLOW CORRECTION
C
C 500 A = SOLF*(100.0/(100.0+S04ERR))
PRINT 17,A
R =1.0
GO TO 502
501 CONTINUE
PRINT 3,1,ISAMP
PRINT 101
PRINT 14
SN=0.0

C CALCULATIONS ASSUMING CAC03 FORMATION PRIOR TO
C REMOVAL OF SAMPLE LIQUOR
C
C B = SOLF
203 SSO4IS =VSS*S04SS
SCAIS = VSS*CASS
C
C P=CAC03 CONTENT OF SAMPLE
60B P = DSOLW*PCAC03/100.0
61
C Q = CALCIUM REMOVED FROM SAMPLE AS CAC03
62B

```

D46J
D46E
D46F
D46G
D46H
D46I
47
48
49

50
51
52
53
54A
D54
54B
55
56

57
58
59

60B
61
62B

C Q = P*0.40 63
 C T = TOTAL CALCIUM DETECTED AS SOLUBLE CALCIUM OR AS CaCO3 64B
 C T = Q+SCAIS 65
 C U = CALCIUM SULFATE DETECTED AS SOLUBLE CALCIUM OR AS CaCO3 66B
 C U = T*136.0/40.0 67
 C ACIDO = (SSO4IS-(T*(96.0/40.0)))*(93.0/96.0)*(B/SSW) 68
 C V = CALCIUM SULFATE PUT INTO SOLUTION OR CONVERTED TO CaCO3 69B
 C V = T*(136.0/40.0) 70
 C INS:) = SOLIDS OUT LESSACID AND V 71B
 C INSSO = B-(ACIDO+V) 72
 C THE COMPOSITION OF THE DRY SAMPLE SOLIDS MUST BE CORRECTED
 C FOR THE CaCO3 CONTENT
 C W = 1.0-(PCaCO3/100.0) 74
 C PCAF2 = PCAF2/W 75
 C CCASO4 = PCASO4/W 76
 C CPSIL = PSIL/W 77
 C CPR2O3 = PR2O3/W 78
 C CAF2O = INSSO*PCAF2/100.0 79
 C TCASO4 = (INSSO*(CCASO4/100.0))+(V) 80
 C SILISO = CPSIL*(INSSO/100.0) 81
 C SO4OUT = (ACIDO*(96.0/98.0))+(FSO4CL)+(TCASO4*(96.0/136.0)) 82
 C SO4OUT=SO4OUT+SSO4 82B
 C SO4ERR = ((SO4OUT-SO4IN)/(SO4IN))*100.0 83

```

84  GAOUT = (CAF20*40.0/78.0)+(TCASO4*(40.0/136.0))+(CACL*CAUSTF)
84B CAOUT=CAOUT+SCL
85  CAERR = ((CAOUT-CAIN)/(CAIN))*100.0
86  FOUT = (CAF20*(38.0/78.0))+(FCL*CAUSTF)
86B FOUT=FOUT+SF
87  FERR = ((FOUT-FIN)/(FIN))*100.0
88  SILOUT = (SILISO)+(SILCL*CAUSTF)
88B SILOUT=SILOUT+SSIL
89  SILERR = ((SILOUT-SILIN)/(SILIN))*100.0

C
C   CALCULATING PER CENT CONVERSIONS
C
90  ACIDR = (ACIDF)-(ACIDO+ACIDCL)
90B ACIDR=ACIDR-SH2SO4
91  PACIDR = (ACIDR/ACIDF)*100.0
92  CAF2R = CAF2IN-CAF2O
93  PCAF2R = (CAF2R/CAF2IN)*100.0
94  SILR = (SILIN-SILISO)
95  PSILR = (SILR/SILIN)*100.0
D95B PRINT 20,CAF2IN
D95C PRINT 21,CO2OUT
D95D PRINT 22,ACIDCL
D95E PRINT 23,ACIDO
D95F PRINT 24,TCASO4
D95G PRINT 25,CAF2O
D95H PRINT 26,CAF2R
D95I PRINT 27,ACIDR
96  PRINT 15,S04ERR,CAERR,FERR,SILERR
97  PRINT 16,PACIDR,PCAF2R,PSILR
98  IF(SN)200,200,201

C
C   SOLIDS OUT FLOW CORRECTION
C
200 B = SOLF*100.0/(100.0+S04ERR)

```

100
101
102
103A
103B
104
105
105B

```

PRINT 17,B
SN=1.0
GO TO 203
201 PRINT 3,I,ISAMP
PRINT 301
TOTIN = SPARF +ACIDF
AHFOUT = FCL*CAUSTF*(40.0/38.0)
AHFOUT=AHFOUT+SHF

```

C
C
C
C
C
C
C
C

CALCULATIONS ON THE BASIS OF ONLY THE SCRUBBER EFFLUENT ANALYSIS

C = SOLIDS OUT.RATE USING CAUSTIC LIQUOR ANALYSIS ONLY 106D

```

SILICL = CAUSTF*SILCL
C = TOTIN - (CO2OUT+AHFOUT+SILICL+ACIDCL)
C=C-S
PRINT 18,C
CAF2R = AHFOUT*78.0/40.0
ACIDR =(AHFOUT*(98.0/40.0))+(CO2OUT*(98.0/44.0))
CAF20 = CAF2IN-CAF2R
ACID0 = ACIDF -(ACIDR+ACIDCL)
ACID0=ACID0-SH2SO4

```

C
C
C

D = INSOLUBLE SOLIDS OUT 113D

```

D = C-ACID0
SILISO = D*PSIL/100.0
CASO40 = D-((SILISO)+(CAF20)+(D*PR203/100.0))
CASO40=CASO40+(SSCASO/100.0)*S*SS
FSO4CL=S04CL*CAUSTF
S04OUT = (ACID0*96.0/98.0)+(CASO40*96.0/136.0)+FSO4CL
S04ERR = ((S04OUT-S04IN)/(S04IN))*100.0
CAOUT = (CAF20*(40.0/78.0))+(CASO40*(40.0/136.0))+(CACL*CAUSTF)

```

114
115
116
116D
117
118
119

```

120 CAERR = ((CAOUT-CAIN)/(CAIN))*100.0
121 SILOUT = SILISO + SILICL
121B SILOUT=SILOUT+SSIL
122 SILERR = ((SILOUT-SILIN)/(SILIN))*100.0
D123B PRINT 20,CAF2IN
D123C PRINT 21,CO2OUT
D123D PRINT 22,ACIDCL
D123E PRINT 23,ACIUO
D123F PRINT 24,CASO4O
D123G PRINT 25,CAF2O
D123H PRINT 26,CAF2R
D123I PRINT 27,ACIDR
123 FERR =0.0
124 PRINT 15,S04ERR,CAERR,FERR,SILERR

C
C
C
CALCULATING PER CENT CONVERSIONS

125 PACIDR = (ACIDR/ACIDF)*100.0
126 PCAF2R = (CAF2R/CAF2IN)*100.0
127 PSILR = ((SILIN-SILISO)/SILIN)*100.0
128 PRINT 16,PACIDR,PCAF2R,PSILR

C
C
C
ACID TO SPAR RATIO CALCULATIONS

C
C
C
CALCULATIONS USING FEED CONDITIONS

129 REQA=SPARF*((0.9036*98.0/78.0)+0.0714*0.98)
RATIO=ACIDF/REQA
PRINT 610,RATIO
610 FORMAT(1H0,1X,@ACID9SPAR RATIO AS FED = @,E14.7)
AA=((ACIDF-SPANF*0.0714*0.98)/98.0)/((SPARF*0.9036)/78.0)
PRINT 611,AA

```

```

C
C
C
ACCOUNTING FOR ACID FUMING
CRATIO=(ACIDF-ACIDCL-SH2SO4)/REQA
PRINT 612,CRATIO
CAA=(ACIDF-ACIDCL-SH2SO4-SPARF*0.0714*0.98)/(SPARF*0.9036*98.00/78.
10)
PRINT 613,CAA
GO TO 50
1 FORMAT(A4,I3,F11.5)
2 FORMAT(F11.5)
3 FORMAT(IH1,10X,0RUN NO. @,A4,11X,@SAMPLE NO. @,I3)
4 FORMAT(IH0,10X,@SPAR FEED RATE = @,F11.5,@GRAMS PER HOUR@)
5 FORMAT(IH0,10X,@ACID FEED RATE = @,F11.5,@GRAMS PER HOUR@)
6 FORMAT(IH0,10X,@SOLIDS OUT RATE = @,F11.5,@GRAMS PER HOUR@)
7 FORMAT(IH0,10X,@RPM OF STIRRERS = @,F11.5)
8 FORMAT(IH0,10X,@CAUSTIC LIQUOR FEED RATE = @F11.5,@LITRES PER HOUR
1@)
9 FORMAT(IH0,10X,@CAUSTIC LIQUOR ANALYSIS@/IH0,10X,@FLUORINE@,6X,
1F11.5,@GRAMS PER LITRE@/11X,@SULFATE@,7X,F11.5,@GRAMS PER LITRE@/
211X,@CALCIUM@,7X,F11.5,@GRAMS PER LITRE@/11X,@SILICA@,8X,F11.5,
3@GRAMS PER LITRE@)
10 FORMAT(IH0,10X,@SAMPLE WEIGHT = @,F11.5,@GRAMS@/IH0,10X,@WEIGHT OF
1 DRY SAMPLE SOLIDS = @,F11.5,@GRAMS@/IH0,10X,@VOLUME OF SAMPLE LIQ
2UOR = @,F11.5,@LITRES@)
11 FORMAT(IH0,10X,@ANALYSIS OF DRY SAMPLE SOLIDS@/IH0,10X,@CALCIUM FL
1UORIDE@,8X,F11.5,@(@/1H,10X,@CALCIUM SULFATE@,9X,F11.5,@(@/1H,10
2X,@SILICA@,16X,F11.5,@(@/11X,@CALCIUM CARBONATE@,7X,F11.5,@(@/11X,
3@R2O3@,20X,F11.5,@(@)
12 FORMAT(IH0,10X,@SOLIDS SAMPLE LIQUOR ANALYSIS@/IH0,10X,@SULFATE@,
18X,F11.5,@GRAMS PER LITRE@/11X,@CALCIUM@,8X,F11.5,@GRAMS PER LITRE
2@)
13 FORMAT(IH0,10X,@RESULTS ASSUMING CaCO3 FORMATION DURING FILTRATION
1@)
129
130
131
132
133
134
135
136
137-1
137-2
138-1
138-2
138-3
138-4
139-1
139-2
139-3
140-1
140-2
140-3
140-4
141-1
141-2
141-3
142-1
142-2

```

14 FORMAT(1H0,10X,@NO SOLIDS OUT CORRECTION FOR SULFATE BALANCE@) 143
 15 FORMAT(1H0,10X,@ERROR IN SULFATE BALANCE = @,F11.5,@(/11X,@ERROR 144-1
 1 IN CALCIUM BALANCE = @,F11.5,@(/11X,@ERROR IN FLUORINE BALANCE 144-2
 2 = @,F11.5,@(/11X,@ERROR IN SILICA BALANCE = @,F11.5,@(@) 144-3
 16 FORMAT(1H0,10X,@PER CENT ACID REACTED = @,F11.5/1H ,10X, 145-1
 1@PER CENT CAF2 REACTED = @F11.5/1H ,10X,@PER CENT SILICA REA 145-2
 CTED = @,F11.5) 145-3
 17 FORMAT(1H0,10X,@WITH SOLIDS OUT CORRECTION FOR A SULFATE BALANCE@/ 146-1
 11H0,10X,@CORRECTED SOLIDS OUT FLOW = @,F11.5,@GRAMS PER HOURS) 146-2
 18 FORMAT(1H0,10X,@SOLIDS OUT FLOW USING CAUSTIC LIQUOR ANALYSIS ONLY 1080-1
 1 = @,F11.5,1X,@GRAMS PER HOUR@) 1080-2
 101 FORMAT(1H0,10X,@RESULTS ASSUMING CACO3 FORMATION PRIOR TO FILTRATI 147-1
 ON@) 147-2
 301 FORMAT(1H0,10X,@CALCULATIONS USING ONLY THE CAUSTIC LIQUOR ANALYSI 148-1
 15@) 148-2
 20 FORMAT(1H0,10X,@CAF2 IN = @,F11.5,@GRAMS PER HOUR@) D1
 21 FORMAT(1H0,10X,@CO2 OUT = @,F11.5,@GRAMS PER HOUR@) D2
 22 FORMAT(1H0,10X,@H2SO4 OUT INTO SCRUJER = @,F11.5,@GRAMS PER HOUR@ 03-1
 1) 03-2
 23 FORMAT(1H0,10X,@H2SO4 OUT WITH SOLIDS = @,F11.5,@GRAMS PER HOUR@) D4
 24 FORMAT(1H0,10X,@CASO4 OUT WITH SOLIDS = @,F11.5,@GRAMS PER HOUR@) D5
 25 FORMAT(1H0,10X,@CAF2 OUT WITH SOLIDS = @,F11.5,@GRAMS PER HOUR@) D6
 25 FORMAT(1H0,10X,@CAF2 REACTED = @,F11.5,@GRAMS PER HOUR@) D7
 27 FORMAT(1H0,10X,@ACID REACTED = @,F11.5,@GRAMS PER HOUR@) D8
 600 FORMAT(4F11.5)
 501 FORMAT(1H0,10X,@TRANSFER LINE SLUDGE@)
 502 FORMAT(1H0,10X,@SLUDGE FLOW RATE = @,F11.5/1H ,10X,@FRACTION OF SL 1
 UIDGE AS LIQUID = @,F11.5/1H ,10X,@GRAMS OF SULFATE PER GRAM OF SLU 2
 DGE LIQUID = @,F11.5/1H ,10X,@GRAMS OF FLOURINE PER GRAM OF SLUDGE 3
 3LIQUID = @,F11.5/1H ,10X,@GRAMS OF SILICA PER GRAM OF SLUDGE LIQUID 4
 4 = @,F11.5/1H ,10X,@FRACTION OF SLUDGE AS SOLID = @,F11.5/1H ,10X, 5
 5@PER CENT CASO4 IN SLUDGE SOLIDS = @,F11.5/1H ,10X,@PER CENT SILIC 6
 6A IN SLUDGE SOLIDS = @,F11.5) 6A
 611 FORMAT(1H0,10X,@AA VALUE USING FEED CONDITIONS ACCOUNTING FOR CALC 11
 IITE = @,E14.7) 11E
 612 FORMAT(1H0,10X,@ACID9SPAR RATIO ACCOUNTING FOR ACID FUMING = @E14. 17)
 17)

613 FORMAT(1H0,1UX,2AA VALUE ACCOUNTING FOR CALCITE AND ACID FUMING =

12,E14.7)

52 STOP

END

149

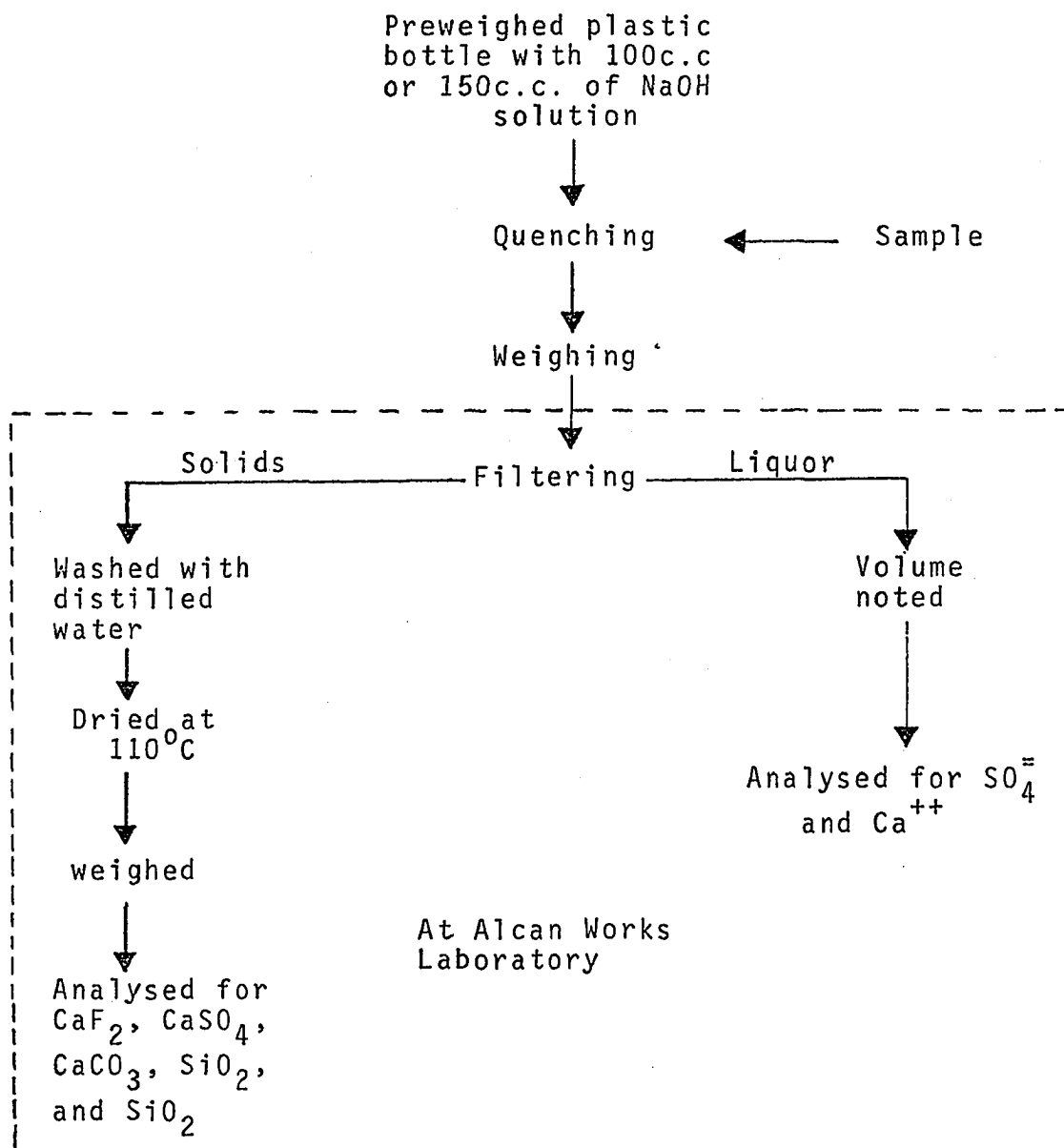


FIGURE AIV.1 Initial Solids Out Samples Handling Scheme

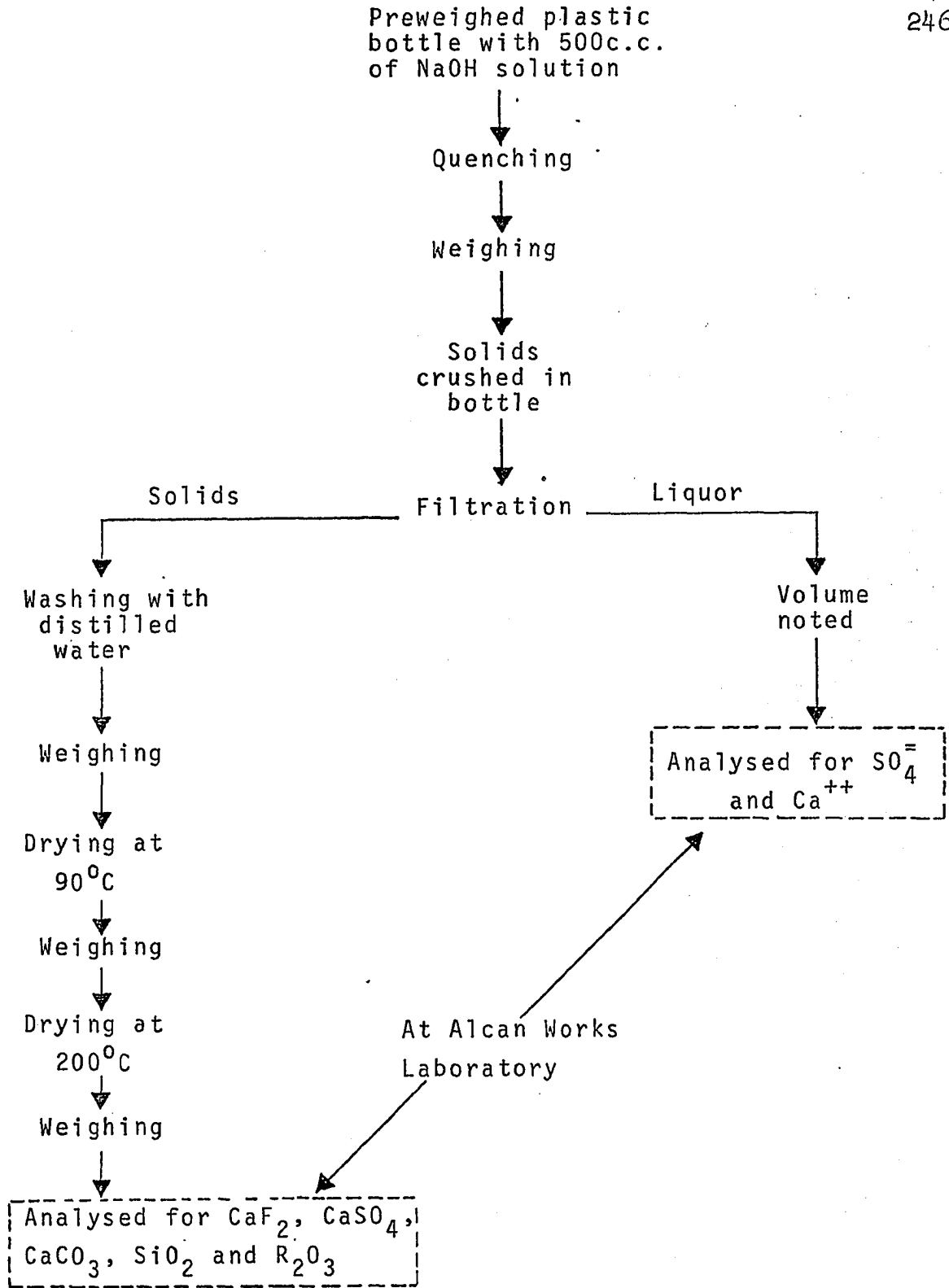


FIGURE AIV.2; Modified Solids Out Samples Handling Scheme

TABLE AIV.1; Utility of Sample Analysis

Sample description	Constituent	Purpose
Solids of solids out sample	%CaF ₂	To calculate the amount of CaF ₂ leaving the reactor in the solids out.
	%CaSO ₄	To calculate the amount of CaSO ₄ leaving the reactor in the solids out.
	%CaCO ₃	To calculate the amount of CaSO ₄ transformed to CaCO ₃ and the amount of SO ₄ ⁼ in the sample liquor due to this transformation.
	%SiO ₂	To calculate the amount of silica leaving the reactor in the solids out.
	%R ₂ O ₃	To calculate the amount of impurities leaving the reactor in the solids out.
Liquor of solids out sample	SO ₄ ⁼ (g./l.)	To determine the total amount of soluble SO ₄ ⁼ in the sample.
	Ca ⁺⁺ (g./l.)	To determine the amount of soluble CaSO ₄ in the sample.

TABLE AIV.1; Continued

Sample description	Constituent	Purpose
Scrubber liquor effluent	$F^{-}(g./l.)$	To calculate the amount of fluorine leaving the reactor into the scrubber.
	$SO_4^{=}(g./l.)$	To calculate the amount of H_2SO_4 vapor entering the scrubber.
	$SiO_2(g./l.)$	To calculate the amount of SiF_4 entering the scrubber.
Solids of sludge sample	% $CaSO_4$	To determine the amount of $CaSO_4$ in the sludge.
	% SiO_2	To determine the amount of SiO_2 in the sludge solids.
Liquid of sludge sample	$SO_4^{=}(g./g.)$	To determine the amount of H_2SO_4 in the sludge.
	$SiO_2(g./g.)$	To determine the amount of silica in the sludge liquor.
	$F^{-}(g./g.)$	To determine the amount of fluorine in the sludge liquor.

TABLE AIV.2. Analysis of Synthetic Samples

Synthetic sample	Reported values			Expected values		
	%CaF ₂ in solids	%CaSO ₄ in solids	SO ₄ ⁼ content of liquor	%CaF ₂ in solids	%CaSO ₄ in solids	SO ₄ ⁼ content of liquor
1	11.66	95.75	25.50	11.67	88.30	24.94
2	6.17	93.00	38.94	6.58	93.92	38.38
3	5.34	95.35	38.17	5.70	94.30	38.35

TABLE AIV.3. Results of Solids Out Sample Analysis

Sample No.	Wht. of sample taken (g.)	Wht. of sample solids after drying at 200°C (g.)	Volume of liquor (calculated) cc.
11A-14	81.32	59.54	498.4
11A-15	93.78	70.77	498.2
11A-16	84.80	62.78	497.7
11A-17	95.11	79.21	496.8
11A-18	92.47	70.35	496.9
11A-19	95.84	74.06	496.9
12A-14	77.58	60.74	499.3
12A-15	92.86	74.36	499.3
12A-16	86.91	68.60	499.3
12A-17	82.11	65.20	499.6
12A-18	82.26	64.52	499.5
12A-19	82.70	65.17	499.4
13A-16	76.81	56.04	498.3
13A-17	83.62	61.50	497.3
13A-18	90.27	67.39	494.9
13A-19	80.15	59.28	498.0
13A-20	81.83	60.20	495.3
13A-21	85.24	64.02	493.4
14A-16	70.10	50.94	497.6
14A-17	87.37	67.04	494.3
14A-18	87.93	67.88	495.1
14A-19	91.12	70.61	499.2
14A-20	83.00	62.82	499.2
14A-21	89.40	68.56	497.6
15A-16	89.70	72.21	497.0
15A-17	83.54	68.98	497.7
15A-18	76.50	59.65	497.6
15A-19	90.08	72.67	498.7
15A-20	80.28	63.36	499.3
15A-21	82.21	65.10	498.4

TABLE AIV.3; Contd.

Sample No.	liquor analysis (g./l.)		solids analysis (g./l.)					
	SO ₄ ⁼	Ca ⁺⁺	CaF ₂	CaSO ₄	CaCO ₃	SiO ₂	R ₂ O ₃	Total
11A-14	41.76	0.46	22.1	70.98	1.51	0.72	0.37	95.68
11A-15	44.17	0.48	20.9	78.10	1.04	0.77	0.32	101.13
11A-16	41.71	0.46	18.5	77.40	1.51	0.75	0.40	98.16
11A-17	45.09	0.46	17.5	78.57	0.90	0.75	0.28	98.00
11A-18	42.68	0.46	20.2	75.18	0.99	0.77	0.29	97.53
11A-19	43.61	0.46	18.2	75.53	1.75	0.76	0.26	96.50
12A-14	23.79	0.32	9.1	NA	1.40	0.83	NA	-
12A-15	29.40	0.51	9.8	NA	2.18	0.76	NA	-
12A-16	26.20	0.47	10.4	NA	1.04	0.82	NA	-
12A-17	26.30	0.45	10.3	NA	1.04	0.83	NA	-
12A-18	20.85	0.43	8.9	NA	1.32	0.79	NA	-
12A-19	21.13	0.38	7.8	NA	1.00	0.94	NA	-
13A-16	26.34	0.47	15.2	79.97	0.94	1.00	NA	97.11
13A-17	30.82	0.42	17.0	83.82	0.94	0.79	NA	102.55
13A-18	15.23	0.41	16.3	83.47	0.76	0.78	NA	101.31
13A-19	24.13	0.38	16.4	79.62	0.94	0.79	NA	97.74
13A-20	22.18	0.44	15.6	82.42	2.54	0.84	NA	101.4
13A-21	25.74	0.37	16.4	81.02	0.76	0.79	NA	98.97
14A-16	19.64	0.37	21.3	NA	1.04	0.92	NA	-
14A-17	17.04	0.50	21.7	71.68	0.94	0.80	NA	95.12
14A-18	28.87	0.44	19.8	74.01	0.94	0.72	NA	95.47
14A-19	21.29	0.34	18.5	NA	0.76	0.92	NA	-
14A-20	21.26	0.40	19.5	NA	0.94	0.78	NA	-
14A-21	22.81	0.44	18.2	76.46	0.84	0.75	NA	96.25
15A-16	17.60	0.44	12.8	NA	0.94	0.82	NA	-
15A-17	16.01	0.41	13.8	NA	0.84	0.81	NA	-
15A-18	13.74	0.38	14.4	NA	0.94	0.84	NA	-
15A-19	13.28	0.43	11.8	NA	0.66	0.81	NA	-
15A-20	11.54	0.39	13.2	NA	0.84	0.82	NA	-
15A-21	19.31	0.36	12.3	NA	0.84	0.78	NA	-

TABLE AIV.4; Scrubber Liquor
Samples Analysis

Sample No.	Liquor Analysis (g/l.)		
	F ⁻ (Average of all replicates)	SO ₄ ⁼	SiO ₂
11A-14	2.46	0.10	0.04
11A-15	2.41	0.08	0.05
11A-16	2.76	0.12	0.07
11A-17	2.79	0.12	0.07
11A-18	2.79	0.11	0.05
11A-19	2.76	0.11	0.07
12A-14	2.61	0.17	0.02
12A-15	2.58	0.16	0.02
12A-16	2.62	0.15	0.02
12A-17	2.62	0.15	0.02
12A-18	2.64	0.16	0.02
12A-19	2.66	0.17	0.02
13A-16	2.46	0.08	0.02
13A-17	2.48	0.08	0.05
13A-18	2.44	0.08	0.02
13A-19	2.50	0.07	0.04
13A-20	2.50	0.09	0.03
13A-21	2.46	0.08	0.03
14A-16	2.26	0.06	0.05
14A-17	2.32	0.01	0.11
14A-18	2.22	0.07	0.05
14A-19	2.28	0.07	0.09
14A-20	2.34	0.07	0.12
14A-21	2.24	0.07	0.12
15A-16	2.40	0.16	0.02
15A-17	2.55	0.17	0.04
15A-18	2.00	0.17	0.03
15A-19	2.50	0.13	0.04
15A-20	2.35	0.16	0.04

TABLE AIV.4. Contd.

Sample No.	Liquor Analysis (g/l.)		
	F ⁻ (Average of all replicates)	SO ₄ ⁼	SiO ₂
15A-21	2.35	0.16	0.04
16A-16	2.55	0.28	0.04
16A-17	2.30	0.27	0.05
16A-18	2.70	0.27	0.03
16A-19	2.65	0.23	0.05
16A-20	2.60	0.22	0.04
16A-21	2.30	0.29	0.05
17A-16	2.57	0.32	0.08
17A-17	2.70	0.36	0.11
17A-18	2.82	0.34	0.07
17A-19	2.87	0.33	0.11
17A-20	2.82	0.32	0.09
17A-21	2.67	0.32	0.11
18A-16	2.45	0.17	0.04
18A-17	2.98	0.22	0.05
18A-18	2.76	0.22	0.04
18A-19	2.52	0.18	0.05
18A-20	2.70	0.20	0.04
18A-21	2.62	0.20	0.05
19A-16	2.68	0.32	0.018
19A-17	2.48	0.26	0.018
19A-18	2.50	0.26	0.018
19A-19	2.47	0.26	0.019
19A-20	2.62	0.24	0.018
19A-21	2.64	0.27	0.018
1F-16	2.54	0.18	0.021
1F-17	2.68	0.19	0.020
1F-18	2.595	0.20	0.020
1F-19	2.57	0.19	0.019

TABLE AIV.4. Contd.

Sample No.	Liquor Analysis (g./l.)		
	F ⁻ (Average of all replicates)	SO ₄ ⁼	SiO ₂
1F-20	2.72	0.21	0.019
1F-21	2.70	0.20	0.019
2F-16	2.65	0.22	0.018
2F-17	2.75	0.25	0.019
2F-18	2.80	0.26	0.020
2F-19	2.85	0.25	0.021
2F-20	2.86	0.27	0.021
2F-21	2.69	0.22	0.020
3F-16	2.71	0.30	0.019
3F-17	2.75	0.30	0.019
3F-18	2.70	0.29	0.019
3F-19	2.74	0.28	0.019
3F-20	2.72	0.27	0.019
3F-21	2.69	0.28	0.020
4F-16	2.61	0.17	0.020
4F-17	2.74	0.19	0.020
4F-18	2.64	0.17	0.019
4F-19	2.62	0.17	0.019
4F-20	2.68	0.17	0.020
4F-21	2.82	0.19	0.021
5F-16	2.80	0.24	0.020
5F-17	2.74	0.24	0.020
5F-18	2.84	0.23	0.020
5F-19	2.71	0.24	0.020
5F-20	2.78	0.23	0.020
5F-21	2.84	0.24	0.020
6F-16	2.68	0.18	0.021
6F-17	2.76	0.18	0.021
6F-18	2.72	0.18	0.020

TABLE AIV.4. Contd.

Sample No.	Liquor Analysis (g/l.)		
	F ⁻ (Average of all replicates)	SO ₄ ⁼	SiO ₂
6F-19	2.71	0.18	0.020
6F-20	2.76	0.19	0.021
6F-21	2.71	0.18	0.021
7F-16	2.62	0.23	0.018
7F-17	2.78	0.27	0.019
7F-18	2.72	0.26	0.018
7F-19	2.72	0.25	0.019
7F-20	2.69	0.24	0.019
7F-21	2.58	0.23	0.019
8F-16	2.67	0.12	0.020
8F-17	2.71	0.13	0.020
8F-18	2.74	0.11	0.021
8F-19	2.78	0.14	0.021
8F-20	2.80	0.14	0.021
8F-21	2.80	0.13	0.022
9F-16	2.67	0.22	0.021
9F-17	2.66	0.19	0.020
9F-18	2.63	0.17	0.021
9F-19	2.61	0.15	0.020
9F-20	2.53	0.18	0.020
9F-21	2.69	0.19	0.021
10F-16	2.66	0.30	0.019
10F-17	2.62	0.35	0.019
10F-18	2.64	0.29	0.018
10F-19	2.63	0.31	0.019
10F-20	2.69	0.42	0.018
10F-21	2.61	0.32	0.018

TABLE AIV.5; Gas Transfer Line Sludge Analysis

Run No.	Fraction Solids In Sludge	Fraction Liquid In Sludge	Liquid Portion (g/g. of Liquid)			Solids Portion (%)	
			SO ₄ ⁼	F ⁻	SiO ₂	CaSO ₄	SiO ₂
16A	0.1060	0.8940	0.8870	0.00054	0.00005	99.0	0.694
17A	0.0528	0.9472	0.8851	0.00516	0.00025	99.0	1.064
18A	0.02850	0.9715	0.8252	0.0038	0.00031	99.0	0.467
19A	0.06177	0.9382	0.8763	0.00482	0.00067	99.0	0.138
2F	0.0515	0.94848	0.91692	0.00310	0.00043	82.50	0.301
3F	0.07146	0.92853	0.96665	0.00291	0.00016	94.70	0.314
5F	0.2470	0.75298	0.7344	0.00373	0.00637	93.51	0.0
7F	0.2614	0.73836	0.97726	0.00176	0.00062	54.74	0.0
10F	0.02615	0.9738	0.94917	0.00370	0.00051	99.73	0.00245

TABLE AIV.6, SiO₂ Content Of Solids, Of Solids
Out Sample Where Only The Scrubber
Effluent Analysis Was Done

Sample No.	%SiO ₂	Sample No.	%SiO ₂	Sample No.	%SiO ₂
16A-16	0.12	19A-19	0.86	4F-16	0.77
16A-17	0.20	19A-20	0.84	4F-17	0.69
16A-18	0.44	19A-21	0.85	4F-18	0.67
16A-19	0.24	1F-16	0.79	4F-19	0.71
16A-20	0.15	1F-17	0.79	4F-20	0.72
16A-21	0.41	1F-18	0.78	4F-21	0.71
17A-16	0.80	1F-19	0.83	5F-16	0.79
17A-17	0.79	1F-20	0.79	5F-17	0.80
17A-18	0.80	1F-21	0.77	5F-18	0.79
17A-19	0.78	2F-16	0.78	5F-19	0.80
17A-20	0.81	2F-17	0.80	5F-20	0.79
17A-21	0.80	2F-18	0.76	5F-21	0.81
18A-16	0.91	2F-19	0.76	6F-16	0.77
18A-17	0.76	2F-20	0.75	6F-17	0.76
18A-18	0.70	2F-21	0.75	6F-18	0.77
18A-19	0.79	3F-16	0.77	6F-19	0.78
18A-20	0.76	3F-17	0.77	6F-20	0.76
18A-21	0.78	3F-18	0.76	6F-21	0.76
19A-16	0.83	3F-19	0.75	7F-16	0.76
19A-17	0.89	3F-20	0.75	7F-17	0.76
19A-18	0.88	3F-21	0.76	7F-18	0.76

TABLE AIV.6, Contd.

Sample No.	%SiO ₂	Sample No.	%SiO ₂
7F-19	0.75	9F-18	0.78
7F-20	0.76	9F-19	0.78
7F-21	0.75	9F-20	0.76
8F-16	0.73	9F-21	0.79
8F-17	0.75	10F-16	0.78
8F-18	0.73	10F-17	0.81
8F-19	0.74	10F-18	0.80
8F-20	0.76	10F-19	0.80
8F-21	0.74	10F-20	0.78
9F-16	0.76	10F-21	0.81
9F-17	0.75		

TABLE AIV.7 Mass Balances and Conversions Using the Reported Solids Out Analysis Assuming CaCO_3 Formation During Filtration; No Solids Out Flow Correction

Run No.	Sample No.	Conversions (%)			Error in Mass Balances (a) (%)		
		CaF_2	H_2SO_4	SiO_2 (b)	Calcium	Sulfate	Fluorine
11A	14	69.09	62.42	27.25	-12.02	-5.04	-2.93
	15	69.95	65.61	20.03	-6.21	-1.64	-5.13
	16	71.54	63.80	23.10	-8.52	-0.60	2.69
	17	74.87	65.07	22.21	-10.86	-0.97	0.16
	18	70.75	66.09	19.46	-3.94	-4.05	4.29
	19	73.54	66.54	20.19	-10.31	-3.18	0.69
	Average	71.62	64.92	22.04	.	.	.
12A	14	85.63	76.23	5.31	-5.57	3.59	-1.37
	15	84.58	75.87	13.64	-4.94	3.57	-0.32
	16	83.49	77.09	5.98	-4.13	2.11	1.09
	17	83.83	75.73	5.90	-5.25	2.69	0.75
	18	85.47	80.42	6.85	-2.36	2.44	-1.22
	19	87.29	80.04	neg.	-3.73	3.22	-3.36
	Average	85.06	77.56	7.54	.	.	.

(a) A negative sign indicates accumulation.

(b) neg. indicates more SiO_2 leaving in solids than entered in spar.

TABLE AIV.7 Continued

Run No.	Sample No.	Conversions (%)			Error in Mass Balances (%)		
		CaF ₂	H ₂ SO ₄	SiO ₂	Calcium	Sulfate	Fluorine
13A	16	75.11	75.13	neg.	-0.54	-4.32	1.31
	17	72.65	73.07	8.19	3.82	-0.41	4.40
	18	70.52	87.58	neg.	14.65	-6.67	5.28
	19	72.51	78.06	4.37	3.16	-6.15	5.12
	20	73.36	80.14	neg.	8.61	-2.32	4.32
	21	72.54	77.81	4.47	4.04	-5.04	3.87
	Average	72.78	78.63	-			
14A	16	65.62	78.45	neg.	4.64	-3.50	3.06
	17	63.19	85.80	1.97	5.77	-12.14	7.32
	18	68.96	74.57	18.47	-3.17	-4.42	-1.49
	19	69.38	81.68	neg.	4.99	-2.51	0.00
	20	68.10	80.14	11.37	4.88	-2.39	3.02
	21	70.20	80.23	12.48	0.63	-4.80	2.12
	Average	68.45	79.01	14.11			

TABLE AIV.7 Continued

Run No.	Sample No.	Conversions (%)			Error in Mass Balances (%)		
		CaF ₂	H ₂ SO ₄	SiO ₂	Calcium	Sulfate	Fluorine
15A	16	79.24	84.29	3.97	-0.64	-1.11	-4.54
	17	77.52	84.79	4.70	0.45	-2.21	1.86
	18	76.43	85.41	0.70	1.36	-3.00	-14.17
	19	80.34	88.27	2.55	1.25	-1.98	-2.52
	20	77.80	88.18	1.14	2.57	-3.10	-4.65
	21	80.51	79.28	10.71	-3.28	1.88	-1.13
	Average	70.86	85.12	3.96			

TABLE AIV.8 Mass Balances and Conversions Using Reported Solids Out Analysis Assuming CaCO_3 Formation During Filtration; Solids Out Flow Rate Corrected to Force a Sulfate Balance

Run No.	Sample No.	Conversions (%)			Error in Mass Balances (a) (%)		
		CaF_2	H_2SO_4	SiO_2 (b)	Calcium	Fluorine	Silica
11A	14	67.45	60.48	23.39	-7.35	-1.29	14.46
	15	69.44	65.05	18.69	-4.64	-4.63	28.63
	16	71.37	63.59	22.63	-7.97	2.86	43.61
	17	74.62	64.73	21.44	-9.99	0.41	44.80
	18	69.51	64.71	16.06	-5.09	5.52	31.26
	19	72.67	65.48	17.57	-7.37	1.56	48.68
	Average	70.84	64.08	19.96			
12A	14	86.12	76.99	8.59	-8.85	-1.87	14.48
	15	85.11	76.64	16.62	-8.22	-0.86	6.45
	16	83.83	77.52	7.39	-6.12	0.75	15.14
	17	84.25	76.31	8.36	-7.73	0.33	14.71
	18	85.82	80.84	9.07	-4.69	-1.56	14.00
	19	87.69	80.60	neg.	-6.73	-3.76	37.08
	Average	85.47	78.15				

(a) A negative sign indicates accumulation.

(b) neg. indicates more SiO_2 leaving in solids than entered in spar.

TABLE AIV.8 Continued

Run No.	Sample No.	Conversions (%)			Error in Mass Balances (%)		
		CaF ₂	H ₂ SO ₄	SiO ₂	Calcium	Fluorine	Silica
13A	16	73.99	74.05	neg.	3.95	2.43	45.47
	17	72.53	72.96	7.81	4.25	4.51	46.85
	18	68.42	86.75	neg.	22.85	7.38	31.03
	19	70.71	76.67	neg.	9.92	6.95	45.63
	20	72.73	79.68	neg.	11.19	4.94	38.86
	21	71.08	76.67	neg.	9.56	5.34	33.39
	Average	71.58	77.80	-			
14A	16	64.38	77.70	neg.	8.43	8.43	64.61
	17	58.10	83.85	neg.	20.37	12.41	129.21
	18	67.53	73.43	14.71	1.30	-0.05	38.71
	19	68.59	81.24	neg.	7.69	0.70	109.06
	20	67.31	79.68	9.-9	7.45	3.81	119.14
	21	68.70	79.29	8.07	5.71	-0.62	120.26
	Average	67.31	79.20	10.66			

TABLE AIV.8 Continued

Run No.	Sample No.	Conversions (%)			Error in Mass Balances (%)		
		CaF ₂	H ₂ SO ₄	SiO ₂	Calcium	Fluorine	Silica
15A	16	79.01	84.14	2.89	0.47	-4.30	19.01
	17	77.01	84.49	2.54	2.73	2.37	41.28
	18	75.70	85.03	neg.	4.49	13.45	35.23
	19	79.95	88.06	0.60	3.29	-2.12	43.23
	20	77.09	87.87	neg.	5.85	-3.94	45.84
	21	80.87	80.13	12.36	-5.06	-1.49	31.45
	Average	78.27	85.79	-			

TABLE AIV.9 Mass Balances and Conversions Using Reported Solids Out Analysis Assuming CaCO_3 Formation Prior to Filtration of Solids Sample; No Solids Out Flow Correction.

Run No.	Sample No.	Conversions (%)			Error in Mass Balances (a) (%)		
		CaF_2	H_2SO_4	SiO_2 (b)	Calcium	Sulfate	Fluorine
11A	14	68.28	63.97	25.37	-12.15	-7.50	-2.12
	15	69.42	66.73	18.62	-6.37	-3.41	-4.61
	16	70.81	65.38	21.12	-8.55	-2.91	3.42
	17	74.51	66.04	21.10	-11.24	-2.66	0.51
	18	70.27	67.17	18.15	-9.32	-5.86	4.76
	19	72.75	68.44	17.82	-10.18	-5.71	1.47
	Average	71.01	66.28	20.36			
12A	14	85.28	77.77	3.01	-5.53	1.77	-1.02
	15	84.00	78.32	10.35	-4.64	0.86	0.26
	16	83.21	78.23	4.39	-4.53	0.32	1.37
	17	83.56	76.88	4.32	-5.69	0.84	1.02
	18	85.16	81.87	4.88	-2.66	0.40	-0.90
	19	87.10	81.08	neg.	-4.09	1.64	-3.17
	Average	84.71	79.01	5.39			

(a) A negative sign indicates accumulation.

(b) neg. indicates more SiO_2 leaving in solids than entered in spar.

TABLE AIV.9 Continued

Run No.	Sample No.	Conversions (%)			Error in Mass Balances (%)		
		CaF ₂	H ₂ SO ₄	SiO ₂	Calcium	Sulfate	Fluorine
13A	16	74.73	76.09	neg.	-1.17	-6.23	1.69
	17	72.22	74.04	6.74	3.52	-2.06	4.83
	18	70.20	88.37	neg.	14.17	-8.22	5.60
	19	72.09	79.03	2.91	2.78	-7.86	5.57
	20	72.20	82.75	neg.	9.22	-5.43	5.47
	21	72.22	78.61	3.33	3.64	-6.51	4.21
	Average	72.27	79.81	-			
14A	16	65.05	79.58	neg.	4.29	-5.57	3.63
	17	62.63	86.87	0.51	5.29	-14.27	7.87
	18	68.47	75.65	17.18	-3.48	-6.33	-1.00
	19	69.02	82.56	neg.	4.73	-4.02	0.27
	20	67.62	81.20	10.05	4.56	-4.28	3.49
	21	69.81	81.20	11.34	0.19	-6.63	-1.73
	Average	67.99	76.44	-			

TABLE AIV.9 Continued

Run No.	Sample No.	Conversions (%)			Error in Mass Balances (%)		
		CaF ₂	H ₂ SO ₄	SiO ₂	Calcium	Sulfate	Fluorine
	16	78.93	85.38	2.42	-0.93	-2.82	-4.21
	17	77.21	85.76	3.40	0.12	-3.84	2.16
	18	76.07	86.46	neg.	1.03	-4.75	-13.82
15A	19	80.14	89.03	1.54	0.80	-3.41	-2.32
	20	77.52	89.12	neg.	2.11	-4.81	-4.37
	21	80.25	80.77	9.54	-3.62	0.31	-0.87
	Average	78.35	86.09	-			

TABLE AIV.10 Mass Balances and Conversions Using the Reported Solids Out Analysis Assuming CaCO_3 Formation Prior to Filtration of Sample Solids; Solids Out Flow Corrected to Force a Sulfate Balance.

Run No.	Sample No.	Conversions (%)			Error in Mass Balances (a) (%)		
		CaF_2	H_2SO_4	SiO_2 (b)	Calcium	Fluorine	Silica
11A	14	65.71	61.14	19.30	-5.03	0.45	18.56
	15	68.35	65.57	15.78	-3.11	-3.53	31.53
	16	69.92	64.38	18.72	-5.78	4.31	47.53
	17	73.82	65.14	18.97	-8.84	1.21	47.28
	18	68.44	65.17	13.11	-3.65	6.59	34.20
	19	71.09	66.60	12.81	-4.73	3.14	53.44
	Average	69.56	64.57	16.45			
12A	14	85.55	78.12	4.8	-7.27	-1.29	18.27
	15	84.13	78.49	11.12	-5.45	0.13	11.96
	16	83.26	78.29	4.66	-4.80	1.33	18.40
	17	83.70	77.06	5.14	-6.50	0.88	17.93
	18	85.22	81.94	5.26	-3.07	-0.97	17.81
	19	87.31	81.36	neg	-5.68	-3.38	40.54
	Average	84.86	79.21	6.20			

(a) A negative sign indicates accumulation.

(b) neg. indicates more SiO_2 leaving in solids than entered in spar.

TABLE AIV.10 Continued

Run No.	Sample No.	Conversions (%)			Error in Mass Balances (%)		
		CaF ₂	H ₂ SO ₄	SiO ₂	Calcium	Fluorine	Silica
13A	16	73.05	74.56	neg.	5.39	3.37	49.93
	17	71.66	73.51	4.88	5.58	5.38	49.77
	18	67.52	87.41	neg.	24.52	8.28	34.13
	19	69.71	77.31	neg.	11.54	7.95	49.10
	20	70.61	81.82	neg.	15.42	7.05	47.08
	21	70.26	77.18	neg.	10.92	6.15	36.25
	Average	70.47	78.63	-			
14A	16	62.97	78.42	neg.	10.49	5.72	69.00
	17	56.42	84.70	neg.	22.76	14.09	133.68
	18	66.37	74.07	neg.	2.92	1.10	41.81
	19	67.70	81.87	neg.	9.22	1.60	112.29
	20	66.18	80.40	6.03	9.23	4.94	122.31
	21	67.65	79.92	5.00	7.35	0.42	122.33
	Average	66.16	78.94	-			

TABLE AIV.10 Continued

Run No.	Sample No.	Conversions (%)			Error in Mass Balances (%)		
		CaF ₂	H ₂ SO ₄	SiO ₂	Calcium	Fluorine	Silica
15A	16	78.31	85.01	neg.	1.94	3.61	22.24
	17	76.32	85.28	neg.	4.06	3.06	44.23
	18	74.88	85.89	neg.	6.04	12.62	38.67
	19	79.45	88.70	neg.	4.30	-1.63	45.69
	20	76.37	88.68	neg.	7.35	-3.21	49.06
	21	80.31	80.82	9.78	-3.88	-0.92	34.02
	Average	77.60	85.73	-			

TABLE AIV.11 Mass Balances and Conversions Based on the Caustic Liquor Analysis

Run No.	Sample No.	Conversions (%)			Error in Mass Balances (a) (%)		
		CaF ₂	H ₂ SO ₄	SiO ₂ (b)	Calcium Sulfate	Silica	
11A	14	66.16	66.47	18.26	0.67	0.66	19.60
	15	64.82	65.18	13.21	0.60	0.60	34.11
	16	74.23	74.24	11.81	0.36	0.36	54.43
	17	75.03	75.01	11.50	0.47	0.46	54.76
	18	75.03	75.01	8.98	0.58	0.58	38.34
	19	74.63	74.24	10.64	0.48	0.48	55.61
	Average	74.63	74.62	12.4			
12A	14	84.26	84.04	neg.	0.95	0.94	25.50
	15	84.26	84.04	neg.	1.02	1.01	16.86
	16	84.59	84.36	neg.	0.96	0.96	24.41
	17	84.59	84.36	neg.	0.95	0.94	25.64
	18	84.26	84.04	2.51	0.99	0.98	20.56
	19	83.93	83.73	neg.	0.79	0.78	46.30
	Average	84.31	84.04	-			

(a) A negative sign indicates accumulation.

(b) neg. indicates more SiO₂ leaving in solids than entered in spar.

TABLE AIV.11 Continued

Run. No.	Sample No.	Conversions (%)			Error in Mass Balances (%)		
		CaF ₂	H ₂ SO ₄	SiO ₂	Calcium	Sulfate	Silica
13A	16	76.42	72.51	neg.	0.83	0.78	41.07
	17	77.04	73.08	5.82	0.77	0.72	48.48
	18	75.80	71.94	7.28	1.03	0.97	14.58
	19	77.66	73.64	5.47	0.85	0.80	38.26
	20	77.66	73.64	neg.	0.89	0.83	33.40
	21	76.42	75.51	5.91	0.94	0.88	26.88
	Average	76.83	73.39	-			
14A	16	68.69	73.21	neg.	0.69	0.73	59.03
	17	70.51	75.08	17.86	0.30	0.31	109.70
	18	67.47	71.97	neg.	0.87	0.92	35.61
	19	69.29	83.83	13.53	0.36	0.37	101.72
	20	71.21	75.70	15.89	0.26	0.27	114.81
	21	68.08	75.29	-	0.28	-.29	112.45
	Average	69.19	73.73				

TABLE AIV.11 Continued

Run No.	Sample No.	Conversions (%)			Error in Mass Balances (%)		
		CaF ₂	H ₂ SO ₄	SiO ₂	Calcium	Sulfate	Silica
15A	16	74.71	79.23	3.01	1.00	1.05	18.90
	17	79.38	84.00	2.33	0.82	0.87	41.48
	18	62.25	66.52	6.35	0.94	0.99	26.51
	19	77.82	82.41	3.01	0.83	0.87	40.81
	20	73.15	77.64	3.87	0.84	0.88	39.95
	21	79.38	84.00	5.95	0.85	0.90	37.86
	Average	78.86	81.45	4.09			
16A	16	77.96	78.63	85.36	1.11	1.11	-42.64
	17	70.31	71.19	76.46	1.04	1.04	-23.15
	18	82.54	83.08	45.23	0.81	0.81	-14.13
	19	81.02	81.60	70.48	1.00	1.00	-17.17
	20	79.49	80.11	81.67	1.08	1.08	-38.94
	21	70.32	71.20	51.66	0.86	0.85	-1.04
	Average	80.26	80.86	68.48			

TABLE AIV.11 Continued

Run No.	Sample No.	Conversions (%)			Error in Mass Balances (%)		
		CaF ₂	H ₂ SO ₄	SiO ₂	Calcium Sulfate	Silica	
17A	16	81.14	77.74	2.93	0.89	0.85	86.03
	17	85.22	81.52	1.18	0.88	0.83	87.78
	18	89.00	85.01	neg.	0.86	0.82	78.34
	19	90.29	-	-	-	-	-
	20	89.00	85.01	neg.	0.85	0.81	101.73
	21	84.28	80.64	1.58	0.88	0.83	120.59
	Average	87.66					
18A	16	77.25	74.07	neg.	0.84	0.80	53.16
	17	93.94	89.49	2.37	0.92	0.88	53.13
	18	84.18	80.47	13.75	1.01	0.96	30.67
	19	79.45	76.10	4.64	0.94	0.89	50.84
	20	85.12	81.34	5.99	0.95	0.90	38.45
	21	82.60	79.01	4.57	0.94	0.89	50.95
	Average	87.66					

TABLE IV.11 Continued

Run No.	Sample No.	Conversions (%)			Error in Mass Balances (%)		
		CaF ₂	H ₂ SO ₄	SiO ₂	Calcium	Sulfate	Silica
19A	16	85.06	89.54	neg.	0.82	0.86	22.79
	17	78.73	83.10	neg.	0.79	0.82	27.16
	18	79.36	83.75	neg.	0.79	0.83	26.26
	19	78.42	82.78	89.69	1.53	1.60	-69.30
	20	83.16	87.62	neg.	0.82	0.86	23.16
	21	83.79	88.25	89.57	1.53	1.60	-69.17
	Average	80.19					
1F	16	78.24	78.57	4.88	1.18	1.18	17.88
	17	82.56	82.75	3.05	1.17	1.16	18.62
	18	79.94	80.21	5.38	1.18	1.18	16.30
	19	79.17	79.47	neg.	1.14	1.14	20.94
	20	83.79	83.94	3.76	1.17	1.17	16.83
	21	85.64	85.74	4.23	1.18	1.17	16.36
	Average	81.17					

TABLE AIV.11 Continued

Run No.	Sample No.	Conversions (%)			Error in Mass Balances (%)		
		CaF ₂	H ₂ SO ₄	SiO ₂	Calcium	Sulfate	Silica
2F	16	84.66	85.23	0.20	1.17	1.16	20.27
	17	87.86	88.23	neg.	1.13	1.12	25.32
	18	89.45	89.72	0.82	1.15	1.15	21.90
	19	91.05	91.22	0.17	1.14	1.14	23.67
	20	91.37	91.52	1.36	1.15	1.14	22.49
	21	85.94	86.43	3.54	1.17	1.17	19.18
	Average	88.27					
3F	16	86.78	86.94	0.61	1.31	1.30	21.01
	17	88.06	88.13	0.08	1.30	1.29	21.54
	18	86.46	86.64	2.03	1.32	1.31	19.59
	19	87.74	87.84	2.80	1.32	1.32	18.82
	20	87.10	87.24	3.06	1.32	1.32	18.56
	21	86.14	86.34	2.17	1.31	1.31	20.57
	Average	86.69					

TABLE AIV.11 Continued

Run No.	Sample No.	Conversions (%)			Error in Mass Balances (%)		
		CaF ₂	H ₂ SO ₄	SiO ₂	Calcium Sulfate	Silica	
4F	16	83.54	84.33	1.62	1.36	1.36	20.93
	17	87.71	88.24	10.30	1.42	1.42	12.25
	18	84.51	85.23	14.05	1.46	1.46	7.38
	19	83.86	84.63	9.16	1.42	1.42	12.26
	20	85.78	86.44	7.14	1.40	1.40	15.41
	21	90.28	90.65	6.72	1.39	1.39	16.95
	Average	85.94					
5F	16	86.45	87.32	2.18	0.81	0.81	20.64
	17	84.60	85.51	1.73	0.80	0.81	21.08
	18	87.69	88.53	neg.	0.78	0.79	23.65
	19	83.68	84.61	2.13	0.80	0.81	20.68
	20	85.84	86.72	2.44	0.81	0.81	20.36
	21	87.69	88.53	neg.	0.78	0.79	23.65
	Average	85.82					

TABLE AIV.11 Continued

Run No.	Sample No.	Conversions (%)			Error in Mass Balances (%)		
		CaF ₂	H ₂ SO ₄	SiO ₂	Calcium	Sulfate	Silica
6F	16	82.69	83.54	5.45	1.18	1.19	17.35
	17	85.16	85.95	5.67	1.19	1.19	17.13
	18	83.93	84.74	4.94	1.18	1.19	16.77
	19	83.62	84.44	3.84	1.17	1.18	17.88
	20	85.16	85.95	5.67	1.19	1.19	17.13
	21	83.62	84.44	6.30	1.19	1.20	16.50
	Average	83.99					
7F	16	83.87	84.14	3.80	0.92	0.91	16.73
	17	88.99	88.92	1.72	0.89	0.89	19.94
	18	87.07	87.13	2.49	0.91	0.90	18.04
	19	87.07	81.13	3.78	0.91	0.91	17.87
	20	86.11	86.23	4.17	0.92	0.91	17.49
	21	82.59	82.94	5.59	0.93	0.92	16.07
	Average	85.07					

TABLE AIV.11 Continued

Run No.	Sample No.	Conversions (%)			Error in Mass Balances (%)		
		CaF ₂	H ₂ SO ₄	SiO ₂	Calcium	Sulfate	Silica
8F	16	85.22	85.64	6.07	1.39	1.39	16.41
	17	86.50	86.83	2.98	1.37	1.36	19.50
	18	87.45	87.73	5.20	1.38	1.37	18.40
	19	88.73	88.93	3.40	1.36	1.36	20.21
	20	89.37	89.52	0.53	1.34	1.33	13.08
	21	89.37	89.52	3.15	1.35	1.35	21.58
	Average	87.87					
9F	16	82.73	83.41	6.66	1.19	1.20	16.23
	17	82.42	83.11	8.02	1.20	1.21	13.79
	18	81.49	82.20	4.73	1.18	1.18	18.17
	19	80.87	81.60	4.99	1.18	1.18	16.82
	20	78.39	79.18	8.44	1.21	1.21	13.37
	21	83.35	80.01	2.71	1.16	1.17	20.18
	Average	81.55					

TABLE AIV.11 Continued

Run No.	Sample No.	Conversions (%)			Error in Mass Balances (%)		
		CaF ₂	H ₂ SO ₄	SiO ₂	Calcium	Sulfate	Silica
10F	16	82.41	82.42	4.65	1.02	1.01	16.41
	17	81.17	81.23	1.53	1.00	1.00	19.54
	18	81.79	81.82	2.48	1.01	1.00	17.51
	19	81.48	81.53	2.61	1.01	1.00	18.46
	20	83.34	83.32	4.26	1.02	1.01	15.72
	21	80.86	80.93	1.66	1.00	0.99	18.32
	Average	81.82					

VITA AUCTORIS

- 1943 Born in Bannia, Italy
- 1963 Completed High School at St. Mary's College,
Sault Ste. Marie, Ontario, Canada
- 1967 Received the Degree of Bachelor of Applied
Science in Chemical Engineering from the
University of Windsor, Windsor, Ontario, Canada.
- 1972 Candidate for the Degree of Doctor of Philosophy
in Chemical Engineering at the University of
Windsor, Windsor, Ontario, Canada